# CRYSTALLIZATION BEHAVIOR

# OF POLY (LACTIC ACID) COMPOSITES

**Somruetai Boonying**

**A Thesis Submitted in Partial Fulfillment of the Requirement for the**

**Degree of Master of Engineering in Polymer Engineering**

**Suranaree University of Technology**

**Academic Year 2009**

# พฤติกรรมการตกผลึกของพอลิแลกติกแอสิดคอมโพสิท

นางสาวสมฤทัย บุญยิ่ง

วิทยานิพนธ์นี้เป็นส่วนหนึ่งของการศึกษาตามหลักสูตรปริญญาวิศวกรรมศาสตรมหาบัณฑิต
สาขาวิชาวิศวกรรมพอลิเมอร์
มหาวิทยาลัยเทคโนโลยีสุรนารี
ปีการศึกษา 2552

**CRYSTALLIZATION BEHAVIOR**

**OF POLY (LACTIC ACID) COMPOSITES**

Suranaree University of Technology has approved this thesis submitted in partial fulfillment of the requirement for a master's degree.

Thesis Examining Committee

(Asst. Prof. Dr. Kasama Jarukumjorn)
Chairperson

(Asst. Prof. Dr. Yupaporn Ruksakulpiwat)
Member (Thesis Advisor)

(Asst. Prof. Dr. Wimonlak Sutapun)
Member

(Asst. Prof. Dr. Nitinat Suppakarn)
Member

(Asst. Prof. Dr. Pranee Chunsamrong)
Member

(Asst. Prof. Dr. Visit Vao-soongnern)
Member

(Prof. Dr. Sukit Limpijumnong)
Vice Rector for Academic Affairs

(Assoc. Prof. Dr. Vorapot Khompis)
Dean of Institute of Engineering

สมฤทัย บุญยิ่ง : พฤติกรรมการตกผลึกของพอลิแลกติกแอสิดคอมโพสิท
(CRYSTALLIZATION BEHAVIOR OF POLY (LACTIC ACID) COMPOSITES
อาจารย์ที่ปรึกษา : ผู้ช่วยศาสตราจารย์ ดร.ยุพาพร รักสกุลพิวัฒน์, 120 หน้า.

งานวิจัยนี้เป็นการศึกษาหน้าที่ของเส้นใยหญ้าแฝกที่ส่งผลต่อพฤติกรรมการเกิดผลึกของพอลิแลกติกแอสิดคอมโพสิท การตรวจสอบสมบัติทางความร้อนของพอลิแลกติกแอสิด ทำโดยใช้เครื่องดิฟเฟอเรนท์เชียล สแกนนิ่ง แคลอรีมิตรี้ หรือ ดีเอสซี ได้มีการศึกษาเปรียบเทียบผลของการก่อเกิดนิวคลีไอของเส้นใยหญ้าแฝกและทัลก์ต่อการเกิดผลึกของพอลิแลกติกแอสิดคอมโพสิท จากการทดลองพบว่าอัตราการเกิดผลึกของพอลิแลกติกแอสิดจะเพิ่มขึ้นเมื่อปริมาณของเส้นใยหญ้าแฝกเพิ่มขึ้น เมื่อเปรียบเทียบอัตราการเกิดผลึกของพอลิแลกติกแอสิดและพอลิแลกติกแอสิดคอมโพสิทพบว่าอัตราการเกิดผลึกของคอมโพสิทระหว่างพอลิแลกติกแอสิดและทัลก์สูงที่สุด นอกจากนี้อุณหภูมิหลอมเหลวที่สภาวะสมดุลของคอมโพสิทระหว่างพอลิแลกติกแอสิดและเส้นใยหญ้าแฝกและคอมโพสิทระหว่างพอลิแลกติกแอสิดและทัลก์ต่ำกว่าของพอลิแลกติกแอสิด ปริมาณเส้นใยหญ้าแฝกที่เพิ่มขึ้นในพอลิแลกติกแอสิดคอมโพสิทนำไปสู่การลดลงของอุณหภูมิหลอมเหลวที่สภาวะสมดุล นอกจากนี้จะพบพีกการเกิดผลึกของคอมโพสิทระหว่างพอลิแลกติกแอสิดและทัลก์ที่อัตราการทำให้เย็นลงที่ 5 องศาเซลเซียสต่อนาที ในขั้นตอนการให้ความร้อนครั้งที่สองด้วยอัตรา 5 องศาเซลเซียสต่อนาที ไม่มีพีกการเกิดผลึกอีกครั้งของคอมโพสิทระหว่างพอลิแลกติกแอสิดและทัลก์ อาจเป็นไปได้ว่าการเกิดผลึกของคอมโพสิทระหว่างพอลิแลกติกแอสิดและทัลก์ได้เกิดขึ้นสมบูรณ์แล้วในขั้นตอนการทำให้เย็นลง ผลการทดลองนี้ตรงข้ามกับผลที่พบในคอมโพสิทระหว่างพอลิแลกติกแอสิดและเส้นใยหญ้าแฝกซึ่งไม่พบพีกการเกิดผลึกของคอมโพสิทระหว่างพอลิแลกติกแอสิดและเส้นใยหญ้าแฝก แม้ว่าอัตราการทำให้เย็นลงจะต่ำลงถึง 1 องศาเซลเซียสต่อนาที เมื่อให้ความร้อนครั้งที่สองกับคอมโพสิทระหว่างพอลิแลกติกแอสิดและเส้นใยหญ้าแฝกจะพบพีกการเกิดผลึกอีกครั้งของคอมโพสิทระหว่างพอลิแลกติกแอสิดและเส้นใยหญ้าแฝก อย่างไรก็ตามเมื่ออัตราการให้ความร้อนมากกว่า 10 องศาเซลเซียสต่อนาทีไม่พบพีกการเกิดผลึกอีกครั้งของคอมโพสิทระหว่างพอลิแลกติกแอสิดและเส้นใยหญ้าแฝก ผลึกของพอลิแลกติกแอสิดเพิ่มขึ้นเมื่อมีเส้นใยหญ้าแฝก สิ่งนี้ชี้ให้เห็นว่าเส้นใยหญ้าแฝกทำหน้าที่เป็นตัวก่อเกิดนิวคลีไอสำหรับพอลิแลกติกแอสิดคอมโพสิท

นอกจากนี้ได้มีการศึกษาอัตราการเติบโตของผลึกของพอลิแลกติกแอสิดและพอลิแลกติกแอสิดคอมโพสิทพบว่ามีการเกิดผลึกแบบทรานคริสตัลไลเซชันที่ผิวของเส้นใยหญ้าแฝกและทัลก์ อัตราการเติบโตของผลึกของพอลิแลกติกแอสิดมากกว่าอัตราการเติบโตของผลึกในบัลค์ของคอมโพสิทระหว่างพอลิแลกติกแอสิดและเส้นใยหญ้าแฝก ในขณะที่อัตราการเติบโตของผลึก

ในบัลค์ของคอมโพสิทระหว่างพอลิแลกติกแอสิดและทัลก์มากกว่าอัตราการเติบโตของผลึกในคอมโพสิทระหว่างพอลิแลกติกแอสิดและเส้นใยหญ้าแฝกและพอลิแลกติกแอสิดคอมโพสิท ยิ่งไปกว่านั้นอัตราการเติบโตของผลึกแบบทรานคริสตัลไลเซชันของคอมโพสิทระหว่างพอลิแลกติกแอสิดและทัลก์มากกว่าในคอมโพสิทระหว่างพอลิแลกติกแอสิดและเส้นใยหญ้าแฝก นอกจากนี้อัตราการเติบโตของผลึกในบัลค์ของคอมโพสิทเร็วกว่าอัตราการเติบโตของผลึกแบบทรานคริสตัลไลเซชัน กราฟความสัมพันธ์ระหว่างอุณหภูมิกับอัตราการเติบโตของผลึกในพอลิแลกติกแอสิดและพอลิแลกติกแอสิดคอมโพสิทมีลักษณะเป็นรูประฆังคว่ำและใช้ได้กับสมการฮอฟฟ์แมน-ลอริเซน อัตราการเติบโตของผลึกสูงสุดของพอลิแลกติกแอสิดและพอลิแลกติกแอสิดคอมโพสิท อยู่ที่อุณหภูมิประมาณ 135 องศาเซลเซียส

สาขาวิชา วิศวกรรมพอลิเมอร์ ลายมือชื่อนักศึกษา _____

ปีการศึกษา 2552 ลายมือชื่ออาจารย์ที่ปรึกษา _____

ลายมือชื่ออาจารย์ที่ปรึกษาร่วม _____

ลายมือชื่ออาจารย์ที่ปรึกษาร่วม _____

SOMRUETAI BOONYING : CRYSTALLIZATION BEHAVIOR OF POLY (LACTIC ACID) COMPOSITES. THESIS ADVISOR : ASST. PROF. YUPAPORN RUKSAKULPIWAT, Ph.D., 120 PP.

VETIVER FIBER/POLY (LACTIC ACID)/THERMAL PROPERTY/ GROWTH RATE

In this research, the role of vetiver fiber on crystallization behavior of vetiver fiber-PLA composite was evaluated. The thermal properties of neat PLA and vetiver fiber-PLA composites were investigated by using a Differential Scanning Calorimeter (DSC). The nucleating effect of vetiver fiber and talc on the crystallization of PLA composites was comparatively studied. Crystallization rate of PLA was increased with increasing vetiver fiber contents. Among that of neat PLA and vetiver fiber-PLA composites, crystallization rate of talc-PLA composites was the highest. Additionally, the equilibrium melting temperatures of vetiver fiber-PLA and talc–PLA composites were lower than that of neat PLA. An increase in vetiver fiber content in the PLA composites led to a decrease in equilibrium melting temperatures of the composites.

In addition, the crystallization peak of talc-PLA composites was observed at the cooling rate of 5°C/min. Upon the second heating scan, re-crystallization peak of talc-PLA composites did not take place with the heating rate of 5°C/min. This might be the indication of complete crystallization of talc-PLA composites during the cooling process. In contrast, the crystallization peak of PLA from vetiver fiber-PLA composites was not observed upon cooling. Even though, the cooling rate was lower down to 1°C/min. During the second heating scan, re-crystallization peak of the vetiver fiber-PLA composites was observed. However, the re-crystallization peak of

vetiver fiber-PLA composites was not observed when the heating rate was higher than 10°C/min. The crystallinity of PLA composites increased with the inclusion of vetiver fiber. This indicated that vetiver fiber acted as a nucleating agent of PLA composites.

Additionally, the spherulitic growth rate of neat PLA and PLA composites was investigated. The transcrystallization (TC) was observed at the vetiver fiber and talc surface. The growth rate of neat PLA was higher than that of PLA in the bulk of the vetiver fiber-PLA composites. While the growth rate of PLA in the bulk of talc-PLA composites was noticeably higher than that of vetiver fiber-PLA composites and neat PLA. Moreover, it was observed that the growth rate at TC region of talc-PLA composites was higher than that of vetiver fiber-PLA composites. In addition, the growth rate of PLA crystallized in the bulk of the composites was faster than that crystallized at TC region. In addition, it was discovered that the growth rate of both neat PLA and PLA composites as function of temperature was illustrated by a bell-shaped curve, and were able to be fitted by Hoffman-Lauritzen growth equation. The maximum growth rate of neat PLA and PLA composites was approximately at 135°C.

School of Polymer Engineering

Academic Year 2009

Student's Signature _____

Advisor' Signature _____

Co-advisor's Signature _____

Co-advisor's Signature _____

# ACKNOWLEDGEMENTS

I would like to thank Suranaree University of Technology and the Center of Excellence for Petroleum, Petrochemical and Advanced Materials, Chulalongkorn University, Thailand for financial support. In addition, I wish to acknowledge the staff in laboratory division of Mettler-Toledo (Thailand) Co., Ltd. for their kind supporting and providing DSC instrument and to Land Development Department (LDD), Nakorn Ratchasima for supplying vetiver grass. I am grateful to all the faculty and staff members of the School of Polymer Engineering and the Center for Scientific and Technological Equipment of Suranaree University of Technology for their help and assistance throughout the period of this study. The grateful thanks and appreciation are given to thesis advisor, Asst. Prof. Dr. Yupaporn Ruksakulpiwat, for her valuable supervision, advice, support and kindness throughout this study.

Moreover, I would like to thank Asst. Prof. Dr. Wimonlak Sutapun and Asst. Prof. Dr. Nitinat Suppakarn, my co-advisors for advices during my research work. I gratefully thank the chairperson, Asst. Prof. Dr. Kasama Jarukumjorn and the committee, Asst. Prof. Dr. Pranee Chumsamrong and Asst. Prof. Dr. Visit Vaosoongnern for him valuable suggestion and encouragement.

Finally, I am deeply grateful to my family and friends who support and encourage me towards the course of this study at the Suranaree University of Technology.

Somruetai Boonying

# TABLE OF CONTENTS

**Page**

# TABLE OF CONTENTS (Continued)

**Page**

# TABLE OF CONTENTS (Continued)

**Page**

# TABLE OF CONTENTS (Continued)

**Page**

# LIST OF TABLES

**Table** **Page**

# LIST OF FIGURES

**Figure** **Page**

# LIST OF FIGURES (Continued)

**Figure** **Page**

# LIST OF FIGURES (Continued)

**Figure** **Page**

# LIST OF FIGURES (Continued)

**Figure** **Page**

# LIST OF FIGURES (Continued)

**Figure** **Page**

# LIST OF FIGURES (Continued)

**Figure** **Page**

# LIST OF FIGURES (Continued)

**Figure** **Page**

# SYMBOLS AND ABBREVIATIONS

| | | |
|---|---|---|
| % | = | Percent |
| $\%X_c$ | = | Degree of crystallinity |
| °C | = | Degree Celsius |
| ΔH | = | Heat of fusion |
| μm | = | Micrometer |
| DSC | = | Differential Scanning Calorimeter |
| g | = | Gram |
| G | = | Growth rate |
| mg | = | Milligram |
| min | = | Minute |
| PLA | = | Poly(lactic acid) |
| POM | = | Polarized Light Optical Microscope |
| rpm | = | Revolution per minute |
| s | = | Second |
| v | = | Volume |
| wt | = | Weight |

# CHAPTER I

# INTRODUCTION

## 1.1 Natural fiber and natural fiber composites

During the last few year it has been an increasing environmental consciousness, which increased the interest to use natural fibers such as kenaf, jute, hemp, flex, and coir instead of traditional fibers. Traditional fiber composites have been composed of either glass or carbon fibers with non-biodegradable material. After their lifetime, the disposal of these products is through either landfill or incineration (Wong, Shank, and Hodzic, 2007). Since traditional fibers products do not degrade in a landfill or composting environments they pose a serious environmental problem.

Natural fibers are subdivided based on their origins, whether they are derived from plants, animals, or minerals. In Figure 1.1 displays images of several natural fibers with reinforcement potential.

The chemical composition as well as the structure of fibers is fairly complicated. The fibers are basically a rigid, crystalline cellulose micro fibril reinforced amorphocellus lignin and/or hemicelluloses matrix. Most plant fibers are composed of cellulose, hemicelluloses, lignin, waxes, and some water-soluble compound. Cellulose, hemicelluloses and lignin are the major constituents.

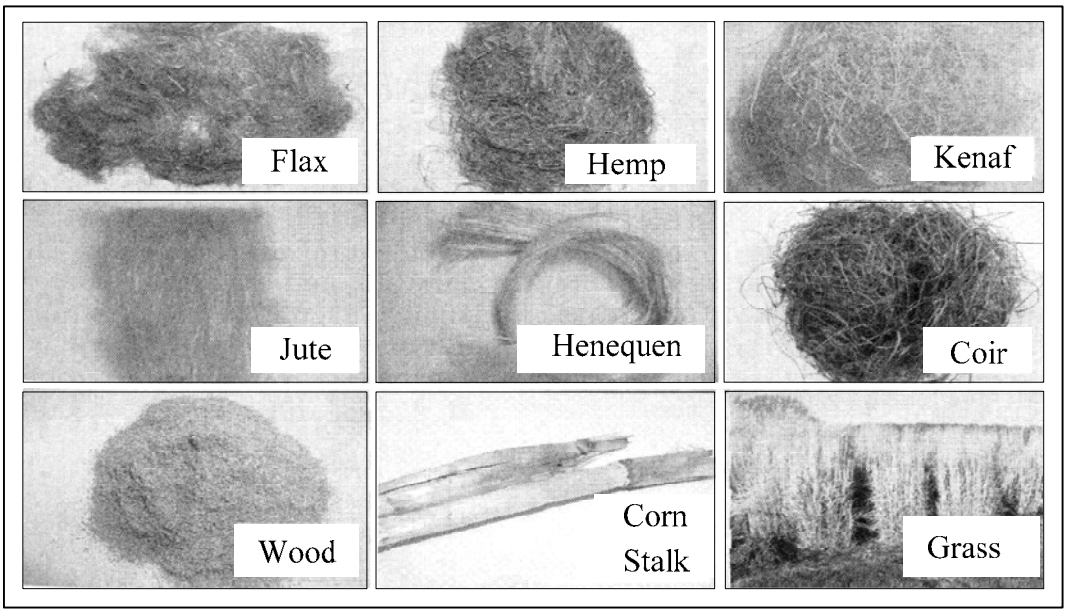


**Figure 1.1** Digital photographs of some natural fibers and sources of natural fibers (Mohanty, Misra, and Drzal, 2005).

The amount of cellulose in lignocellliulosic system depends on the species and age of the plant. Cellulose is a hydrophilic glucan polymer consisting of a linear chain of 1, 4 - β anhydroglucose unite, which contain alcoholic hydroxyl group (Figure 1.2). These hydroxyl groups form intermolecular and intramolecular hydrogen bonds with the macromolecule itself and also with other cellulose macromolecules or polar molecules. Therefore, all natural fibers are hydrophilic in nature. Although the chemical structure of cellulose from different natural fiber is the same, the degree of polymerization varies.

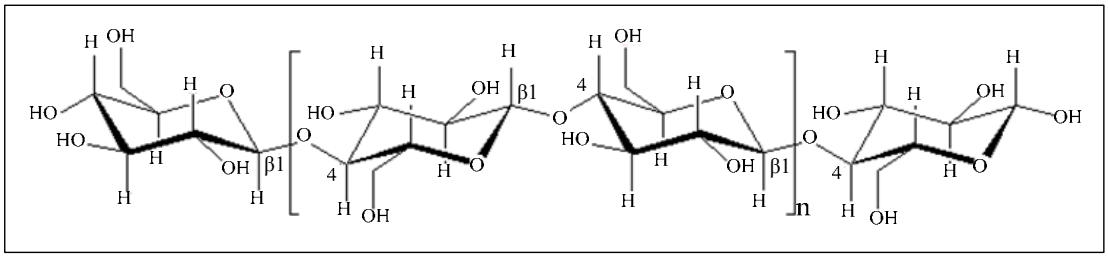

**Figure 1.2** Cellulose structure (Mohanty et al., 2005).

Hemicelluloses are polysaccharides composed of a combinanation of 5- and 6-ring carbon ring sugars. The polymer chains are much shorter and branched, containing pendant side groups giving rise to its noncrystalline nature. Hemicelluloses form the supportive matrix for cellulose microfibrils. Hemicelluloses are very hydrophilic and soluble in alkali and easily hydrolyzed in acid.

During the biological synthesis of plant walls, polysaccharide such as cellulose and hemicelluloses are produced, and simultaneously lignin fills the spaces between the polysaccharide fibers, cementing them together. This lignification process causes a stiffening of cell walls, and the carbohydrate is protected from chemical and physical damage. A probable structure of lignin is represented in Figure 1.3. Although the exact mode of linkages of lignin with cellulose in lignocellulosic natural fiber is not well known, lignin is believed to be linked with the carbohydrate through two types of linkages, one alkali sensitive and the other alkali resistant. The alkali sensitive linkages forms an ester-type combination between lignin hydroxyls and carboxyls of hemicellulose uronic acid.

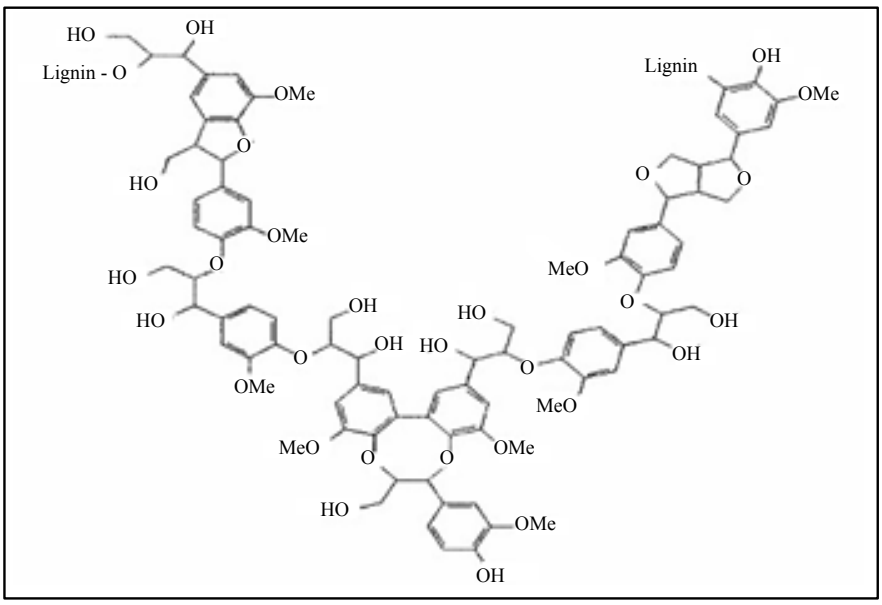


**Figure 1.3** Lignin structure (Mohanty et al., 2005).

Waxes make up the part of the fiber, which can be extracted with organic solutions. These waxy materials consist of different types of alcohols, which are insoluble in water as well as in several acids (palmitic acid, oleaginous acid, stearic acid) (Bledzki and Gassan, 1999).

The mechanical properties of plant fibers are much lower when compared to those of the most widely used competing reinforcing glass fibers. However, a value of low density, the specific properties, strength, and stiffness plant fibers were high compared to the glass fibers. Moreover, natural fibers have several advantages, such as low cost, ease of separation, biodegradability, renewability, recyclability and locally availability (Lee and Wang, 2006).

## 1.2 Vetiver grass

In order to expand the use of agro-fibers for composites, it is useful to have the information on fiber characteristics and the factors, which affect performance of the fiber. Vetiver grass (*Vetiveria zizanioides*) as shown in Figure 1.4 belongs to the same grass family as maize, sorghums, sugarcane and lemon grass. Vetiver grass is well known as a useful plant for erosion control. Chemical composition, the physical and mechanical properties of vetiver fiber are shown in Table 1.1 and 1.2, respectively. In Thailand, His Majesty the King Bhumipol Adulyadej has initiated and supported the use of vetiver grass for soil and water conversation since 1991. Various activities on other applications of this grass have been promoted since then. Normally, leaves of the vetiver grass are cut every few months to keep vetiver row in order and left as a residue. Only a miner portion of the residues is reserved as animal feed or household fuel. On the other hand, huge quantities of the remaining residues are burnt in fields or on the side of road. To help farm gains some extra incomes from the residue has been an interesting. Moreover, the advantages of vetiver grass include their low cost, low density, biodegradability and renewability. Therefore, investigations aiming to improve the value of such residue are challenging attempts (Somnuk, U., Eder, G., Phinyocheep, P., Suppakarn, N., Sutapun, W., and Ruksakulpiwat, Y., 2007).

**Figure 1.4** Photograph of vetiver grass (*Vetiveria zizanioides*)

**Table 1.1** Chemical composition of vetiver fiber after treated with 1% (wt/v) NaOH for five days (Ruksakulpiwat, Y., Suppakarn, N., Sutapun, W., and Thomthong, W., 2007).

| **Chemical compositions** | **Vetiver fiber (wt%)** |
|---|---|
| C | 97.30 |
| $SiO_2$ | 1.17 |
| $K_2O$ | 0.21 |
| $P_2O_5$ | 0.12 |
| $SO_3$ | 0.05 |
| $Al_2O_3$ | 0.05 |
| MgO | 0.07 |
| Cl | 0.02 |
| MnO | 0.04 |
| $Na_2O$ | 0.01 |
| Others | 0.07 |

**Table 1.2** The physical and mechanical properties of vetiver fiber after treated with 1% (wt/v) NaOH for five days (Ruksakulpiwat, Y., et al., 2007).

| Properties | Vetiver fiber |
|---|---|
| Density (g/cm$^3$) | 1.5 |
| Diameter (μm) | 100-200 |
| Tensile strength (MPa) | 247-723 |
| Young's modulus (GPa) | 12.0-49.8 |
| Elongation at break (%) | 1.6-2.4 |

## 1.3 Polylactic acid (PLA)

With increasing demands on renewable resources for consumer products, the use of biodegradable materials is of high interest. Traditional polymeric materials derived from petro-chemical sources do not degrade and the disposal of such materials is of concern (Wong et al., 2007). In recent years, the development of biocomposites from biodegradable polymers and natural fibers have attracted great interests in the composite science, because they could allow complete degradation in soil or by composting process and do not emit any toxic or noxious components (Lee and Wang, 2006). Plastic materials produced from petrochemicals are widely used in packaging, automotive, healthcare application, and communication or electronic industries. As these conventional synthetic polymers are not easily degraded because of their high molecular mass and hydrophobic character. They may accumulate in the environment and represent a significant source of environmental pollution potentially harming wildlife (Iovin, Zullo, Rao, Cassar, and Gianfreda, 2008).

Polylactic acid (PLA) is the first commodity polymer produced from annually renewable resources. The benefits of PLA included low energy to produce and

reduced green house gas production. Moreover, it has high-strength, high-modulus polymer that can be made from renewable resources to yield articles for use in either the industrial packaging field or the biocompatible/bioabsorbable medical device market. It is one of the few polymers in which the stereochemical structure can easily be modified by polymerizing a controlled mixture of the L- or D-isomers to yield high molecular-weight amorphous or crystalline polymers (Garlotta, 2001). It is a rigid polymer that can be semicrystalline or totally amorphous, depending on the stereopurity of the polymer backbone (Mohanty et al., 2005).

In order to PLA to be processed on large-scale production lines in applications such as injection molding, blow molding, thermoforming, and extrusion, the polymer must possess adequate thermal stability to prevent degradation and maintain molecular weight and properties. PLA degradation is dependent on time, temperature, low-molecular-weight impurities, and catalyst concentration. Catalysts and oligomers decrease the degradation temperature and increase the degradation rate of PLA. In addition, they can cause viscosity and rheological changes during processing, and poor mechanical properties (Garlotta, 2001).

The basic building block for PLA was lactic acid. Lactic acid (2-hydroxy propionic acid) is the simplest hydroxyl acid with an asymmetric carbon atom and exists in two optically active configurations. L(+) and D(–) lactic acids, as a consequence of the presence of the hydrogen atom connected to an asymmetric carbon atom. The L- isomer is produced in humans and other mammals, whereas both the D- and L- enantiomers are produced in bacterial systems. Poly(L(+) lactic acid) (PLLA) is synthesized by two methods: (1) the polymerisation of L-lactide (cyclic dimer of lactic acid) and (2) the polycondensation of L(+) lactic acid (LA), which is carried out

in the bulk or in solution. The best results of polycondensation of L(+) lactic acid in solution were obtained using diphenyl ether as the solvent. The temperature of the synthesis of poly (L(+) lactic acid) should not exceed 140°C (Dutkiewicz, Grochowska-Lapienis and Tomaszewski, 2003). The synthesis of D-lactic acid from rice by fermentation using microorganisms were describes by Lee (2005). Some microorganisms were found to be active for producing D-lactic acid of high optical purity after an intensive screening test for D-lactic acid bacteria using glucose as substrate. Rice powder was hydrolyzed with a combination of enzymes: α-amylase, β-amylase, and pullulanase, and the resultant rice saccharificate were subjected to the fermentation with the selected D-lactic acid bacteria.

The majority of the world's commercially produced lactic acid is made by the bacterial fermentation of carbohydrates, using homolactic organisms such as various optimized or modified strains of the genus *Lactobacilli*, which exclusively form lactic acid. The organisms that predominantly yield the L -isomer are *Lactobacilli amylophilus, L. bavaricus*, *L. casei*, *L. maltaromicus*, and *L. salivarius*. Strains such as *L. delbrueckii*, *L. jensenii*, or *L. acidophilus* yield the D-isomer or mixtures of both (Hartmann, 1998).

Commercial fermentation is usually conducted in a batch process, which takes three to six days to complete. Sugar concentrations of 5–10% are used, which give the production rates of 2 grams of acid per 1 liter of broth per hour. A high final lactic acid concentration is desired in the final broth to give the greatest process efficiencies, but high concentrations lead to lactic acid toxicity and growth inhibition. The method of separation of the produced acid consists of adding calcium hydroxide or calcium

carbonate to neutralize the fermentation acid and give soluble calcium lactate solutions. This calcium lactate broth is filtered to remove the cell biomass and other insoluble, then evaporated, recrystalllized, and acidified with sulfuric acid to yield the crude lactic acid. Higher purity is obtained by distillation of the acid as the methyl or ethyl ester, followed by hydrolysis back to the acid (Garlotta, 2001).

The synthesis of lactic acid into high-molecular weight PLA can follow two different routes of polymerization, as depicted in Fig. 1.6. Lactic acid is condensation polymerized to yield a low-molecular-weight, brittle, glassy polymer, which, for the most part, is unusable for esterification of any applications unless external coupling agents are used to increase the molecular weight of the polymer. The molecular weight of this condensation polymer is low due to the viscous polymer melt, the presence of water, impurities, the statistical absence (low concentration) of reactive end-groups, and the "back-biting" equilibrium reaction that forms the six-member lactide ring. The second route of producing PLA is to collect, purify, and ring-open polymerize (ROP) lactide to yield high-weight average molecular weight ($M_w$ > 100,000) PLA. The lactide method is the only method of producing pure, high-molecular-weight PLA until Mitsui Toatsu Chemicals recently commercialized a process wherein lactic acid and catalyst are azeotropically dehydrated in a refluxing, high-boiling, aprotic solvent under reduced pressures to obtain PLA with weight-average molecular weights greater than 300,000 (Garlotta, 2001).

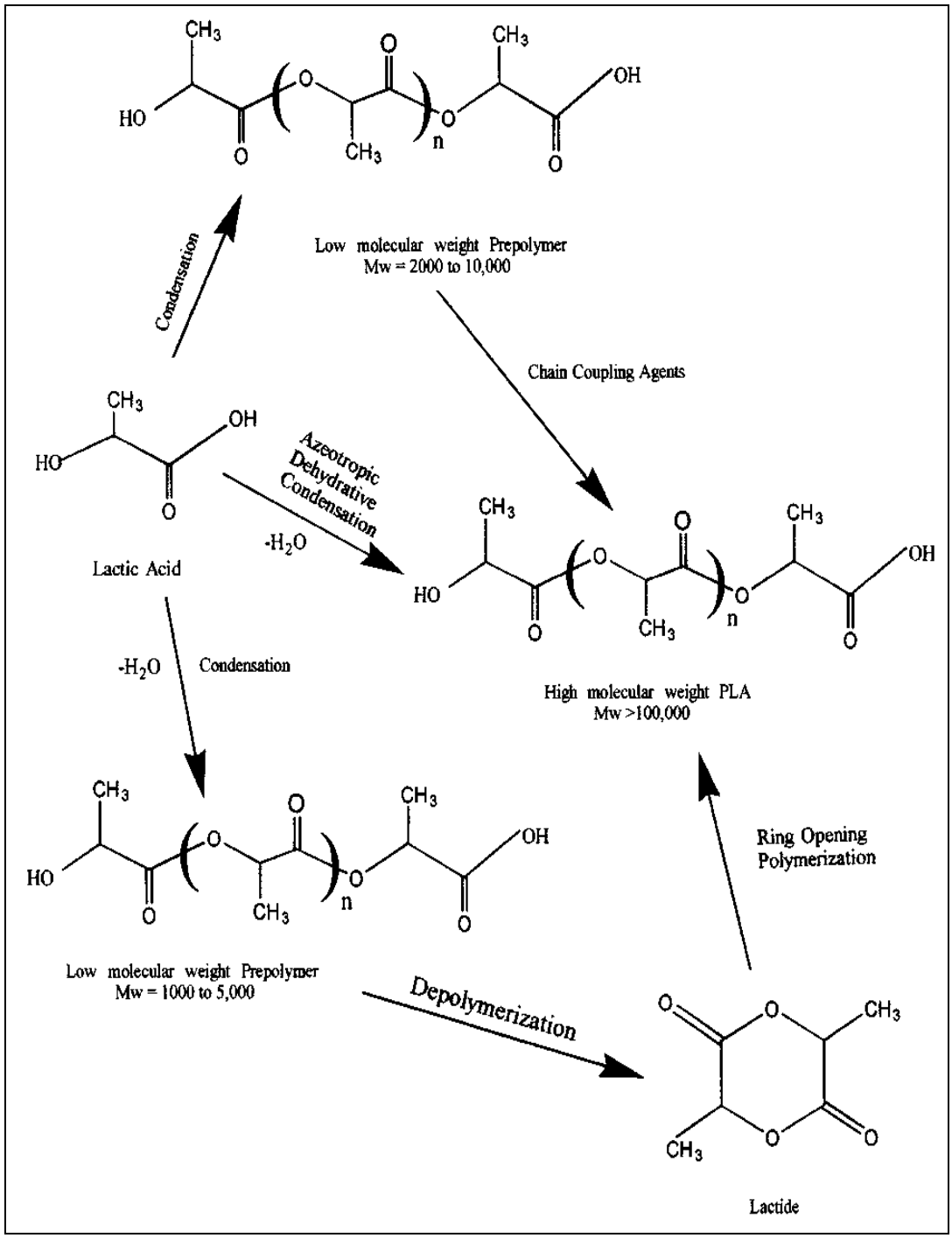


**Figure 1.5** Synthesis methods for high-molecular-weight PLA

(Hartmann, 1998)

The synthesis of lactic acid into high-molecular weight PLA can follow two different routes of polymerization, as depicted in Fig. 1.5. Lactic acid is condensation polymerized to yield a low-molecular-weight, brittle, glassy polymer, which, for the most part, is unusable for esterification of any applications unless external coupling agents are used to increase the molecular weight of the polymer. The molecular weight of this condensation polymer is low due to the viscous polymer melt, the presence of water, impurities, the statistical absence (low concentration) of reactive end-groups, and the "back-biting" equilibrium reaction that forms the six-member lactide ring. The second route of producing PLA is to collect, purify, and ring-open polymerize (ROP) lactide to yield high-weight average molecular weight ($M_w$ > 100,000) PLA. The lactide method was the only method of producing pure, high-molecular-weight PLA until Mitsui Toatsu Chemicals recently commercialized a process wherein lactic acid and catalyst are azeotropically dehydrated in a refluxing, high-boiling, aprotic solvent under reduced pressures to obtain PLA with weight-average molecular weights greater than 300,000 (Garlotta, 2001).

The self-condensation of lactic acid results in a low-molecular- weight product with an equimolar concentration of hydroxyl and carboxyl end-groups. To increase the molecular weight, chain-coupling agents must be added, and these will preferentially react with either the hydroxyl or carboxyl group, which leads to different kinetic reaction rates of coupling. The condensed PLA can be modified to produce either all hydroxyl or all carboxyl groups.

The azeotropic condensation polymerization is a method to obtain high-molecular-weight polymer without the use of chain extenders or adjuvant. Copolymers using various diacids, diols, or hydroxy-acids are possible with molecular the use of

solvents and residual catalyst the main draw-puribacks. A general procedure for this route consists of reduced pressure distillation of lactic acid for 2 to 3 hours at 130°C to remove the majority of the condensation water. Catalyst and diphenyl ether are added; then a tube packed with 3-A° molecular sieves is attached to the reaction vessel. The refluxing solvent is returned to the vessel by way of the molecular sieves for additional 30 – 40 hours at 130°C. The polymer can then be isolated as is or dissolved and precipitated for further purification.

Various esterification-promoting adjuvant and chain-extending agents have been reported that they can be used to increase the molecular weight of the PLA condensation products. Some examples of the esterification promoting adjuvents are bis(trichloromethyl) carbonate, dicyclohexylcarbodiimide, and carbonyl diimidazole. These adjuvant produce reaction byproducts that must be either neutralized or removed. Bis(trichloromethyl) carbonate creates hydrochloric acid, which can degrade the polymer, or dicyclohexylcarbodiimide forms unreactive and insoluble dicyclohexylurea, which can be filtered out during the final purification steps. The advantages of esterification-promoting adjuvents are that the final product is highly purified, free from residual metals, catalyst, and low-molecular-weight oligomers. The disadvantages are higher costs due to the increased number of reaction steps, the use of dangerous or flammable solvents, inability to form copolymers containing different functional groups, and the additional purification and separation steps of nonrecoverable byproducts

The ring-opening polymerization of lactide was first demonstrated by Carothers in 1932, but high molecular weights were not obtained until improved lactide purification techniques were developed by DuPont in 1954. Lactide is obtained by the

depolymerization of low molecular-weight PLA under reduced pressure to give a mixture of L-lactide, D-lactide, or meso-lactide. The different percentages of the lactide isomers form was depend on the lactic acid isomer feedstock, temperature, and catalyst (Hartmann, 1998).

**Table 1.3** Properties of some commercial PLA (NatureWork, 2005: Biomer, 2006).

| **Properties** | **NatureWork® PLA** | **Biomer® L9000** |
|---|---|---|
| Density (g/ml) | 1.24 | 1.25 |
| $T_g$ (°C) | 56.7 - 57.9 | n/a |
| $T_m$ (°C) | 140 - 152 | n/a |
| HDT (°C) | 40 - 45 (amorphous)<br>135 (crystalline) | n/a |
| Tensile strength (MPA) | 53 | 70 |
| Elongation (%) | 6 | 2.4 |
| Flexular Modulus (MPa) | 350 - 450 | 3,600 |

Poly (lactic acid) homopolymers have some properties as shown in Table 1.3. They require processing temperatures in excess of 185–190°C (Garlotta, 2001). $T_g$ and $T_m$ are strongly affected by overall optical composition, primary structure, thermal history, and molecular weight. Below $T_g$, PLA will only behave as a brittle polymer.

## 1.4 PLA composites

PLA is brittle polymer (Oksmana, Skrifvarsb, and Selinc, 2003). It needed modifications for more practical applications. The improvement of the properties of PLA is added of fillers or reinforcement material. Several studies have reported that

fillers such as talc sodium stearate calcium lactate (Li, 2007) and calcium metaphosphate (Junga et al., 2005) synthetic fibers such as glass fiber (Huda, Drzal, Mohanty, and Misra, 2006) man-made cellulose fiber (Ganster, Fink, and Pinnow, 2006) cabon (Kim, Chae, Park, Yoon, Kang, and Jin, 2007); (Kuana, Chena, Kuana, Lina, Chiangb, and Peng, 2008); (Tsuji, Kawashima, Takikawa, and Tanaka, 2007); organoclay (Day, Victoria, Nawaby, and Liao, 2006); (Krikorian and Pochan, 2004) and natural fibers such as kenaf (Huda et al., 2008); (Nishino, Hirao, and Kotera, 2003) flax (Wong et al., 2007) bamboo (Lee and Wang, 2006) coir (Iovino et al., 2008) jute (Hu, Lim, Kim, and Yoon, 2007); (Khondker, Ishiaku, Nakai, and Hamada, 2006) were used as reinforcement materials in PLA composites to enhance it's mechanical properties. For natural fibers, a major disadvantage of natural fibers is their hydrophilic character that makes them, in principle, immiscible with less polar or nonpolar polymers. Therefore, to develop such biocomposites with optimum properties, it has been customary to decrease the hydrophilicity of the lignocellulosic materials by chemical modification (Bledzki and Gassan, 1999) or to promote interfacial adhesion through the use of compatibilizers (Parka, Kima, and Kimb, 2003).

Generally, the properties of composites were affected by its crystallization behavior. Therefore, the studies on crystallization behavior of composites are significant. Previously, crystallization of PLA composites in the presence of nucleating agents was also studied (Li, 2007). Nucleating agent is a chemical substance which can form nuclei for the growth of crystals in the polymer melt. A nucleating agent has recognized that it influenced on the crystalline morphology. Usually, the crystallinity increased and the crystalline rate is accelerated with the nucleating agent effect (Xu, Lei, and Xie, 2003). Li (2007) found that talc was an effective nucleating agent for

PLA. In the same way, natural fibers were reported that they can induce crystal nucleation of polymers at the fiber surface, i.e. the so-called transcrystallinity effect in several polymer matrix such as PP (Choudhury, 2008), PE (Vaisman, Gonzalez, and Marom, 2003) and PHA (Dufresne, Kellerhals, and Witholt, 1999).

From the previous study, the vetiver grass was shown to be an effective filler in polypropylene (PP) composites. It was found that the presence of vetiver grass led to an increase in tensile strength and Young's modulus of PP composites (Ruksakulpiwat,Y., Suppakarn, N., Sutapun, W., and Thomthong, W., 2007). As mentioned above, PLA is biodegradable polymer while PP is not. Therefore, the use of PLA biopolymer in the composites instead of PP polymer is interesting. Moreover, the using of vetiver grass as a filler in PLA composites has never been published. Talc filled PLA composites were also prepared and their crystallization were compared with those of vetiver grass filled PLA composites.

## 1.5 Research objectives

The purpose of this research is to study the role of vetiver fiber on crystallization behavior of vetiver fiber-PLA biocomposite. Talc as a nucleating agent was used to compare the nucleating effecting between talc and vetiver fiber.

## 1.6 Scope and limitations of the study

In this study, vetiver grass and talc were used as fillers in PLA composites. Before used, vetiver grass was cut and modified by alkalization. The vetiver fiber-PLA and talc-PLA composites were prepared by mixing vetiver fiber or talc into PLA at 180°C in an internal mixer. The crystallization behavior of both composites was investigated. Sperulitic growth rate was determined by using a Hot Stage under a

Polarized Light Optical Microscope (POM). Glass transition temperature ($T_g$), melting temperature ($T_m$), crystallization temperature ($T_c$), equilibrium melting temperature ($T^o_m$) and degree of crystallinity of the composites were obtained by differential scanning calorimeter (DSC).

## 1.7 References

Bledzki, A. K., and Gassan, J. (1999). Composites reinforced with cellulose based fibres. **Prog. Polym. Sci.** 24: 221-274.

Choudhury, A. (2008). Isothermal crystallization and mechanical behavior of ionomer treated sisal/HDPE composites. **Mater. Sci. Eng.** 491: 492-500.

Day, M., Victoria, A., Nawaby, and Liao, X. (2006). A DSC study of the crystallization behavior of polylactic acid its nanocomposites. **J. Therm. Anal. Calorim.** 86: 623-629.

Dufresne, A., Kellerhals, M. B., and Witholt, B. (1999). Transcrystallization in Mcl-PHAs/Cellulose Whiskers Composites. Macromolecules. 32: 7396-7401.

Ganster, J., Fink, H.-P., and Pinnow, M. (2006). High-tenacity man-made cellulose fibre reinforced thermoplastics–Injection moulding compounds with polypro-pylene and alternative matrices. **Compos. Part A.** 37: 1796-1804.

Garlotta, D. ( 2001). A Literature Review of Poly(Lactic Acid). **J. Polym. Environ.** 9: 63-84.

Hartmann, M. H. (1998). **Biopolymers from Renewable Resources.** Berlin: Springer-Verlag.

Hongbo Li, M. A. H. (2007). Effect of nucleation and plasticization on the crystallization of poly(lactic acid). **Polymer.** 48:6855-6866.

Hu, R.-H., Lim, J.-K., Kim, C.-I., and Yoon, H.-C. (2007). Biodegradable Composites Based on Polylactic Acid(PLA) and China Jute Fiber. **Eng. Mater.** 353-358: 1302-1305.

Huda, M. S., Drzal, L. T., Mohanty, A. K., and Misra, M. (2006). Chopped glass and recycled newspaper as reinforcement fibers in injection molded poly(lactic acid) (PLA) composites: A comparative study. **Compos. Sci. Technol.** 66: 1813-1824.

Huda, M. S., Drzal, L. T., Mohanty, A. K., and Misra, M. (2008). Effect of fiber surface-treatments on the properties of laminated biocomposites from poly(lactic acid) (PLA) and kenaf fibers. **Compos. Sci. Technol.** 68: 424-432.

Iovino, R., Zullo, R., Rao, M. A., Cassar, L., and Gianfreda, L. (2008). Biodegradation of poly(lactic acid)/starch/coir biocomposites under controlled composting conditions. **Polym. Degrad. Stab.** 93: 147-157.

Junga, Y., Kim, S.-S., Kim, Y., Kim, S.-H., Byung-Soo Kimb, SukyoungKim, YongChoi, C., and Kim, S. H. (2005). A poly(lactic acid)/calcium metaphosphate composite for bone tissue engineering. **Biomaterials.** 26: 6314-6322.

Khondker, O. A., Ishiaku, U. S., Nakai, A., and Hamada, H. (2006). A novel processing technique for thermoplastic manufacturing of unidirectional composites reinforced with jute yarns. **Compos. Part A.** 37: 2274-2284.

Kim, H.-S., Chae, Y. S., Park, B. H., Yoon, J.-S., Kang, M., and Jin, H.-J. (2007). Thermal and electrical conductivity of poly(L-lactide)/multiwalled carbon nanotube nanocomposites. **Current Applied Physics**.

Krikorian, V., and Pochan, D. J. (2004). Unusual Crystallization behavior of organoclay reinforced poly(L-lactic acid) nanocomposites. **Macromolecules.** 37: 6480-6491.

Kuana, C.-F., Chena, C.-H., Kuana, H.-C., Kun-Chang Lina, Chiangb, C.-L., and Peng, H.-C. (2008). Multi-walled carbon nanotube reinforced poly (L-lactic acid) nanocomposites enhanced by water-crosslinking reaction. **J. Phys. Chem. Solids.** 69: 1399-1402.

Lee, S.-H., and Wang, S. (2006). Biodegradable polymers/bamboo fiber biocomposite with bio-based coupling agent. **Compos. Part A.** 37: 80-91.

Mohanty, A. K., Misra, M., and Drzal, L. T. (2005). **Natural fiber, Biopolymer, and Biocomposites.** Boca Raton: Taylor & Francis Group.

Nishino, T., Hirao, K., and Kotera, M. (2006). X-ray diffraction studies on stress transfer of kenaf reinforced poly(L-lactic acid) composite. **Compos. Part A.** 37: 2269-2273.

Nishino, T., Hirao, K., Kotera, M., Nakamae, K., and Inagaki, H. (2003). Kenaf reinforced biodegradable composite. **Compos. Sci. Technol.** 63: 1281-1286.

Oksmana, K., Skrifvarsb, M., and Selinc, J.-F. (2003). Natural fibres as reinforcement in polylactic acid (PLA) composites. **Compos. Sci. Technol.** 63: 1317-1324.

Parka, J.-M., Kima, D.-S., and Kimb, S.-R. (2003). Interfacial properties and microfailure degradation mechanisms of bioabsorbable fibers/poly-l-lactide composites using micromechanical test and nondestructive acoustic emission. **Compos. Sci. Technol.** 63: 403-419.

Ruksakulpiwat, Y., Suppakarn, N., Sutapun, W., and Thomthong, W. (2007). Vetiver–polypropylene composites: Physical and mechanical properties **Compos. Part A.** 38: 590-601.

Somnuk, U., Eder, G., Phinyocheep, P., Suppakarn, N., Sutapun, W., and Ruksakulpiwat, Y. (2007). Quiescent crystallization of natural fiber-polypropylene composites. **J. Appl. Polym. Sci.** 106: 2997-3006.

Tsuji, H., Kawashima, Y., Takikawa, H., and Tanaka, S. (2007). Poly(L-lactide)/nano-structured carbon composites: Conductivity, thermal properties, crystallization, and biodegradation. **Polymer.** 48: 4213-4225.

Vaisman, L., Fernanda Gonzalez, M., and Marom, G. (2003). Transcrystallinity in brominated UHMWPE fiber reinforced HDPE composites: morphology and dielectric properties. **Polymer.** 44: 1229-1235

Wong, S., Shanks, R. A., and Hodzic, A. (2007). Effect of additives on the interfacial strength of poly(L-lactic acid) and poly(3-hydroxy butyric acid)-flax fibre composites. **Compos. Sci. Technol.** 67: 2478-2484.

Xu, T., Lei, H., and Xie, C. S. (2003). The effect of nucleating agent on the crystalline morphology of polypropylene (PP). **Mater. Des.** 24: 227-230.

# CHAPTER II

# LETURATURE REVIEW

## 2.1 Crystallization behavior of PLA and PLA composites

PLA is attracting much attention, particularly from the ecological point of view due to the producibility from renewable resources. Because of its biodegradable property, PLA is expected to be used for medical devices, such as controlled drug release matrices. It is known that the rate of hydrolytic degradation of PLA is strongly affected by the degree of crystallinity. Therefore, it is well expected that the solid-state structure including a crystalline lamellar organization plays an important role for controlling the degradation rate. The study on the crystallization of PLA is, thus, of great importance not only from the academic interest but also from the engineering viewpoint. It is well-known that the physical properties of semicrystalline polymer are strongly affected by the solid-state structure, such as crystallinity, crystalline form, and morphology. The properties change upon heating according to structural changes, including lamellae thickening, crystal transformation, and melting.

Crystallization kinetic of PLLA was analyzed by many researchers (Kalb and Pennings, 1980); (Kawai et al., 2007); (Lorenzo, 2005); (Vasanthakumari and Penning, 1983); (Yasuniwa et al., 2006). From the curve of radius growth rate (G), as a function of crystallization temperature ($T_C$), Kawai and co-worker found that the value of G increased with $T_C$, and after reaching the maximum it then decreased with increasing

$T_c$ (Kawai et al., 2007). This result is similar to that of Vasanthakumari and Penning. However, the spherulite growth rate curve shown discontinuity, first maximum at around 130°C and a second at around 105°C (Kawai et al., 2007). The appearance of the discontinuity is reported to be dependent on the molecular weight, tacticity, and species for copolymerization. Most possible explanation might be the difference in the crystal modification (Kawai et al., 2007); (Lorenzo, 2005); (Yasuniwa et al., 2006-2008). Three crystalline forms (α, *β*, and *γ*) have been reported for PLLA. Crystallization from the melt or from solution leads to α form crystal, which is the most common polymorph. In the α form, two chains with $10_3$ helical conformation are packed into an orthorhombic unit cell with dimensions of $a$ = 10.7 Å, $b$ = 6.45 Å, and $c$ (fiber axis) = 27.8 Å. The second phase, *β* form, is obtained under high drawing conditions and high temperatures, containing three chains in a trigonal unit cell with $a = b$ = 10.52 Å and $c$ = 8.8 Å. A third crystal modification, *γ* form, was obtained via epitaxial crystallization on hexamethylbenzene substrate. It has two antiparallel $3_1$ helices packed in an orthorhombic unit cell with $a$ = 9.95 Å, $b$ = 6.25 Å, and $c$ = 8.8 Å. Recently, Kawai and coworker reported a new crystalline form with hexagonal packing, namely, the α′ form. Moreover they found that the crystal structure changes between α′ form and α form at around 150ºC led to the discontinuity of the spherulite growth rate (Kawai et al., 2007). In addition, melting behavior of PLLA was also studied with X-ray by Yasuniwa et al. (2008). It was elucidated from the change in the X-ray diffraction pattern that the phase transition from the low-temperature ($T_c \leq T_b$) crystal modification (α′-form) to the high temperature ($T_b \leq T_c$) one crystal modification (α -form) occurred in a range 155-165 °C. Besides, Yasuniwa and co-worker reported $T_c$ dependence of log peak

crystallization time ($\tau_p$) discretely changed at 113°C (refered as boundary temperature, $T_b$). Meanwhile, the $T_c$ dependence of G and the size of the spherulite also discretely changed at $T_b$. They suggested that the crystal structure discretely changes at $T_b$ between orthorhombic crystal modification (α-form) and trigonal (β-form) (Yasuniwa et al., 2006). The discontinuity in spherulite growth rate curve was also reported by Lorenzo. He found that crystallization rate of PLLA was very high at temperatures between 100 and 118°C and a discontinuity was observed around 116–118°C. This discontinuity has been ascribed to a sudden acceleration in spherulite growth. Moreover, the sudden change in crystallization rate may be due to growth in a different crystal modification (Lorenzo, 2005). The discontinuity in crystallization rate of PLLA has also been correlated with a transition in crystallization regime. Crystallization regime II–III transition temperature around 130°C was reported by Lorenzo (2005). Vasanthakumari and Penning (1983) also reported the boundary temperature between regime I and regime II about 163°C. Yasuniwa and co-worker also studied the effects of $T_c$ and time on the melting behavior of PLLA. They found that when $T_c$ was lower than 135°C, the double melting peaks appeared. The melting behavior, especially $T_c$ dependence of the melting temperature ($T_m$), discretely changed at 113°C, in accordance with the discrete change of the crystallization behavior at 113°C. When $T_c$ was higher than 135°C, a single melting peak appeared. In addition, $T_c$ dependence of $dT_m/dT_c$ discretely changed at 135°C. That is, the melting behavior, especially $T_c$ dependence of $T_m$ and $dT_m/dT_c$, are different in three temperature regions of $T_c$ divided by 113°C and 135°C Regions I ($T_c \leq 113$°C), II (113°C $\leq T_c \leq$ 135°C), and III (135°C $\leq T_c$) (Yasuniwa et al., 2007).

The growth rate results for samples of different molecular weight were also studied by Vasanthakumari and Penning (1983). It is clear that the growth rate increases with the decrease of molecular weight. In addition, Wang and Mano (2005) reported in the case of lower-molecular-weight PLLA ($M_n$ = 86,000) that a single exothermic peak could be observed at cooling rate of 2ºC/min. The obtained peak temperature and degrees of crystallinity dramatically increased with an increase of melting temperature or time. It may be attributed to the degradation of PLLA. With the increasing of prior melting temperature or time, the molecular weight of PLLA could decrease, which results in the increase of the degrees of crystallinity of PLLA obtained after cooling. Double cold crystallization peaks are observed in the DSC traces during heating for PLLA ($M_n$ = 86,000) obtained from fast cooling (at 20 °C/min). Double melting behaviors were observed and it was suggested that the low-temperature and high-temperature peaks were attributed to the melting of some amount of the original crystals and the melting of crystals formed through the melt/re-crystallization process, respectively. The competition between the crystallization from the nuclei remained after cooling, and the crystallization from spontaneous nucleation may be responsible for the appearance of double peaks. They also found that the influence of the melting conditions on the thermal behaviors of PLLA is also dependent on its initial molecular weight. For example, for a higher molecular weight PLLA ($M_n$ = 269,000), a double exothermic peak appears during cooling processes.

The equilibrium melting temperature of PLLA was determined by Kalb and Pennings (1980) and Vasanthakumari and Pennings (1983) and found to be about 215ºC and 207ºC, respectively.

The effects of incorporated poly (D-lactic acid) (PDLA) as PLA stereo complex crystallites on the crystallization behavior of PLLA were investigated by Tsuji and co-worker. In isothermal crystallization from the melt, the radius growth rate of PLLA spherulite (crystallization temperature ($T_c$) ≥125 °C), the induction period for PLLA spherulite formation ($t_i$) ($T_c$ ≥125 °C), the growth mechanism of PLLA crystallites (90 °C ≤ $T_c$ ≤ 150 °C) were not affected by the incorporation of PDLA or the presence of stereocomplex crystallites as a nucleating agent. By contrast, the presence of stereocomplex crystallites significantly increased the number of PLLA spherulites per unit area or volume. In isothermal crystallization from the melt, at PDLA content of 10 wt%, the starting, half, and ending times for overall PLLA crystallization ($t_c$(S), $t_c$(1/2), and $t_c$(E), respectively) were much shorter than those at PDLA content of 0 wt%, due to the increased number of PLLA spherulite . Reversely, at PDLA content of 0.1 wt%, the $t_c$(S), $t_c$(1/2), and $t_c$(E) were longer than or similar to those at PDLA content of 0 wt%, probably due to the long $t_i$ and the decreased number of spherulites. This seems to have been caused by free PDLA chains, which did not form stereocomplex crystallites. In the non-isothermal crystallization of as-cast or amorphous-made PLLA films during cooling from the melt, the addition of PDLA above 1 wt% was effective to accelerate overall PLLA crystallization (Tsuji et al., 2006). While Yuryev et al. (2008) measured spherulite growth rates of poly (L/D-lactide) in the range of 100-160°C and of PLLA in the range of 100-170°C. Extremely short induction time was observed in both cases. It can be noted that there is very short nucleation time in all polylactide samples and a very fast heating allows crystallization without delay. PLLA exhibited a spherulite growth rate about two times higher than that of poly (L/D-lactide). It is the 2% D-lactide repeat unit content in the poly (L/D-

lactide) which causes the decrease of the spherulite growth rate. The randomly distributed D-lactide repeat units create steric impediments during crystallization thus decreasing the overall spherulite growth rate (Yuryev et al., 2008).

Besides, the thermal properties of plasticized PLA with modified and unmodified clays were studied by Paul and co-worker. DSC analyses have shown that the nature of the clay does not affect the glass transition temperature or the melting temperature of the PLA matrix, except for the modified clays based composite where a slight decrease in both $T_g$ and $T_m$ can be detected (Paul et al., 2003). In addition, Krikorian and Pochan (2004) studied the effect of organically modified montmorillonite clay addition on crystallization of a polymer matrix. Two types of commercially available organoclays with different extent of miscibility with a polymer matrix were employed, leading to fully exfoliated (high miscibility) and intercalated (low miscibility) nanocomposite morphologies. Bulk kinetics studies and radial spherulite growth rates indicate that when a high degree of filler polymer matrix miscibility is present, nucleation properties of the organoclay are low relative to the less miscible organoclay. Therefore, the overall bulk crystallization rate was increased in the intercalated system and somewhat retarded in the exfoliated system. Spherulite growth rates were significantly increased relative to the bulk in the fully exfoliated nanocomposite. This phenomenon, linked with less effective nucleation properties, resulted in significantly bigger spherulite sizes in the exfoliated nanocomposite. The overall percent of crystallinity and the size of crystalline domains decreased by the addition of organoclay and are the lowest in the fully exfoliated case.

Crystallization and melting behavior of the chopped glass fiber- and recycled newspaper cellulose fiber (RNCF) - reinforced PLA composites were studied by Huda

et al. (2006). The $T_g$ and $T_m$ of the composites do not change significantly with the addition of RNCF to the PLA matrix. They suggest that RNCF do not significantly affect the crystallization properties of the PLA matrix. The melting enthalpy ($\Delta H_m$), crystallization enthalpy ($\Delta H_c$) and $T_c$ of the PLA composites decreased for the presence of RNCF. The crystallization temperature of the RNCF reinforced composite decreases, which signifies that the fibers hinder the migration and diffusion of PLA molecular chains to the surface of the nucleus in the composites. This result is similar to report of Paul et al. (2003). They also found that the $\Delta H_m$, $\Delta H_c$ and $T_c$ of the PLA composite decreases in the presence of RNCF.

The effect of nucleation on the crystallization of PLA was studied by Li (2007). The effect of heterogeneous nucleation was assessed by adding talc, sodium stearate and calcium lactate as potential nucleating agents and 10 wt% acetyl triethyl citrate (ATC) and polyethylene glycol (PEG) as plasticizers. From this study, Li and Huneault found that talc was an effective nucleating agent while calcium lactate and sodium stearate had little or no nucleating ability. Polyethylene glycol (PEG) and acetyl triethyl citrate (ATC) were shown to be efficient plasticizers that increased the achieved crystallinity even at high cooling rates when used in combination with talc.

In addition, the effects of filler content and coupling treatment on thermal and mechanical properties of wood flour/talc-filled PLA composites were studied by Lee et al. (2008). The use of talc (10 wt%) in composites led to decreasing of $T_g$ and $\Delta H_c$. On the other hand, the addition of talc (10 wt%) and silane (1 and 3 wt%) to PLA/WF composites showed no significant effects on the $T_c$, $T_m$ and $\Delta H_m$ of composites. This result suggested that the addition of talc had resulted in tertiary interfaces in the composites and the added silane acted as a dispersing agent in the interfaces. In

contrast to the report of Paul et al. (2003) talc filled RNCF-reinforced PLA hybrid composites were studied. They found that when talc filled PLA hybrid composites do exhibit an increase in $T_g$ compared to neat PLA. These observations indicate that a higher $T_g$ consequently promotes a change from soft and flexible properties to hard and tough properties of the composites.

Besides, the addition of 1wt% silane to the PLA/WF/talc combinations led to higher $T_g$ values than those of the combinations with 3wt% silane. The higher $T_g$ of the composites with 1wt% silane could be ascribed to an improved interfacial adhesion between polymer matrix and fillers (Lee et al., 2008).

## 2.2 PLA/Natural fiber composites

Lee and Wang studied PLA/bamboo fiber composite by using lysine-diisocyanate (LDI) as a coupling agent. They found that crystallization temperature was increased and enthalpy decreased with increasing LDI content. The increase in $T_c$ could be due to the nucleation effect of the BF and LDI. In particular, the urethane linkage between polymer matrix and BF produced by the addition of LDI might further enhance nucleation of polymer matrix. The molecular motion of the polymer matrix could be restricted by the addition of LDI, resulting in a decrease of crystallization enthalpy, whereas there was no significant change in melting temperature (Lee and Wang, 2006).

In addition, Cheung and co-worker studied silk fibers reinforced PLA where crystallization and melting behavior of PLA and silk/PLA biocomposite were determined by DSC. It was found that the crystallization temperature ($T_c$) decreased with the addition of silk fibers. These results indicated that there were two main factors that control the crystallization of polymeric composite systems: (i) the

additives hinder the migration and diffusion of polymer molecular chains to the surface of the growing polymer crystal in the composites, thus providing a negative effect on polymer crystallization which results in a decrease in the $T_c$; (ii) the additives have a nucleating effect which gives a positive effect on polymer crystallization and leads to an increase in $T_c$ (Cheung et al., 2008).

Recently, the thermal properties of solvent cast biocomposites of poly (lactic acid) containing purified alfa micro-cellulose fibers were studied. It was found that the broad single melting peak of PLA is seen to become multiple in the biocomposites, which show two melting peaks with one of them having higher melting point than the neat biopolymer. This latter effect strongly reveals the nucleating role of the fibers, which are able to promote a more robust crystalline morphology (Sanchez-Garcia et al., 2008).

Degrees of crystallinity ($X_c$) of PLA were also investigated. Lee et al. (2008) presented the effect of filler on thermal properties of wood flour/talc-filled PLA composites. The large decrease in the $X_c$ of the composites with the addition of WF was observed. This may be caused by the partial inhibition effect of WF on polymer crystal formation. They also found that when wood flour content increased, double peaks were observed in DSC thermograms, and the $T_g$, $T_m$, $\Delta H_m$, $\Delta H_c$ decreased. Besides, the effect of fiber content on the crystallinity of PLA was also investigated by Tokoro et al. (2008). Two kinds of PLA/BF composites whose fiber fraction were 20% and 50% in weight were used. The crystallinities of PLA in those composites were 51% and 42%, respectively. It indicated that crystallinity of PLA in PLA/BF was affected insignificantly by the space of spherulites for crystal formation and growth.

## 2.3 Transcrystallization

Semi-crystalline polymers are usually reinforced with various types of organic or inorganic reinforcements like fibers to form composites with improved mechanical properties. It is well known that these reinforcements can result in changes in morphology and crystallinity of the interphase regions. Some of the substrates, especially fibers, may act as heterogeneous nucleating agents and nucleate crystallization along the interface with sufficiently high density of nuclei. These nuclei will hinder the lateral extension and force growth in one direction, namely perpendicularly to the fiber surfaces and result in a columnar crystalline layer, known as transcrystallinity (TC) or transcrystalline layers (TCL), with limited thickness (Quan et al., 2005).

### 2.3.1 Structure of transcrystallization

The structure of TC was studied in iPP fiber reinforced iPP composites. It was found that in one region close (<300 nm) to the fibers, lamellae exist very densely and the c-axes of the crystal lattices were oriented along the longitudinal direction of the fiber. In the other region, a little away (>300 nm) from the fiber, a cross-hatched structure composed of the parent lamellae (whose c-axes were parallel to the fiber surface) and the daughter lamellae (whose c-axes were perpendicular both to the fiber surface and the parent lamellae), was observed. A schematic illustration of the lamellae orientation near the fiber surface was shown in Figure 2.1 (Varga and Karger-Kocsis, 1995).

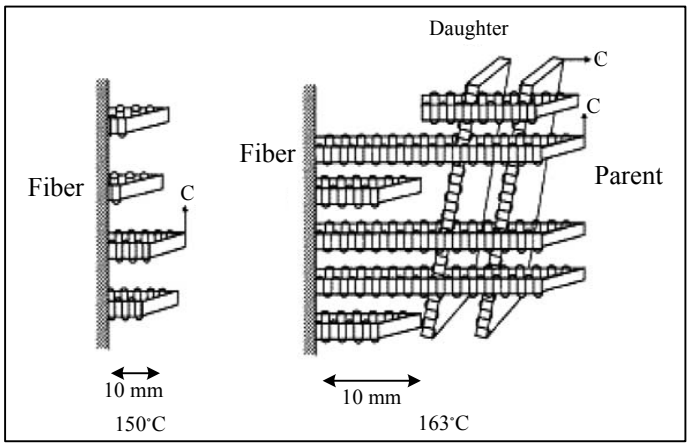


**Figure 2.1** Schematic illustration of lamellae orientation near the fiber surface (Varga and Karger-Kocsis, 1995).

### 2.3.2 Transcrystallization in PLA composites

Tokoro and co-worker studied a bamboo fiber (BF)/PLA. They found that when BF was put into PLA, crystallization of PLA was promoted in comparison with PLA only. Some papers show that natural fibers could also promote the crystallization of polymers on the surface of fillers as well as inorganic fillers. It is found that the surface topography of the fiber is the decisive factor on crystallinity development. In their study, which the result of surface topography of bamboo reinforcements in SEM photographs and result of crystallinity ($X_c$) of PLA in differential scanning calorimetry analysis (DSC). It was found that a low crystallinity ($X_c$) of PLA was obtained in the composite where smooth surface topography was observed at the BF. It is considered that the surface roughness of short bamboo fiber bundles was expected to initiate and growth of crystals in PLA/BF due to defects and imperfection of short bamboo fiber bundles. On the other hand, the effects of annealing on the thermal properties of PLA and BF/PLA composite were also studied by Tokoro et al. From the DSC thermograms of PLA and PLA/BF composites after

annealing, it was found that the endothermic peak of crystallization disappeared in all cases. The crystallinities ($X_c$) of PLA and PLA in PLA/BF composites after annealing increased when compared to that of neat PLA without annealing. It is known that the crystal formation is not initiated on the smooth surface of reinforcement. If a reinforcing fiber had a smooth surface, bulk crystallization occurred in many locations around the fiber. It has also been found that in composites with a high fiber volume fraction, transcrystallinity occurred only in the interface. Spherulites are not formed in the space between fibers because the distance between fibers is too short. PLA/BF composites in this study had high fiber content so that the bulk crystallization did not occur in small areas between fibers. The low crystallinity of PLA in PLA/BF composites was attributed to two reasons; smooth surface and high volume fraction of fiber reinforcement (Tokoro et al., 2008).

Besides, the crystallization at interface between PLA and N,N-Ethylenebis (1,2hydroxystearamide) (WX1) was observed. The well-developed layer of transcrystallite grown from WX1 surface is the evidence of the epitaxial crystallization of PLA in the presence of WX1 (Nam et al., 2006), while solvent cast composites of PLA and purified cellulose fibers were studied by Sanchez-Garcia and co-worker. The transcrystallinity event is not observable in the optical micrographs here, possibly because the crystallinity of the cast PLA samples is very low (Sanchez-Garcia et al., 2008).

## 2.4 Kinetics of crystallization

Crystallization occurs in two stages: nucleation and growth. The overall crystallization kinetics has been largely analyzed by the Hoffman and Lauritzen analysis (Vasanthakumari and Penning, 1983). Kinetic theories, as apposed to theories that emphasize the characterization of the equilibrium aspects of polymer crystal, are essential nucleation theories. These kinetic theories differ from classical nucleation theory in that the emphasis is not only on the formation of the nucleus but also on its subsequent growth. The well-established Hoffman and Lauritzen theory has been used to quantify the isothermal crystallization kinetics because of the applicability and straightforward quantitative nature of the theory.

Under normal circumstances, flexible linear molecules crystallize into the form of thin platelets whose upper and lower surface consist of an array of molecular folds. These folded structures in polymer crystallizing from the melt are referred to as "chain folded lamellae" These lamellas grow to from sperulites, so commonly encountered in crystallized linear polymers. The growth rate of Hoffman and Lauritzen theory is based on surface or secondary nucleation theory. The following treatment does not consider the fluctuations of the fold but still predicts growth rates over a wide range of supercooling. The Hoffman and Lauritzen growth rate equation was given as (Hoffman et al., 1976):

$$G(T) = G_o \exp\left[\frac{-U^*}{R(T_c - T_\infty}\right] \exp\left[\frac{-K_g}{T_c(\Delta T) f}\right] \tag{2.1}$$

Where G(T) is the radial growth rate.

$G_0$ is the pre-exponential factor containing quantities not strongly dependent on temperature.

$U^*$ is a universal constant characteristic of the activation energy of chain motion (reptation) in the melt.

R is a gas constant.

$K_g$ is the nucleation constant.

$T_\infty$ is the theoretical temperature at which all motion associated with viscous flow or reptation ceases, and is defined as $T_\infty = T_g - 30$ (K).

$f$ is the correction factor $f = 2T_C /(T°_m + T_c)$, which account for the temperature dependence of $\Delta h_f$, $f$ has little effect at small supercoolings, but decrease $\Delta h_f$ considerarable near the glass transition temperature.

$T°_m$ is the equilibrium melting temperature.

$\Delta T$ is the supercooling and is equal to $T°_m - T_C$

## 2.5 References

Cheung, H.-Y., Lau, K.-T., Tao, X.-M., and Hui, D. (2008). A potential material for tissue engineering: Silkworm silk/PLA biocomposite. **Comp. Part B: Eng.** 39: 1026-1033.

Hoffman, J. D., Davis, G. T., and Lauritzen, L. I. (1976). **Treatise on solid state chemistry: Crystalline and non-crystalline solids** *Vol. 3*. New York: In: Hannay JB Editor.

Kawai, T., Rahman, N., Matsuba, G., Nishida, K., Kanaya, T., Nakano, M., Okamoto, H., Kawada, J., Usuki, A., Honma, N., Nakajima, K., and Matsuda, M. (2007).

Crystallization and melting behavior of poly (L-lactic acid). **Macromolecules.** 40: 9463-9469.

Krikorian, V., and Pochan, D. J. (2004). Unusual Crystallization Behavior of Organoclay Reinforced Poly(L-lactic acid) Nanocomposites. **Macromolecules.** 37: 6480-6491.

Lee, S.-H., and Wang, S. (2006). Biodegradable polymers/bamboo fiber biocomposite with bio-based coupling agent. **Compos. Part A.** 37: 80-91.

Lee, S.-Y., Kang, I.-A., Doh, G.-H., Yoon, H.-G., Park, B.-D., and Wu, Q. (2008). Thermal and Mechanical Properties of Wood Flour/Talc-filled Polylactic Acid Composites: Effect of Filler Content and Coupling Treatment. **J. Thermo. Compos. Mater.** 21, 209-223.

Lorenzo, M. L. D. (2005). Crystallization behavior of poly (L-lactic acid. **Euro. Polym. J.** 41: 569-575.

Nam, J. Y., Okamoto, M., Okamoto, H., Nakano, M., Usuki, A., and Matsuda, M. (2006). Morphology and crystallization kinetics in a mixture of low-molecular weight aliphatic amide and polylactide. **Polymer.** 47: 1340-1347.

Paul, M.-A. l., Alexandre, M. l., Dege´e, P., Henrist, C., Rulmont, A., and Dubois, P. (2003). New nanocomposite materials based on plasticized poly(L-lactide) and organo-modified montmorillonites: thermal and morphological study. **Polymer.** 44: 443-450.

Quan, H., Li, Z.-M., Yang, M.-B., and Huang, R. (2005). On transcrystallinity in semi-crystalline polymer composites. **Compos. Sci. Technol.** 65: 999-1021.

Sanchez-Garcia, M. D., Gimenez, E., and Lagaron, J. M. (2008 ). Morphology and barrier properties of solvent cast composites of thermoplastic biopolymers and purified cellulose fibers. **Carbo. Polym.** 71: 235-244.

Tokoro, R., Vu, D. M., Okubo, K., Tanaka, T., Fujii, T., and Fujiura, T. (2008). How to improve mechanical properties of polylactic acid with bamboo fibers. **J. Mater. Sci.** 43: 775-787.

Tsuji, H., Takai, H., and Saha, S. K. (2006). Isothermal and non-isothermal crystallization behavior of poly(L-lactic acid):Effects of stereocomplex as nucleating agent. **Polymer.** 47: 3826-3837

Varga, J., and Karger-Kocsis, J. (1995). Interfacial morphologies in carbonfiber-reinforced polypropylene microcomposites. **Polymer.** 36: 4877-4881.

Vasanthakumari, R., and Penning, A. J. (1983). Crystallization kinetics of poly(L-lactic acid). **Polymer.** 24:175-178.

Wang, Y., and Mano, J. o. F. (2005). Influence of melting conditions on the thermal behaviour of poly(L-lactic acid). **Europ. Polym. J.** 41: 2335-2342.

Yasuniwa, M., Iura, K., and Dan, Y. (2007). Melting behavior of poly(L-lactic acid): Effects of crystallization temperature and time. **Polymer.** 48: 5398-5407.

Yasuniwa, M., Tsubakihara, S., Iura, K., Ono, Y., Dan, Y., and Takahashi, K. (2006). Crystallization behavior of poly(L-lactic acid). **Polymer.** 47: 7554-7563.

Yuryev, Y., Wood-Adams, P., Heuzey, M.-C., Dubois, C., and Brisson, J. (2008). Crystallization of polylactide films: An atomic force microscopy study of the effects of temperature and blending. **Polymer.** 49: 2306-2320.

# CHAPTER III

# THE STUDY OF THERMAL PROPERTIES OF POLY (LACTIC ACID) AND POLY (LACTIC ACID) COMPOSITES

## 3.1 Abstract

In this work, vetiver fiber was used as a filler for poly (lactic acid) (PLA). The thermal properties of neat PLA and vetiver fiber-PLA composites were investigated by using a Differential Scanning Calorimeter (DSC). Talc as a nucleating agent was used to compare the nucleating effecting between talc and vetiver fiber. It was found that crystallization rate of talc-PLA composites was the highest among neat PLA and vetiver fiber- composites. Besides, the crystallization rate of PLA with 20% vetiver fiber content was higher than that of neat PLA and 1-10% (w/w) vetiver fiber-PLA composites. The equilibrium melting temperatures ($T_m^0$) of neat PLA and PLA composites were obtained from Hoffman-Weeks plot. It was found that the presence of vetiver fiber and talc caused $T_m^0$ values of PLA decreased compared to that of neat PLA. In addition, $T_m^0$ values of PLA decreased with increasing vetiver fiber content. For non-isothermal crystallization, it was found that an exothermic peak of vetiver fiber-PLA composite was not observed upon cooling. However, the exothermic peak appeared upon heating. The crystallization temperature of vetiver fiber-PLA composites decreased with increasing vetiver fiber content. This could be implied that

vetiver fiber acted as nucleating sites for PLA. In cases of talc-PLA composites, crystallization can be observed to take place during both heating and cooling process. The talc-PLA composites showed the lowest crystallization temperature compared to that of neat PLA and vetiver-PLA composites. In addition, a degree of crystallinity, $\%X_C$, increased with the presence of vetiver fiber compared to that of neat PLA. As vetiver fiber content was increased, $\%X_C$ increased. Similarly, the incorporation of talc led to an increase of $\%X_C$ compared to that of neat PLA. PLA with 1% talc content showed the the highest $\%X_C$ among neat PLA and other PLA composites. Moreover, $\%X_C$ decreased with increasing talc content. It could be concluded that vetiver fiber and talc acted as a nucleating agent on PLA composite system.

KEYWORDS: Vetiver fiber, Poly (lactic) acid, Thermal properties, Talc

## 3.2 Introduction

With increasing demands on renewable resources for consumer products, the use of biodegradable materials is of high interest which is result of traditional polymeric materials derived from petro-chemical resources degrade in the long time. Moreover, the disposal of such materials is of concern (Wong et al., 2007). In recent years, the development of biocomposites from biodegradable polymers and natural fibers have attracted great attention in field of the composite science because they allow complete degradation in soil or by composting process and emit none of toxic or noxious components (Lee and Wang, 2006). Polylactic acid (PLA) is the first commodity polymer produced from annually renewable resources. The benefits of PLA include low energy to produce and reducing green house gas production. However, PLA is a brittle polymer (Oksmana et al., 2003). It needs modifications for

more practical applications. The improvement of the properties of PLA is added of fillers or reinforcement material. Several studies have reported that fillers such as talc, sodium stearate, calcium lactate (Li and Huneault, 2007), organoclay (Day et al., 2006); (Krikorian and Pochan, 2004) and calcium metaphosphate (Junga et al., 2005) were used in PLA matrix. At the same time, the addition of synthetic fibers such as glass fiber (Huda et al., 2006), man-made cellulose fiber (Ganster et al., 2006), carbon fiber (Kuana et al., 2008); (Tsuji et al., 2007) in PLA were also studied. In case of natural fibers such as kenaf (Huda et al.; 2008); (Nishino et al., 2003), flax (Wong et al., 2007), bamboo (Lee and Wang, 2006), coir (Iovino et al., 2008), jute (Hu et al., 2007); (Khondker et al., 2006) were also used as filler in PLA composites. However, a major disadvantage of natural fibers is their hydrophilic character that makes them, in principle, immiscible with PLA that it is less polarity polymers. These results are affecting to properties of composites. Therefore, to develop the natural fiber-PLA composites with optimum properties, it has been customary to decrease the hydrophilicity of natural fiber by chemical modification (Bledzki and Gassan, 1999) or to promote interfacial adhesion through the use of compatibilizers (Parka et al., 2003).

In this work, vetiver fiber was modified by alkalization to decrease the hydrophilic. The alkali-treated vetiver fiber was used to mix with neat PLA to prepare vetiver fiber-PLA composites. The ratios of vetiver fiber to neat PLA were varied from 1-20% (w/w). Talc filled PLA composites were also prepared and its nucleating effect on crystallization of PLA was investigated. The thermal properties of neat PLA, vetiver fiber-PLA and talc-PLA composites were examined by using a Differential Scanning Calorimeter (DSC). Glass transition temperature ($T_g$), melting temperature

($T_m$), crystallization temperature ($T_c$), equilibrium melting temperature ($T^o_m$) and degree of crystallinity of the composites were further determined.

## 3.3 Experimental

### 3.3.1 Materials and chemical reagents

Poly (lactic acid) (PLA 4042D) was purchased from Nature Works, LLC. Vetiver grass *(Vetiveria Zizanioides)* was obtained from The Land Development Department, Nakhon Ratchasima, Thailand. The ages of vetiver grass are around 6–8 months. Sodium hydroxide (NaOH) (laboratory grade) was purchased from Italmar (Thailand) Co., Ltd. Talc (86255) with average particle size of 45 μm was purchased from Fluka.

### 3.3.2 Vetiver fibers preparation

To obtain the vetiver fiber, vetiver grass was washed by water to get rid of dirt and dried by sunlight for one day. The washed vetiver leaves were ground by a Retsch grinder machine and then sieved into the length of 2 mm. Vetiver fiber with 2 mm length was firstly washed by water to eliminate dirt and then dried in an oven at 100°C overnight. After that, the vetiver fiber was immersed in a solution of 4% (wt/v) NaOH for 2 h at 40°C and the vetiver-to-solution ratio is 1:25 (wt/v) to obtain the alkali-vetiver fiber. The alkali-vetiver fiber was then washed thoroughly with water and dried in an oven at 100°C for 24 h. These vetiver fibers were used to prepare the PLA composites throughout this study.

### 3.3.3 Preparation of vetiver fiber-PLA and talc-PLA composites

The ratio of vetiver fiber to neat PLA was varied from 1-20% (wt/wt). Vetiver fiber was mixed with neat PLA at 180°C in an internal mixer (Haake Rheomix 3000P). Mixing speed and mixing time were 50 rpm and 13 minutes, respectively.

After that, PLA composites were ground and dried before use. To prepare talc-PLA composites, the same mixing procedure was applied to mix 1% and 20% (wt/wt) talc with neat PLA.

### 3.3.4 Sample preparation

The films with a thickness about 2 mm of neat PLA, talc-PLA and vetiver fiber-PLA composite were prepared by compression molding at 180 ºC. The glass transition temperature ($T_g$), melting temperature ($T_m$), crystallization temperature ($T_c$), equilibrium melting temperature ($T^o_m$) and degree of crystallinity of these films were determined by Differential Scanning Calorimeter (DSC) (Perkin-Elmer: model 7)

### 3.3.5 Isothermal crystallization

Isothermal crystallization of neat PLA, talc-PLA and vetiver fiber–PLA composites was determined using a Differential Scanning Calorimeter. Thermal programming for rate of crystallization measurement was divided into 5 stages as shown in Figure 3.1.

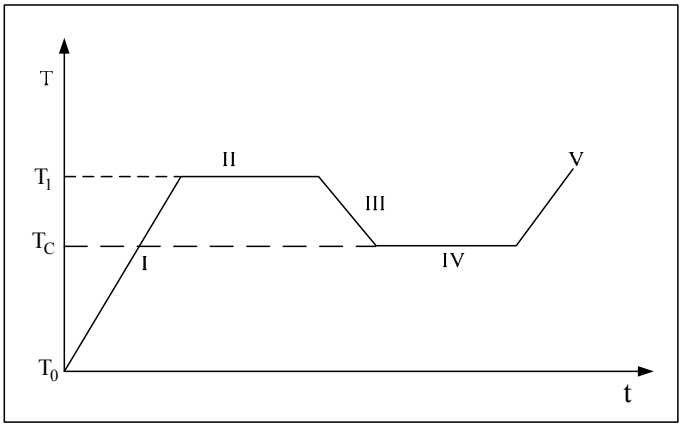


**Figure 3.1** Thermal programming for isothermal crystallization $T_0$ = 25°C, $T_1$ = 220°C, and $T_c$ = isothermal crystallization temperature.

Stage I : Heating a sample in the calorimeter with a heating rate of 20°C/min from 25°C to 220°C.

Stage II : Isothermal annealing the sample at the temperature, $T_1$ = 220°C for 5 min to remove thermal history of sample. This step called isothermal crystallization.

Stage III : Cooling the sample in the calorimeter to the $T_C$ with a cooling rate of 50°C/min.

Stage IV : Performing isothermal crystallization at various crystallization temperatures.

Stage V : Reheating the sample in the calorimeter from studied crystallization temperatures to 220°C with a heating rate of 20°C/min.

To measure rate of crystallization of the sample, the sample was heated from 25°C to 220°C and held at 220°C for 5 minutes under a nitrogen atmosphere in order to eliminate its thermal history. Then, the sample was cooled down with a rate of 50°C/min to various predetermined crystallization temperatures ($T_c$) and maintained at that temperature until the crystallization was completed.

After the completion of crystallization, the samples were heated to 220°C at a rate of 20°C. The melting temperature ($T_m$) of the sample was obtained from the maximum of the endothermic peaks. The equilibrium melting temperatures ($T^0_m$) was determined from Hoffman-Weeks plot (the extrapolation plot of $T_c$ versus $T_m$) (Vasanthakumari and Penning, 1983).

### 3.3.6 Non-isothermal crystallization

For non-isothermal crystallization of the PLA and PLA composites, the sample was heated from 25°C to 180°C with a heating rate of 10ºC/min and held at

180°C for 5 minutes under a nitrogen atmosphere. Then, the sample was cooled down with a rate of 10°C/min from 180°C to 25°C. After that the sample was heated again from 25°C to 180°C with a heating rate 10ºC/min. Thermal programming for rate of measurement was divided into 4 stages as shown in Figure 3.2.

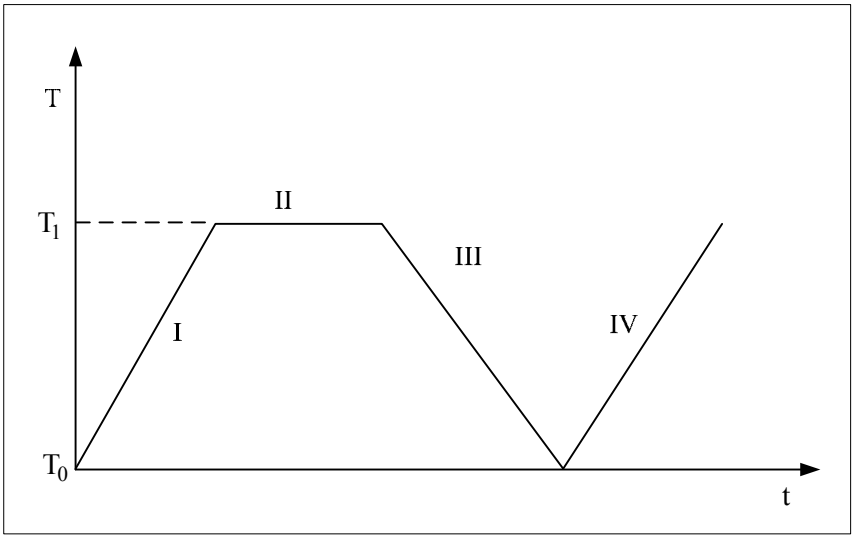


**Figure 3.2** Thermal programming for rate of non-isothermal crystallization measurement $T_0$ = 25°C, $T_1$ = 180°C.

Stage I : Heating a sample in the calorimeter with a heating rate of 10°C/min from 25°C to 180°C. (First heating scan)

Stage II : Isothermal annealing the sample at the temperature, $T_1$ = 180°C for 5 min to remove thermal history of sample.

Stage III : Cooling the sample in the calorimeter to the $T_0$= 25°C with a cooling rate of 10°C/min. (Cooling scan)

Stage IV : Heating the sample in the calorimeter again from $T_0$= 25°C to 180°C with a heating rate of 10°C/min. (Second heating scan)

The glass transition temperature, $T_g$, melting temperature, $T_m$, crystallization temperature, $T_c$ and degree of crystallinity, $\%X_C$ of neat PLA and PLA composites were measured.

The degree of crystallinity, $\%X_C$ in the composites can be obtained by:

$$\%X_C = \frac{\Delta H_m}{\Delta H_{mo}(\varnothing_{PLA})} \times 100 \quad (3.1)$$

In which $\Delta H_m$ is the measured melting enthalpy, $\Delta H_{mo}$ is the melting enthalpy of purely crystalline sample (93 J/g for PLA according to (Cheung et al., 2008) and $Ø_{PLA}$ is the PLA weight fraction in the composites.

## 3.4 Results and discussion

### 3.4.1 Isothermal crystallization

Figure 3.3 shows DSC thermograms of neat PLA during isothermal crystallization. In general, the time required to complete crystallization increased with increasing crystallization temperature. However, in this study, it was found that the time required to complete crystallization for the crystallization temperature at 95°C was longer than at the crystallization temperature at 100°C. S´anchez et al. (2005) also found that the minimum of the crystallization exotherms increased and moved to shorter times as $T_c$ increased up to 110°C. From this temperature, the height of crystallization peak decreased and moved to longer times. When the vetiver fiber at various ratios (1-20% w/w) was added in neat PLA, a similar result was observed as shown in Figure 3.4-3.7. The time required to complete crystallization for the

crystallization temperature at 95°C was longer than at the crystallization temperature at 100°C. In addition, DSC thermograms of PLA with 1% talc content during isothermal crystallization were shown in Figure 3.8. It was found that the time required to complete crystallization increased with increasing crystallization temperature. From Figure 3.3-3.8, the time required to reach the maximum rate of crystallization ($t_{max}$) was used to construct the graphs as shown in Figure 3.9.

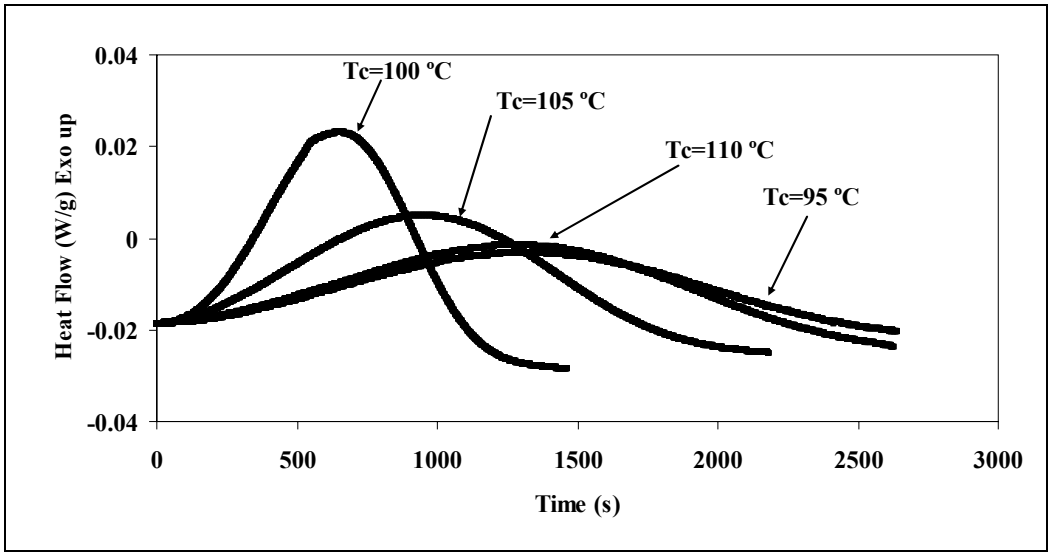


**Figure 3.3** DSC curves of the isothermal crystallization at various crystallization temperatures of the neat PLA.

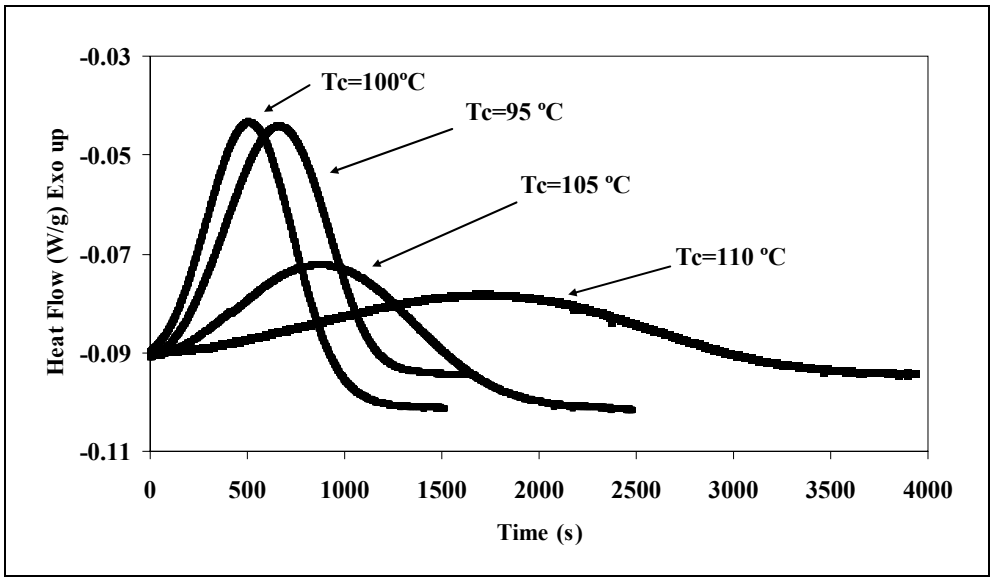


**Figure 3.4** DSC curves of the isothermal crystallization at various crystallization temperatures of 1% vetiver fiber- PLA composite.

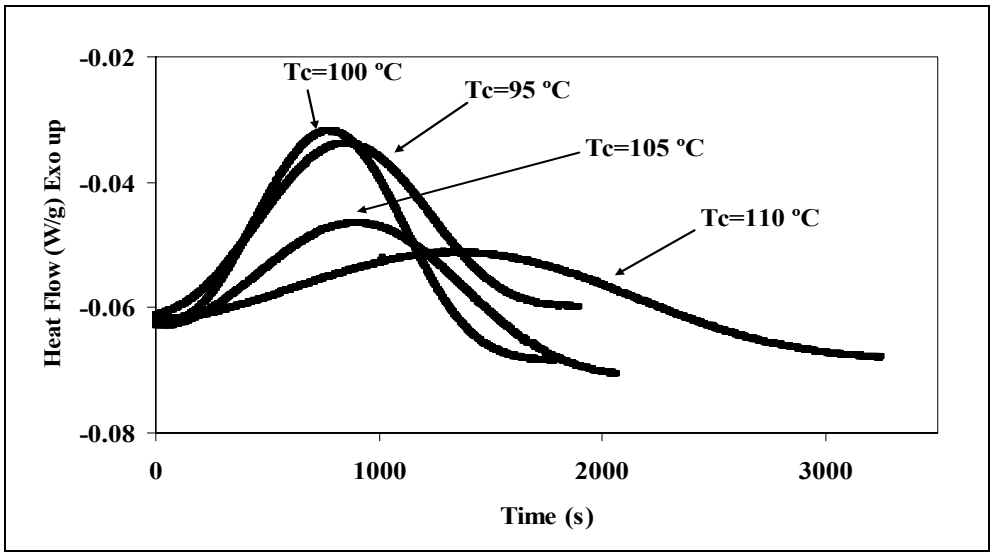


**Figure 3.5** DSC curves of the isothermal crystallization at various crystallization temperatures of 5% vetiver fiber- PLA composite.

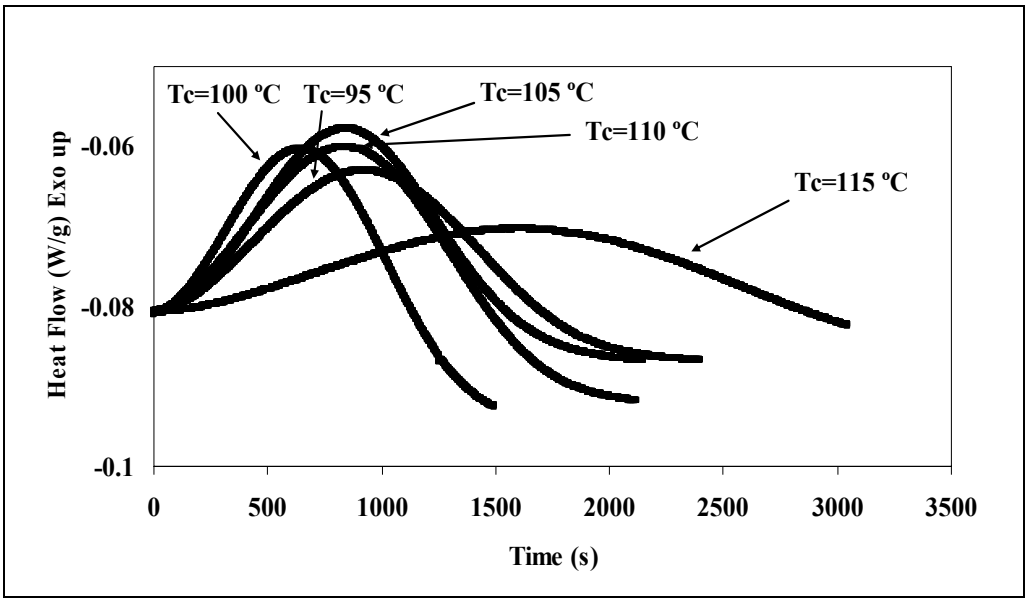


**Figure 3.6** DSC curves of the isothermal crystallization at various crystallization temperatures of 10% vetiver fiber- PLA composite.

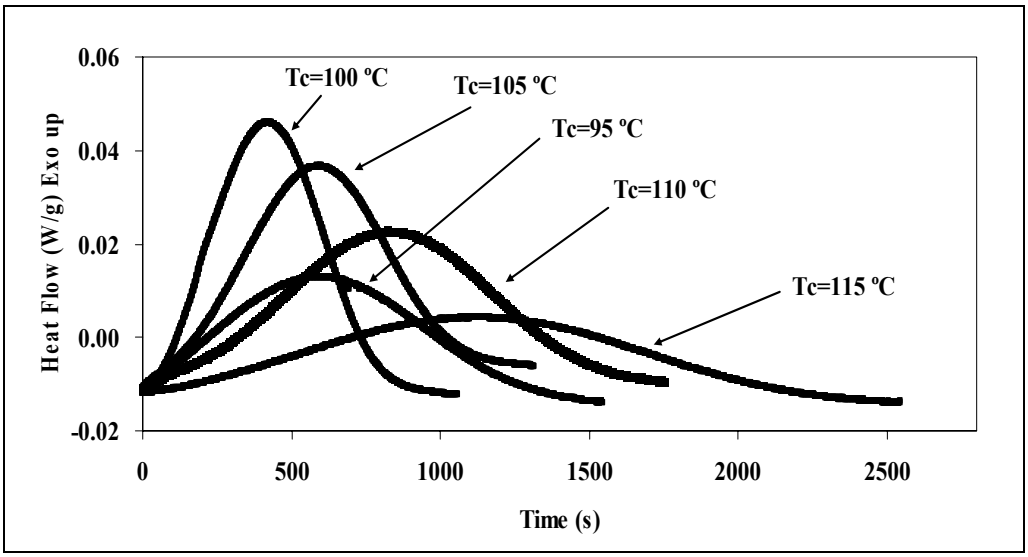


**Figure 3.7** DSC curves of the isothermal crystallization at various crystallization temperatures of 20% vetiver fiber- PLA composite.

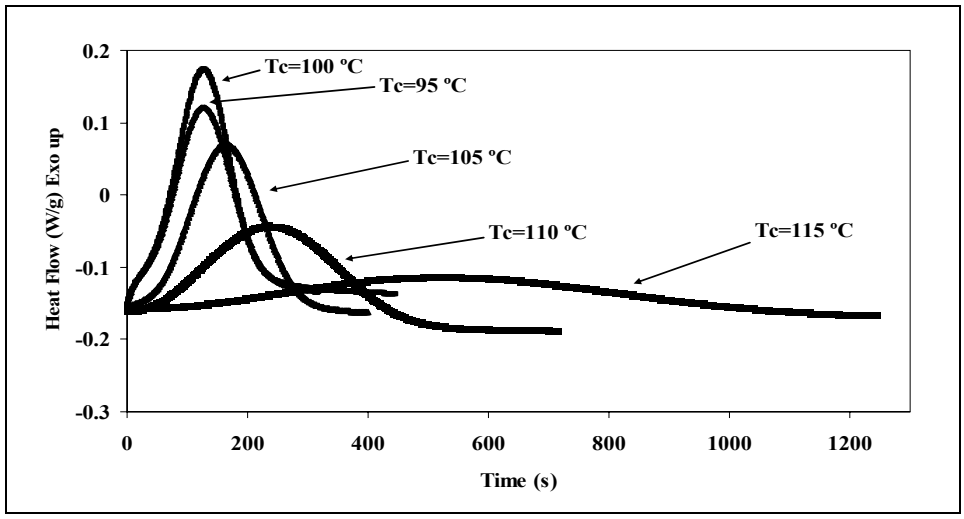


**Figure 3.8** DSC curves of the isothermal crystallization at various crystallization temperatures of 1% talc- PLA composite.

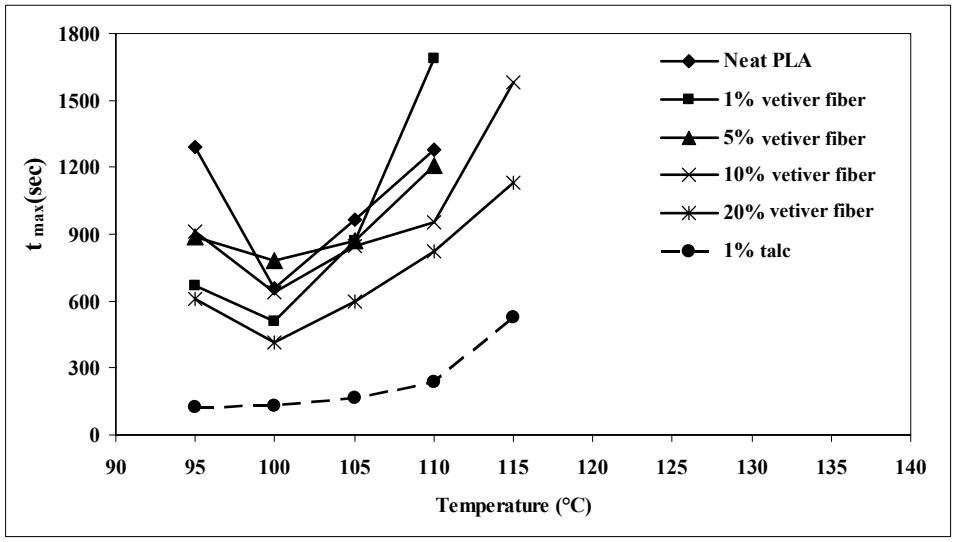


**Figure 3.9** Plot of crystallization temperature versus the time required to reach maximum rate of crystallization ($t_{max}$) of neat PLA and PLA composite obtained from isothermal crystallization at various crystallization temperatures.

In this study, $t_{max}$ was used to describe the crystallization rate. It was found that addition of talc in neat PLA led to the lowest $t_{max}$ among neat PLA and vetiver-PLA composites. This indicates the the highest crystallization rate of talc-PLA composites compared to that of neat PLA and vetiver-PLA composites. Talc was also showed to decrease the rate of crystallization of neat PP (Albano et al., 2003). In cases of vetiver fiber-PLA composites, $t_{max}$ values of 1-10% vetiver fiber-PLA composites were not significant difference compared to that of neat PLA. At 20% vetiver fiber, a $t_{max}$ value was lower compared to that of neat PLA and 1-10% vetiver fiber-PLA composites. This indicates that the crystallization rate of vetiver fiber at 20% content was the the highest compared to 1-10% vetiver fiber content. These results can be suggested that vetiver fiber at 20% content and talc acted as a good nucleating agent for PLA.

In addition, $t_{max}$ of neat PLA and vetiver fiber-PLA composites at crystallization temperature of 100°C was the lowest among the other crystallization temperatures. In this study, these can be suggested that the maximum crystallization rate of neat PLA and vetiver fiber-PLA composites were found at crystallization temperatures of 100°C.

Figure 3.10 showed the DSC melting endotherms for neat PLA during heating after isothermal crystallization at each crystallization temperature. The double melting endotherms for neat PLA were observed in the sample obtained after isothermally crystallization at 105°C, 100°C and 95°C. This result can also be observed when vetiver fibers at various ratios from 1-20% were added in neat PLA as shown in Figure 3.11-3.14, respectively. Similarly, 1% talc-PLA composites also

showed the double melting endotherms after isothermally crystallized at 95°C and up to 105°C as shown in Figure 3.11.

The double melting endotherms of talc-PLA composites indicate that several crystallite forms of PLA were taken place. The low and high-temperature melting endotherms of  have been reported by several authors (Chen et al., 2007); (He et al., 2007); (Thanomkiat, P., et al., 2004). The low-temperature melting endotherms were found to associate with the melting of the primary crystallites formed at isothermal crystallization temperature and shifted to higher temperature with increasing crystallization temperature. While the high-temperature melting endotherms were attributed to the melting of re-crystallized crystallites formed during a heating scan. This high-temperature melting endotherms showed less dependence on the isothermal crystallization temperature. From this reason, the melting temperature values that obtained from low-temperature melting endotherms were used to determine the equilibrium melting temperature ($T^o_m$) according to Hoffman and Weeks (1976) as shown in Figure 3.16.

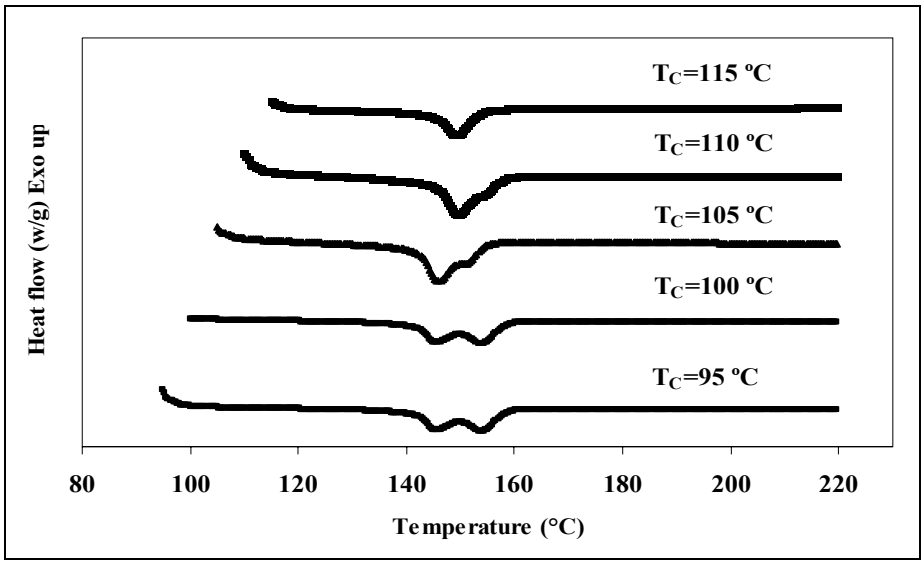


**Figure 3.10** DSC thermograms of neat PLA during heating after isothermal crystallization at various crystallization temperatures.

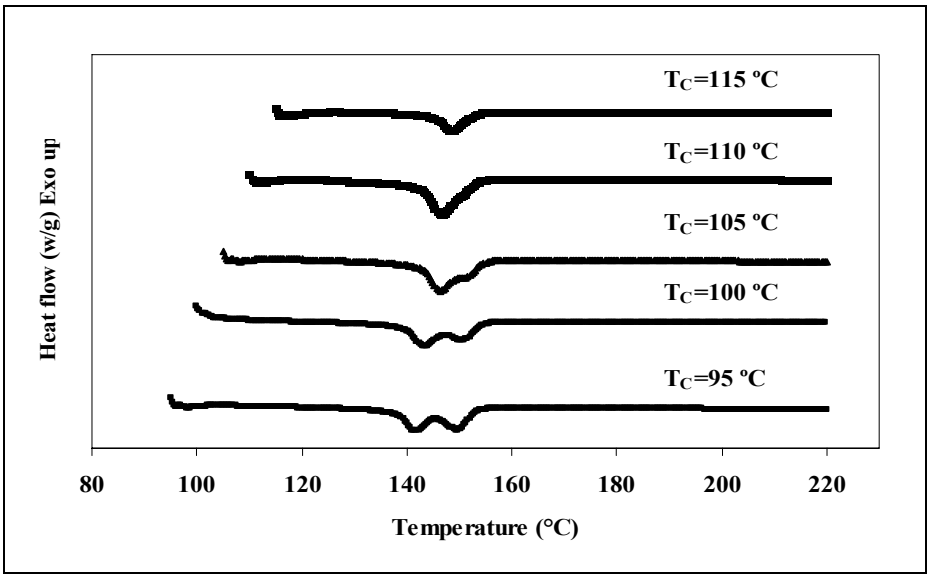


**Figure 3.11** DSC thermograms of 1% vetiver fiber-PLA composite during heating after isothermal crystallization at various crystallization temperatures.

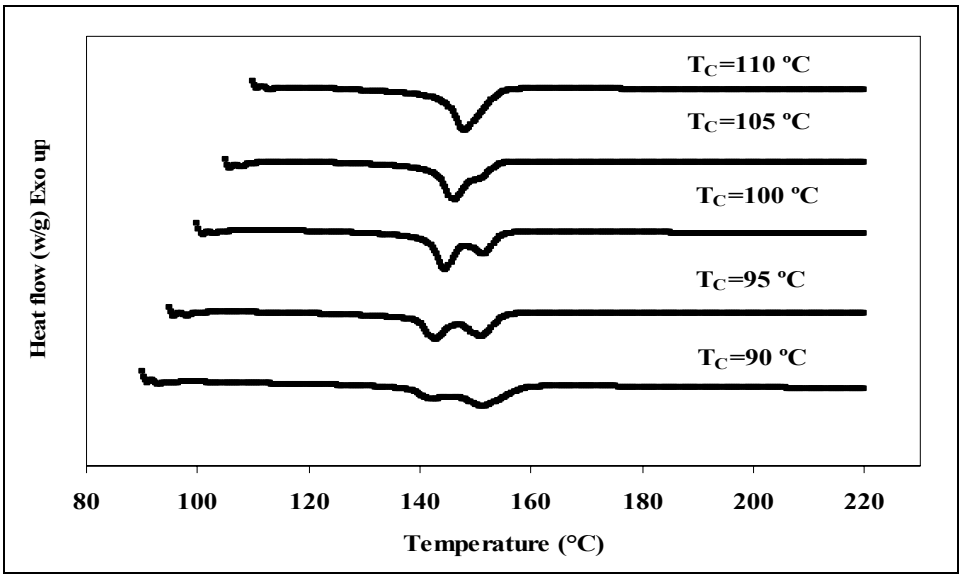


**Figure 3.12** DSC thermograms of 5% vetiver fiber-PLA composite during heating after isothermal crystallization at various crystallization temperatures.

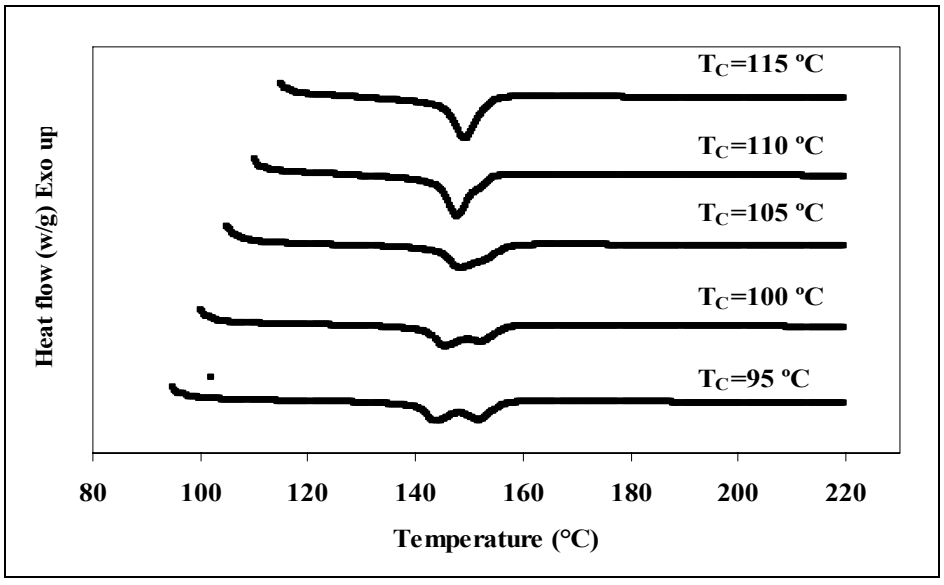


**Figure 3.13** DSC thermograms of 10% vetiver fiber-PLA composite during heating after isothermal crystallization at various crystallization temperatures.

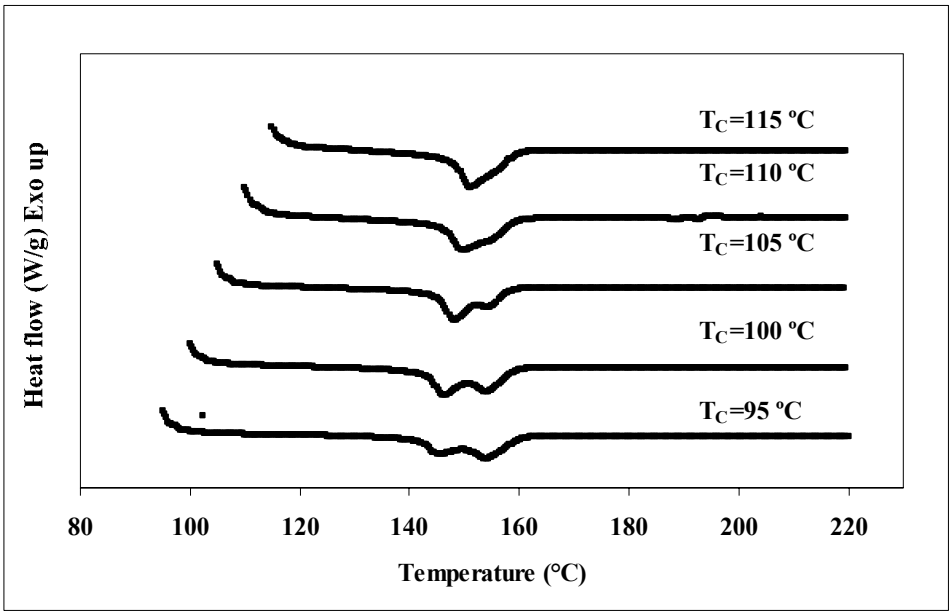


**Figure 3.14** DSC thermograms of 20% vetiver fiber-PLA composite during heating after isothermal crystallization at various crystallization temperatures.

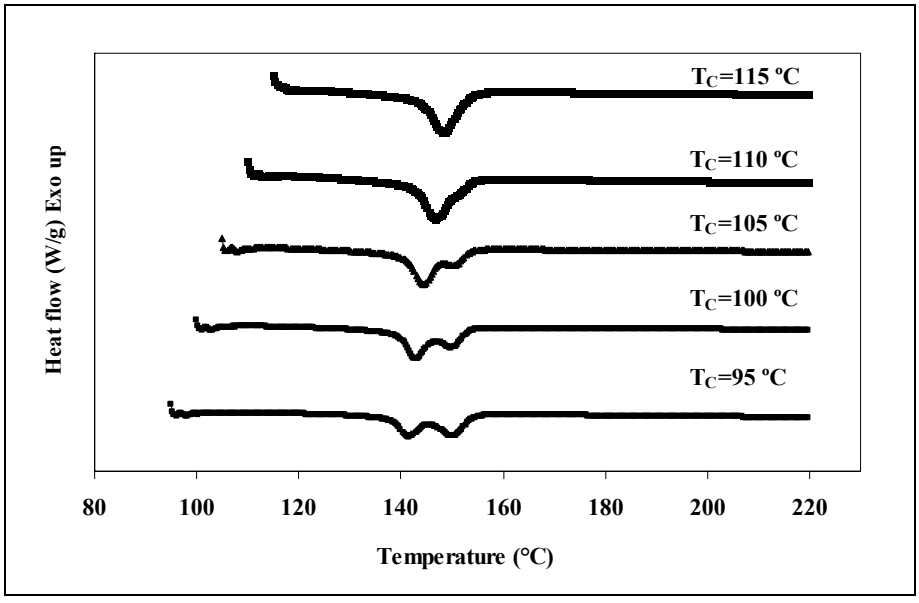


**Figure 3.15** DSC thermograms of 1% talc-PLA composite during heating after isothermal crystallization at various crystallization temperatures.

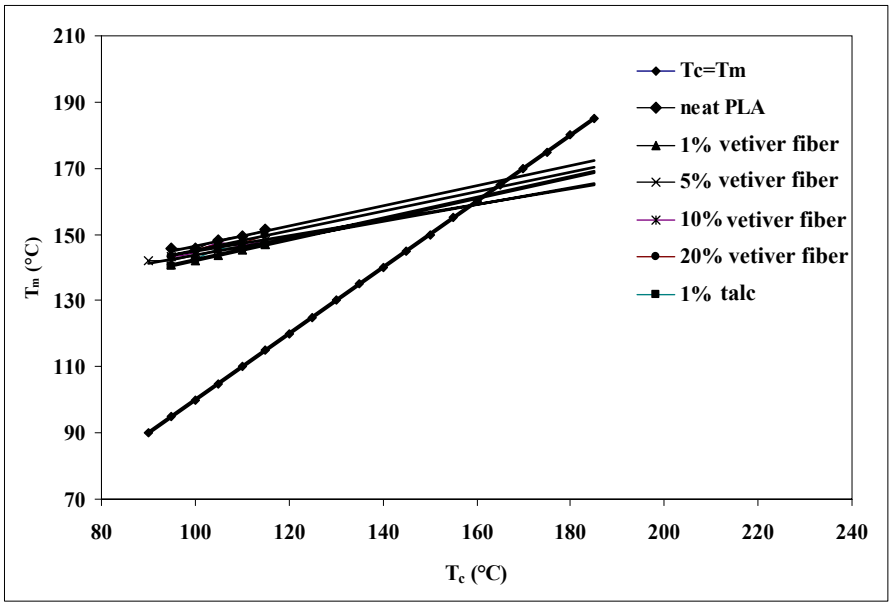


**Figure 3.16** Hoffman–Weeks plots for determining the equilibrium melting temperatures ($T^o_m$) of neat PLA, vetiver fiber-PLA and talc-PLA composites.

Figure 3.16 represents the relationship between crystallization temperature and melting temperature of neat PLA and PLA composites obtained from DSC measurements. Table 3.1 shows the equilibrium melting temperatures ($T^0_m$) of neat PLA and PLA composites obtained from the extrapolation of $T_m$ versus $T_C$ to the line which $T_m = T_C$ according to Hoffman and Weeks (1976). From Table 3.16, it was found that the presence of vetiver fiber and talc in PLA composites led to a decrease in $T^o_m$ of PLA. It was also found that $T^o_m$ slightly decrease with increasing the fiber content. This may be because vetiver fiber and talc interrupted the lamella formation and led to less perfect crystal of PLA. Previously, Krikorian and Pochan (2004) added organically modified montmorillonite clay in PLA composites. They also found that

$T^o_m$ decreased with increasing clay content. Arroyoa et al. (2000) also found that a decrease in $T^o m$ of PP was observed when aramid fibers content increased.

**Table 3.1** The equilibrium melting temperatures ($T^o_m$) of neat PLA, vetiver fiber-PLA and talc-PLA composites.

| Samples | The equilibrium melting temperatures ($T^o_m$) (°C) |
|---|---|
| Neat PLA | 164.10 |
| 1% vetiver fiber | 162.05 |
| 5% vetiver fiber | 159.90 |
| 10% vetiver fiber | 159.59 |
| 20% vetiver fiber | 158.03 |
| 1% talc | 161.09 |

### 3.4.2 Non-isothermal crystallization

Figure 3.17-3.19 showed the curve of DSC thermograms of neat PLA and vetiver fiber-PLA composites recorded during the first heating, the cooling and the second heating at a rate of 10°C/min, respectively.

In Figure 3.17, the glass transition temperature ($T_g$), the crystallization temperature ($T_c$) (indicated by exothermic peak) and melting temperature ($T_m$) (indicated by endothermic peak) of neat PLA and vetiver fiber-PLA composite could be observed. From the DSC curves, it was found that the $T_g$ of the vetiver fiber-PLA composites were not changed comparing to that of neat PLA. $T_c$ of vetiver fiber-PLA composite was shifted to lower temperature with increasing vetiver fiber content. However, $T_m$ of vetiver fiber-PLA composites was not significantly changed compared to that of neat PLA. Nevertheless, at 20% vetiver fiber content, multiple melting peaks were clearly observed. Upon cooling, no exothermic peak could be

observed in both neat PLA and PLA composites as shown in Figure 3.18. Then, neat PLA and vetiver fiber-PLA composites were heated again and DSC curves from the second heating scan were shown in Figure 3.19. Similar to the first heating scan, The $T_g$ of the vetiver fiber-PLA composites were not changed. Moreover, $T_C$ of vetiver fiber-PLA composites was slightly lower than that of neat PLA. With increasing vetiver fiber content, $T_C$ of vetiver fiber-PLA composites decreased.

The $T_C$ of PLA in neat PLA and PLA composites were not observed upon cooling scan (Figure 3.18). It is probable that the samples were not completely amorphous and may form very small crystal. The very small crystal might be act as initially nuclei. Even though, these nuclei may represent a small crystalline fraction. They increased the crystallization rate upon heating led to a decrease in $T_C$ of PLA with the presence of vetiver fiber. Li and Huneault (2007) studied effect of talc and polyethylene glycol on the crystallization of PLA. They have found thin TC upon heating shifted to a lower temperature with increasing polyethylene glycol.

From the first heating scan (Figure 3.17) and the second heating scan (Figure 3.19), PLA composites with 20% vetiver fiber content showed the lowest crystallization peak compared to PLA composites with 1-10% vetiver fiber content. This implied that PLA composites with 20% vetiver fiber content act as a good nucleating agent. Meanwhile, double melting peaks could be clearly observed with 20% vetiver fiber-PLA composites. This indicated that the several crystal forms were taken place. The double melting peaks of PLA were also observed in purified cellulose fibers-PLA composites (Sanchez-Garcia et al., 2008) and chicken feather fiber-PLA composites (Cheng et al., 2009).

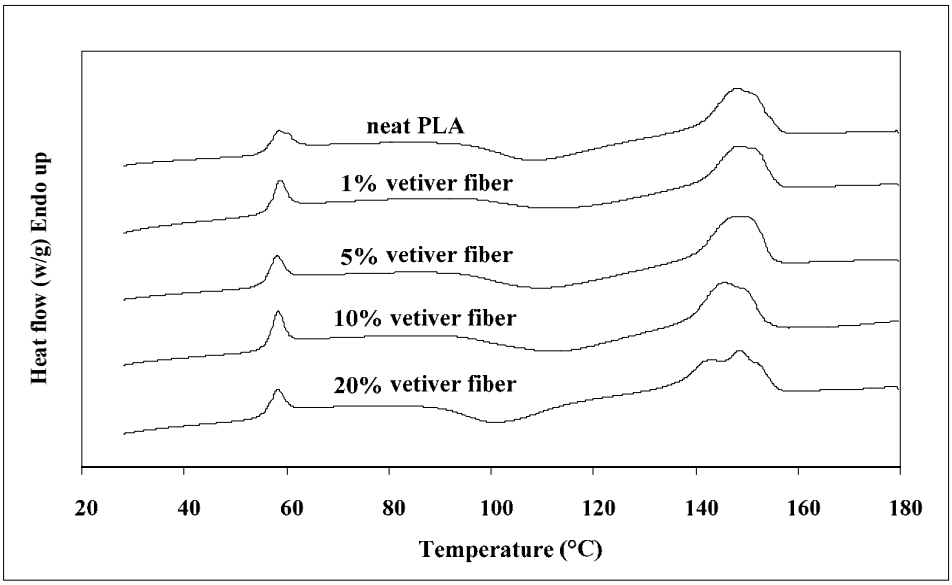


**Figure 3.17** DSC thermograms of neat PLA and vetiver fiber-PLA composites recorded during first heating at the rate of 10ºC/min.

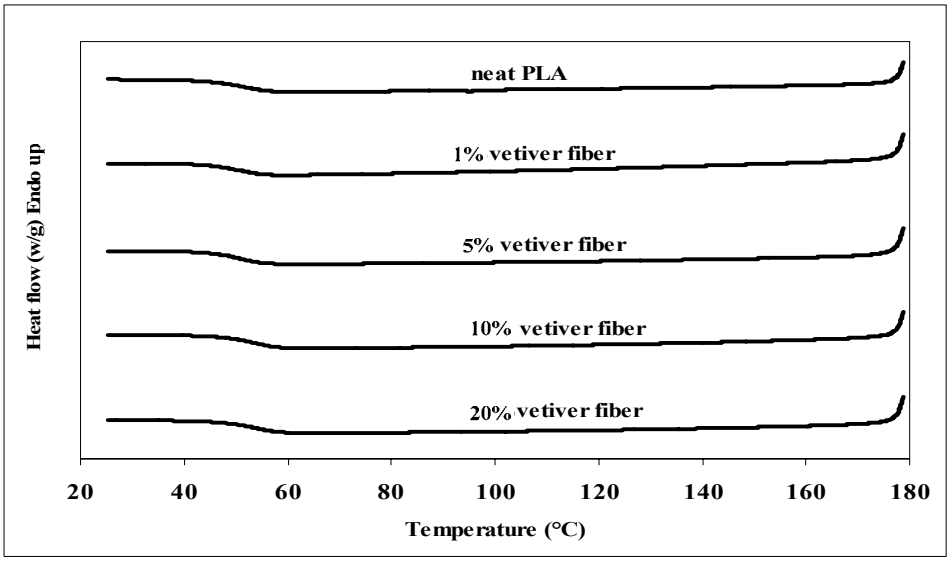


**Figure 3.18** DSC thermograms of neat PLA and vetiver fiber-PLA composites recorded during cooling at the rate of 10ºC/min.

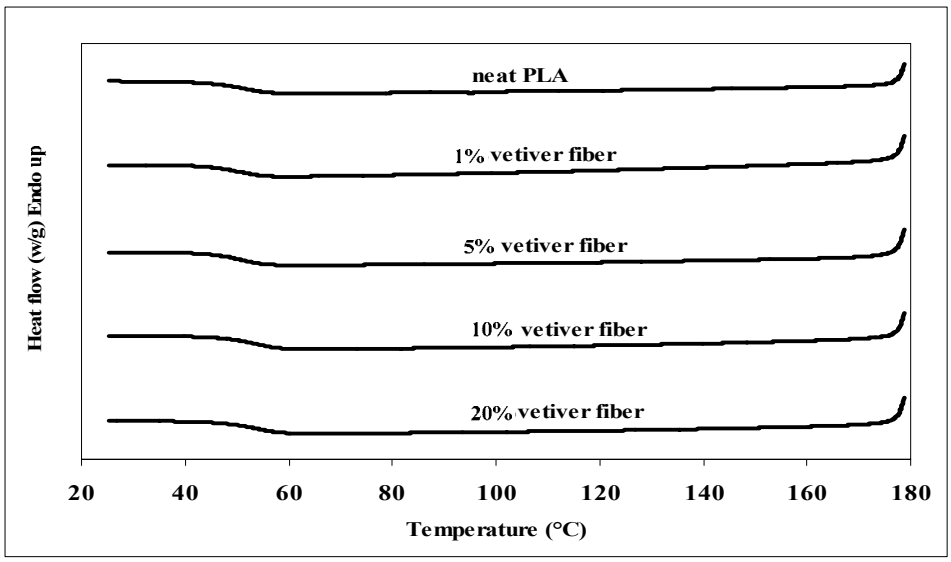


**Figure 3.19** DSC thermograms of neat PLA and vetiver fiber-PLA composites recorded during second heating at the rate of 10 ºC/min.

In order to compare the nucleating effect of talc with that of vetiver fiber, talc with 1% and 20% (w/w) were used. DSC thermograms of neat PLA, talc-PLA, and vetiver fiber-PLA composites recorded during the first heating, the cooling, and the second heating scan were shown in Figure 3.20-3.22, respectively. From Figure 3.20, when talc was added, $T_g$ of talc-PLA composites was similar to that of neat PLA. However, $T_C$ of talc-PLA composites was lower than that of neat PLA. Meanwhile, increasing talc content led to a decrease in $T_C$ of talc-PLA composites. At 20% talc-PLA composite, the double melting peaks of PLA were clearly observed and shifted to higher temperature compared to neat PLA and other PLA composites. These could be implied that a perfect and more stable crystal was formed with the incorporation of 20% talc content. DSC thermograms of neat PLA, vetiver fiber-PLA and talc-PLA composites recorded during cooling were shown in Figure 3.21. It could

be seen that for 20% talc-PLA composites, a small crystallization peak appeared around 90°C. However, the crystallization peak was not observed either in 1% talc-PLA composites or other vetiver fiber-PLA composites and neat PLA. Figure 3.22 showed DSC thermograms recorded during the second heating of neat PLA, vetiver fiber-PLA and talc-PLA composites. Similar to the result of the first heating scan, $T_g$ of the PLA composites were the same as that of neat PLA. The presence of talc in PLA composites led to a decrease in $T_C$ of talc-PLA composites compared to neat PLA and other vetiver fiber-PLA composites. $T_C$ of talc-PLA composites decreased with increasing talc content. In addition, double melting peaks could be observed in 20% vetiver fiber-PLA composites. For talc-PLA composites, double melting peaks were observed in both 1% and 20% talc-PLA composites.

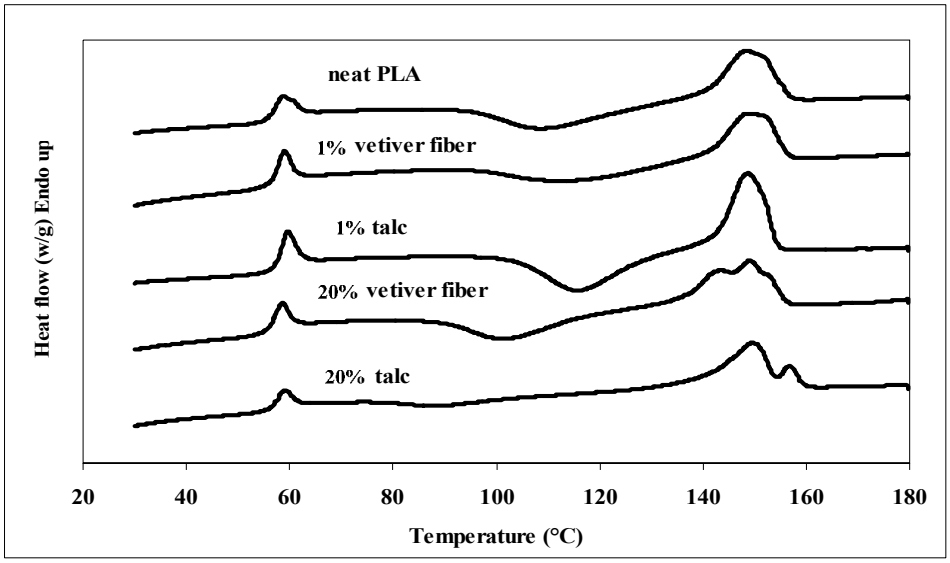


**Figure 3.20** DSC thermograms of neat PLA, vetiver fiber-PLA and talc-PLA composites recorded during the first heating at the rate of 10 ºC/min.

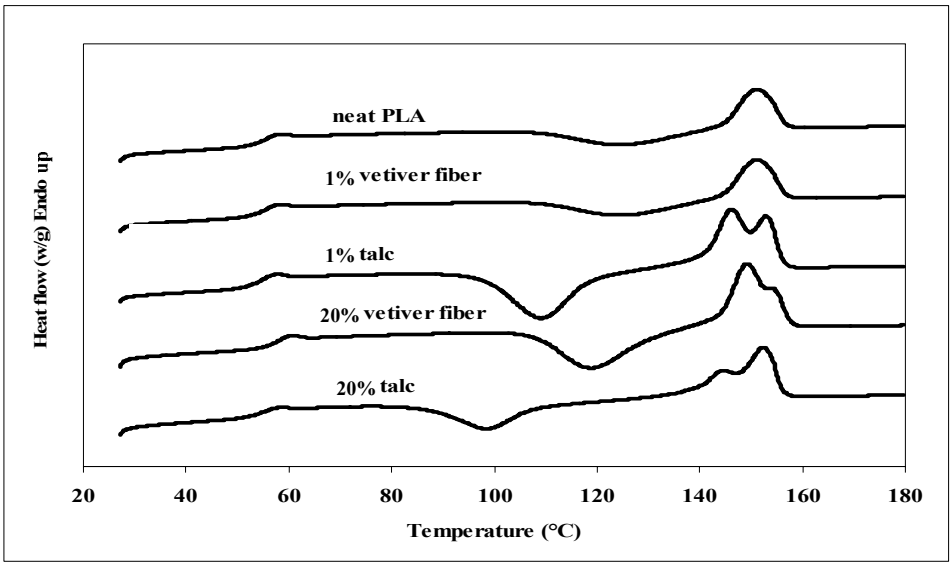


**Figure 3.21** DSC thermograms of neat PLA, vetiver fiber-PLA and talc-PLA composites recorded during cooling at the rate of 10 ºC/min.

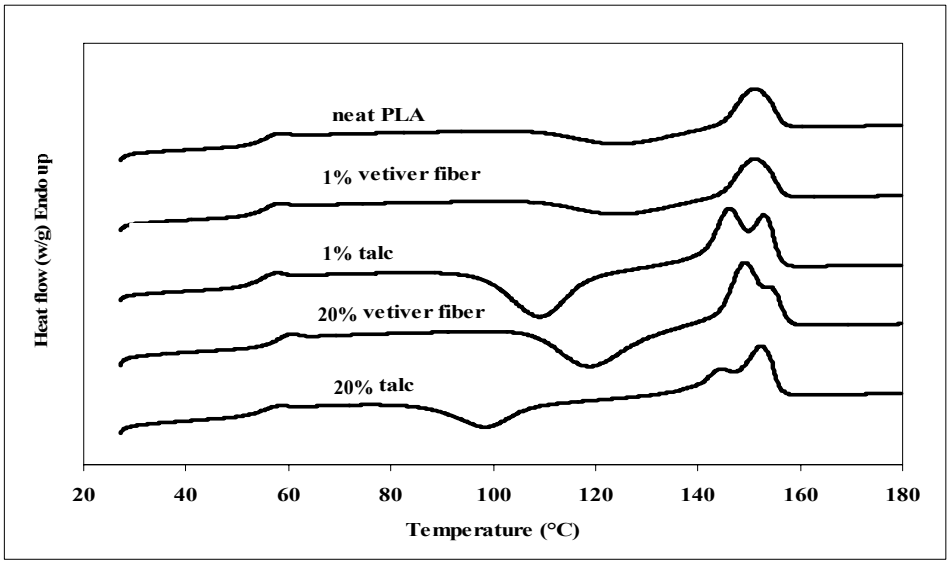


**Figure 3.22** DSC thermograms of 10ºC/min of neat PLA, vetiver fiber-PLA and talc-PLA composites recorded during the second heating.

From the previous results, a small crystallization peak of PLA in 20% talc-PLA composites was observed upon the cooling scan (Figure 3.18). Neat PLA, 1% talc-PLA and vetiver fiber-PLA composites showed no crystallization peak upon the cooling scans. From these results, it might be that the cooling rate of 10°C/min was too rapid that the time for the diffusion of the molecular segments onto the growing crystallites was not sufficient. So, it was interesting to observe the melt crystallization of talc-PLA and vetiver fiber composites at the cooling rate lower than 10°C/min

DSC thermograms of neat PLA and vetiver fiber-PLA composites recorded during cooling were shown in Figure 3.23a-b with the rate of 5°C/min and 10°C/min, respectively. Similar to the result obtained from the cooling rate of 10°C/min (Figure 3.23b), none of exothermic peak was observed in both neat PLA and vetiver fiber-PLA composites with the rate of 5°C/min as shown in Figure 3.23a. Then, neat PLA and vetiver fiber-PLA composites were heated again with the rate of 5°C/min. DSC thermograms of the second heating were shown in Figure 3.24a. The DSC thermograms clearly showed the separation of crystallization peak and melting peak. Meanwhile, double melting peak was clearly observed in neat PLA and PLA composites compared to that obtained with the heating rate of 10°C/min (Figure 3.24b). In addition, it was found that double melting peak of vetiver fiber-PLA composites were shifted to lower temperature when the content of vetiver fiber rise from 1% to 20%. This implied that less perfect crystals were generated with the incorporation of vetiver fiber.

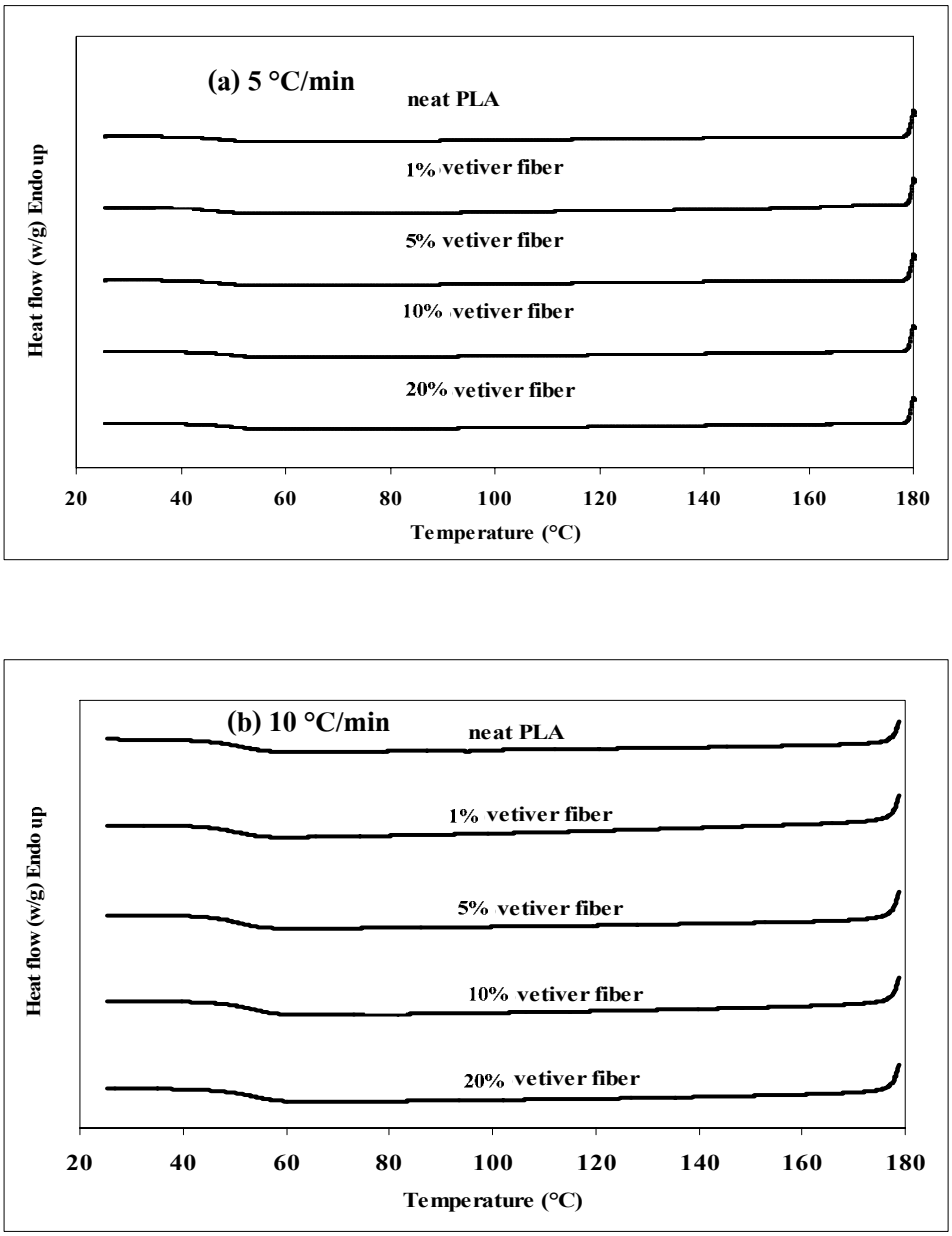


**Figure 3.23** DSC thermograms of neat PLA and vetiver fiber-PLA composites recorded during the cooling at the rate of 5ºC/min (a) and 10ºC/min (b).

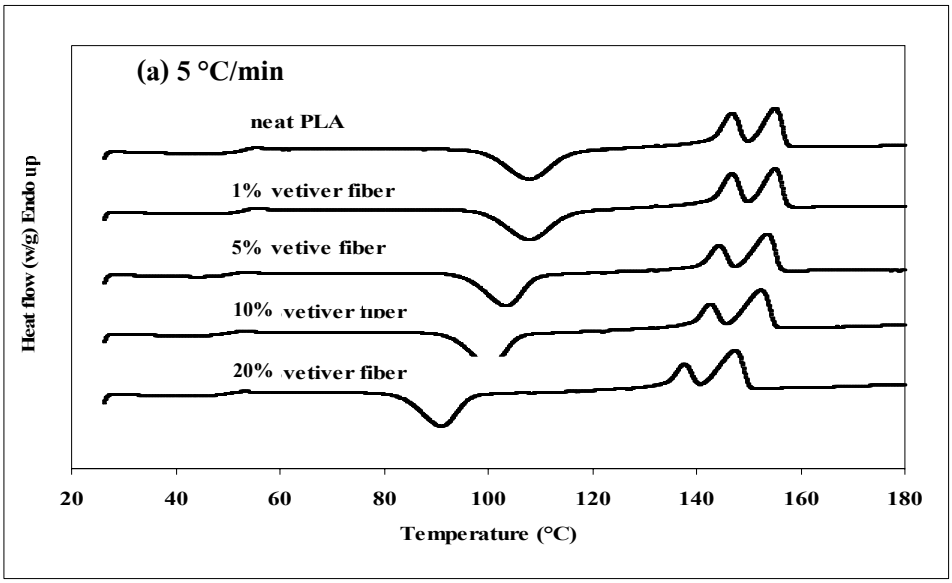


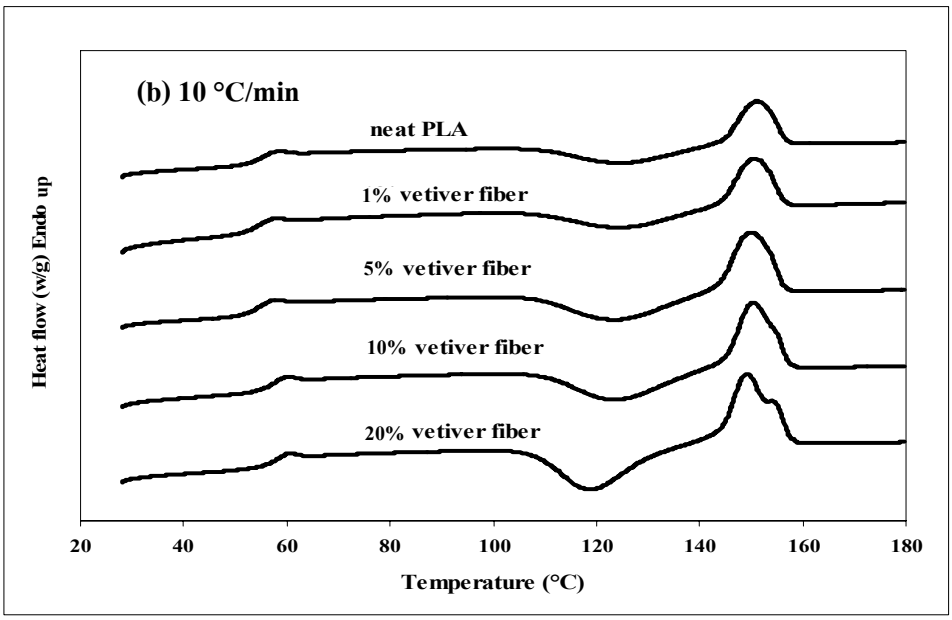


**Figure 3.24** DSC thermograms of neat PLA and vetiver fiber-PLA composites recorded during the second heating at the rate of 5ºC/min (a) and 10ºC/min(b).

DSC thermograms of neat PLA, vetiver fiber-PLA and talc-PLA composites recorded during cooling scan with the rate of 5°C/min and 10°C/min were shown in Figure 3.25a and b, respectively. From Figure 3.25a, interestingly, it showed thin TC of PLA with the incorporation of talc was clearly observed compared to the rate of 10°C/min (Figure 3.25b). This can be suggested that cooling rate of 5°C/min was slow enough for crystallization of talc-PLA composites to take place.

DSC thermograms of the second heating scan of neat PLA, vetiver fiber-PLA and talc-PLA composites were shown in Figure 3.26a in which crystallization peaks were not observed. These ascribed to the crystallization of talc-PLA composites was already taken place upon cooling. However, at the heating rate of 10°C/min (Figure 3.26b), crystallization peak of talc-PLA composites were clearly observed.

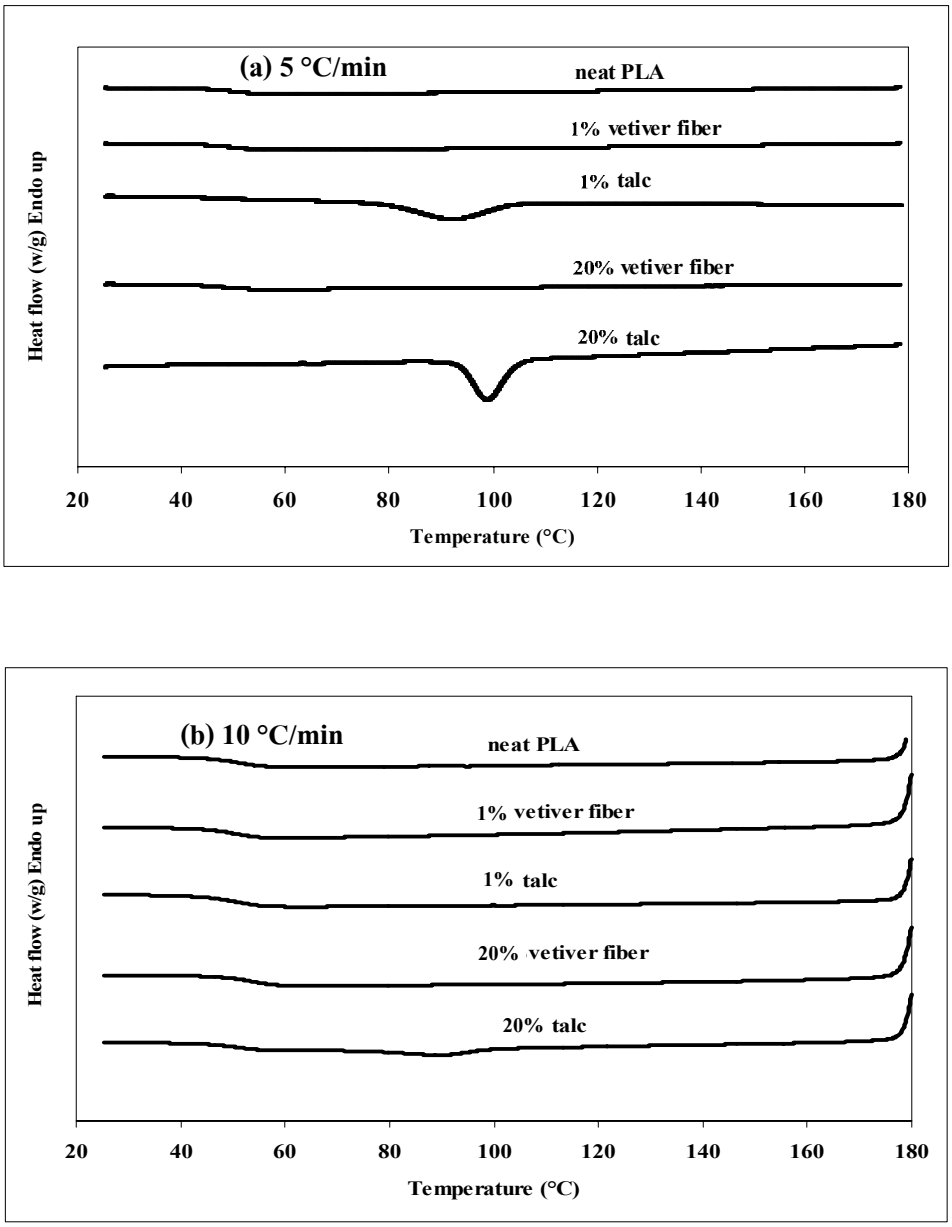


**Figure 3.25** DSC thermograms of neat PLA, vetiver fiber-PLA and talc-PLA composites recorded during the cooling at the rate of 5ºC/min (a) and 10ºC/min (b).

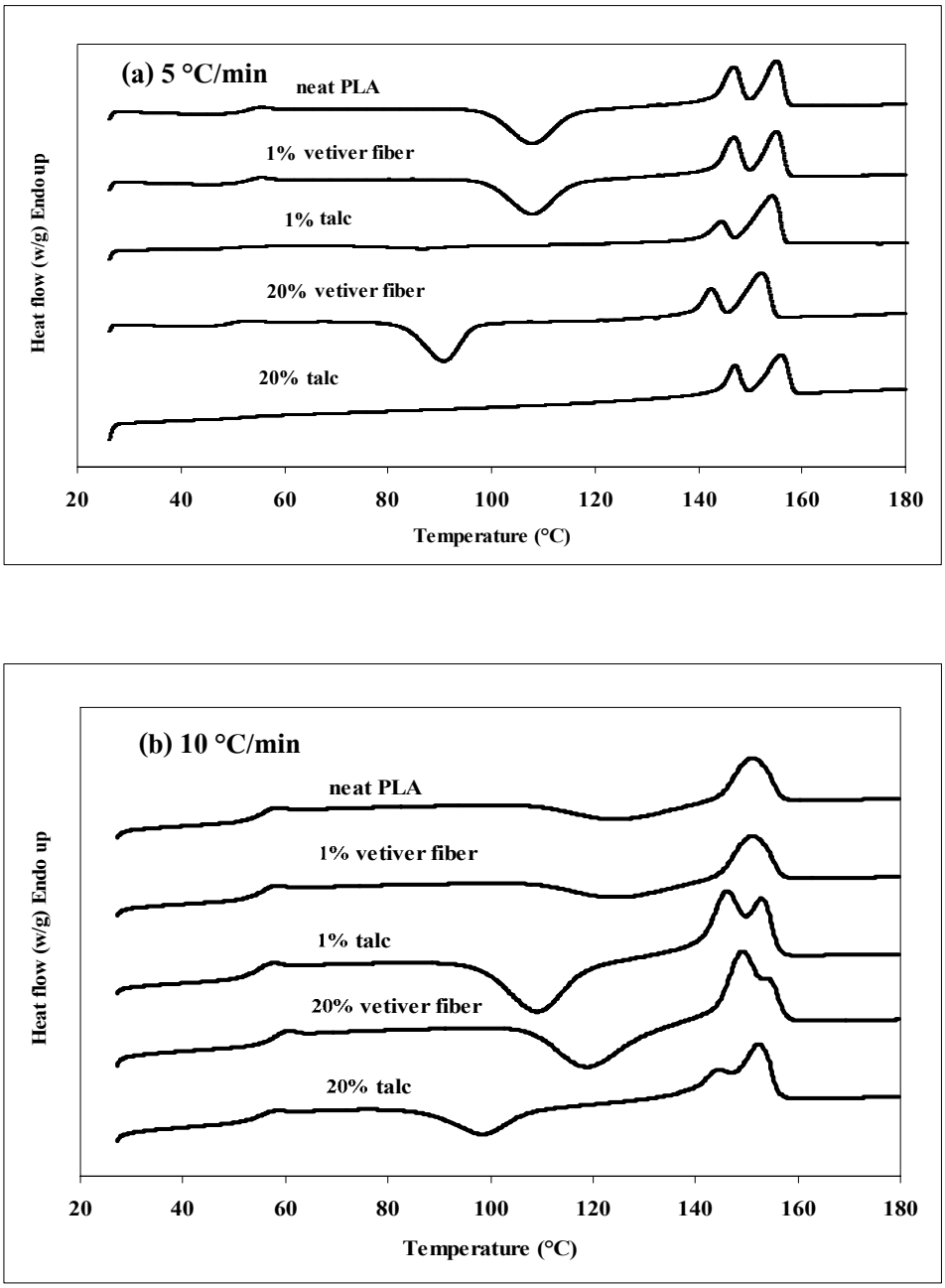


**Figure 3.26** DSC thermograms of neat PLA, vetiver fiber-PLA and talc-PLA composites recorded during the second heating at the rate of 5ºC/min (a) and 10ºC/min (b).

From Figure 3.24a and 3.26a, $T_g$ and $T_C$ of neat PLA and PLA composites from the seco nd heating scan with the rate of 5ºC/min and 10ºC/min were summarized in Table 3.2. From Table 3.2, $T_g$ of neat PLA and PLA composites increased as the heating rates increased. This result was attributed to the delayed heat response of the PLA molecules at the high scanning rates (Yeh et al., 2009). At the heating rate of 10°C/min, it was found thin TC of neat PLA and PLA composites were higher compared to those observed at the heating rate of 5°C/min. This suggested that an increasing induction time to chain arrangement for crystallization was found with a lower heating rate.

In addition, it was noteworthy to mention thin TC of vetiver fiber-PLA composite was not observed in a cooling scan with the cooling rate of 5ºC/min. It might be that the cooling rate was still rapid led to the crystallization of PLA was not taken place in vetiver fiber-PLA composites. Therefore, the effect of cooling and heating rate on crystallization of vetiver fiber-PLA composites was elucidated in the next section.

**Table 3.2** Glass transition temperatures ($T_g$) and crystallization temperature ($T_C$) of neat PLA and PLA composites from the second heating scan with the rate of 5ºC/min and 10ºC/min.

| Samples | $T_g$ (ºC) | | $T_C$ (ºC) | |
|---|---|---|---|---|
| | **5 ºC/min** | **10 ºC/min** | **5 ºC/min** | **10 ºC/min** |
| Neat PLA | 51.08 | 54.45 | 107.52 | 124.54 |
| 1% vetiver fiber | 51.00 | 53.90 | 108.44 | 124.51 |
| 5% vetiver fiber | 49.76 | 54.22 | 103.19 | 123.54 |
| 10% vetiver fiber | 49.84 | 55.53 | 100.00 | 123.38 |
| 20% vetiver fiber | 49.80 | 55.12 | 92.74 | 118.74 |
| 1% talc | 49.95 | 54.07 | - | 108.97 |
| 20% talc | 49.46 | 54.31 | - | 98.55 |

### 3.4.3 Effect of cooling and heating rate on crystallization of 20% vetiver fiber-PLA composites

From the previous section, PLA composites with 20% vetiver fiber content showed the lowest crystallization peak compared to 1-10% vetiver fiber-PLA composites. These implies that a good nucleating agent by 20% vetiver fiber content. Therefore, 20% vetiver fiber-PLA composites were chosen to use in this study. Figure 3.27 shows DSC curves with different cooling rate of 20% vetiver fiber-PLA composites after heating from 25ºC to 180ºC with rate of 10ºC/min. Upon cooling at different rates, exothermic peak of neat PLA and vetiver fiber-PLA composites was not observed at all cooling rates. Even though, the cooling rate was lower down to 1°C/min. It was well-known that the crystallization rate of PLA was very slow compared with those of other semi-crystalline polymers (Wang and Mano, 2005). As a

result, it was possible that a slow nucleation and a very small crystal may be taken place. Therefore, the change of heat of fusion was very small.

After cooling from 180ºC to 25ºC with the rate of 10ºC/min, PLA composites was heated again from 25ºC to 180ºC using different heating rates. Figure 3.28 showed effect of the heating rate on crystallization of PLA in 20% vetiver fiber-PLA composites. From DSC curve, it was found that the $T_g$ and $T_C$ of PLA composites shifted to higher temperatures with increasing the heating rate. $T_g$ values of the PLA composites significantly increased as the heating rates increased. It was attributed to the delayed heat response of the PLA molecules at high scanning rates (Yeh et al., 2009). Crystallization peak became larger and shifted to higher temperature with increasing heating rate from 1°C/min to 10°C/min (Smith, Drews, and Vasanthan, 2005).

When a heating rate was faster than 10°C/min, $T_C$ of PLA composites was not observed. For melting peak, it was observed that the double melting peaks of 20% vetiver fiber-PLA composites were found at the heating rates of 1°C/min and 5°C/min. With increasing a heating rate, the low-temperature melting peak increased while the high-temperature melting peak decreased. When heating rate increased to 20°C/min, the double melting peak was transformed into a single melting peak. This result suggested that at a higher heating rates, the process of re-crystallization was hindered, resulting in only one low-temperature melting peak. This work was similar to the study of PP nucleated by supported β-nucleating agent with different heating rates (Zhang et al., 2008). Besides, melting peak of 20% vetiver fiber-PLA composites almost disappeared while exothermic peak was not observed with a high heating rate

(50°C/min). These may be due to the short time for the diffusion of the molecular segments onto the growing crystallites of PLA composite. (Srimoaon, et al., 2004).

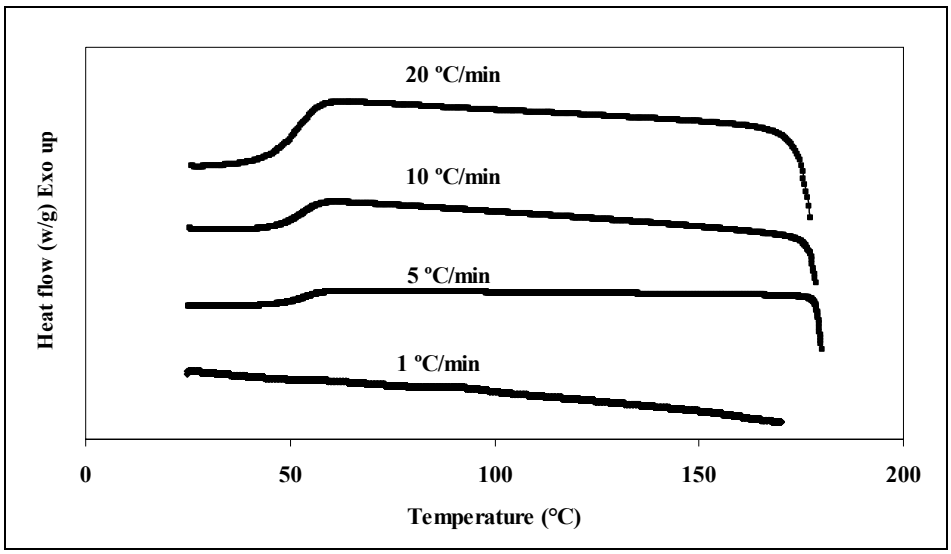


**Figure 3.27** DSC thermograms of 20% vetiver fiber-PLA composites recorded during cooling at the different rates.

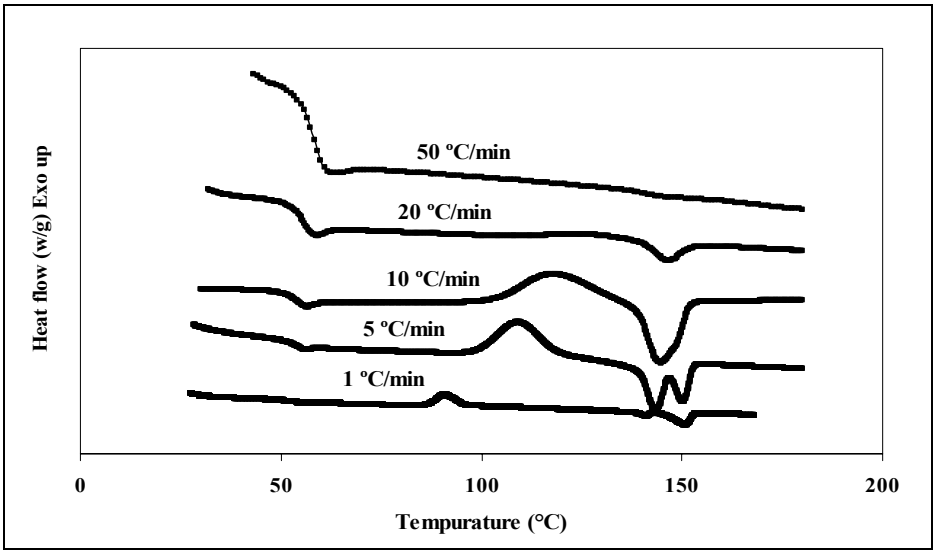


**Figure 3.28** DSC thermograms of 20% vetiver fiber-PLA composites recorded during heating at the different rates.

From Figure 3.24a and 3.26a, melting enthalpy ($\Delta H_m$) and crystallization enthalpy ($\Delta H_c$) were obtained from peak area under melting peak and crystallization peak (Mathot, 1994) respectively. Degree of crystallinity ($\%X_C$) of neat PLA and PLA composites determined from equation 3.1 was shown in Table 3.3. From Table 3.3, when vetiver fiber and talc were added in PLA matrix, it was found that ($\Delta H_c$) of PLA with the addition of 1% and 5% vetiver fiber content slightly increased compared to that of neat PLA. However, 10% and 20% vetiver fiber-PLA composites showed the decrease of ($\Delta H_c$) compared to that of neat PLA. In addition, when talc was added in neat PLA, ($\Delta H_c$) was not observed for 1% talc-PLA and 20% talc-PLA composites upon heating (Figure 3.26a). This result suggested that the crystallization of PLA in talc-PLA composites was already taken place in the cooling cycle as shown in Figure 3.25a.

From Table 3.3, it was found that the presence of vetiver fiber and talc in PLA composites led to an increase of $\%X_C$ compared to the neat PLA. With increasing vetiver fiber from 1-10% content, the $\%X_C$ of PLA composites were found to increase compared to that of neat PLA. When vetiver fiber rise to 20% content, a decrease in $\%X_C$ of PLA in vetiver fiber-PLA composites were observed compared to that of other vetiver fiber-PLA composites. The decrease in $\%X_C$ of PLA in PLA composites at 20% vetiver fiber could be ascribed with a high fiber volume fraction, transcrystallinity was occurred only at the interface. Spherulites were not formed in the space between fibers because the distance between fibers was too narrow. Besides, 20% vetiver fiber-PLA composites had high fiber content so that the bulk crystallization did not or less occur in space areas between fibers. Similarly, Tokoro et al. (2007) also found that an increase of bamboo content in PLA/bamboo composites

led to a decrease in $\%X_C$ of PLA. For talc-PLA composites, the $\%X_C$ of PLA in 20% talc-PLA composites decreased compared to that of 1% talc content. This result can be ascribed that high talc content has a lot of interference to crystal growth. Therefore, a large number of small and less perfect crystals were generated. This led to the decrease in $\%X_C$. Medeiros et al. (2001) also found that $\%X_C$ of PP decreased with increasing talc content.

**Table 3.3** Melting enthalpy ($\Delta H_m$), crystallization enthalpy ($\Delta H_c$), and degree of crystallinity ($\%X_C$) of neat PLA and PLA composites from the second heating with the rate of 5ºC/min.

| **Samples** | $\Delta H_m$ **(J/g)** | $\Delta H_c$**(J/g)** | $\%X_C$ |
|---|---|---|---|
| Neat PLA | 31.12 | -29.64 | 33.46 |
| 1% fiber | 32.87 | -30.00 | 35.70 |
| 5% fiber | 33.26 | -31.59 | 37.65 |
| 10% fiber | 33.21 | -28.99 | 39.68 |
| 20% fiber | 26.20 | -20.09 | 35.22 |
| 1% talc | 38.18 | - | 41.47 |
| 20% talc | 28.58 | - | 38.41 |

## 3.5 Conclusions

Isothermal rate of crystallization of talc-PLA composites was the the highest among neat PLA and vetiver fiber-PLA composites. Crystallization rate of 20% vetiver fiber-PLA composites was higher than that of neat PLA and 1% - 10% vetiver fiber composites. Additionally, the equilibrium melting temperature of vetiver fiber-PLA and talc–PLA composites was lower than that of neat PLA. An increase of vetiver fiber content in vetiver fiber-PLA composites led to a decrease in equilibrium

melting temperature of the PLA composites. In addition, at a cooling rate of 10°C/min, crystallization peak of talc-PLA composites was not observed. However, when the cooling rate was slow down to 5°C/min, the crystallization peak of talc-PLA composites was observed. Moreover, upon the second heating scan, re-crystallization peak of talc-PLA composites was found with a heating rate of 10°C/min. Nevertheless, re-crystallization peak of talc-PLA composites was not found with a heating rate of 5°C/min.

In contrast, the crystallization peak of PLA in vetiver fiber-PLA composites was not observed upon cooling even though with lowering cooling rate to 1°C/min. Upon the second heating scan, re-crystallization peak of vetiver fiber-PLA composites was not observed with the heating rate of 20 and 50°C/min. The crystallinity of PLA increased with the presence of talc and vetiver fiber. These indicated that talc and vetiver fiber act as a nucleating agent for the PLA composites.

## 3.6 References

Albano, C., Papa, J., Ichazo, M., González, J., and Ustariz, C. (2003). Application of different macrokinetic models to the isothermal crystallization of PP/talc blends. **Comp. Struct.** 62: 291–302.

Arroyoa, M., Zitzumbob, R., andAvalos, F. (2000). Composites based on PP/EPDM blends and aramid short fibres. Morphology/behaviour relationship. **Polymer.** 41: 6351–6359.

Bledzki, A. K., and Gassan, J. (1999). Composites reinforced with cellulose based fibres. **Prog. Polym. Sci.** 24: 221-274.

Chen, X., Hou, G., Chen, Y., Yang, K., Dong, Y., and Zhou, H. (2007). Effect of molecular weight on crystallization, melting behavior and morphology of poly(trimethylene terephalate).**Polym. Test.** 26: 144–153.

Cheung, H.-Y., Lau, K.-T., Tao, X.-M., and Hui, D. (2008). A potential material for tissue engineering: Silkworm silk/PLA biocomposite. **Comp. Part B: Eng.** 39: 1026-1033.

Day, M., Victoria, A., Nawaby, and Liao, X. (2006). A DSC study of the crystallization behavior of polylactic acid its nanocomposites. **J. Therm. Anal. Calorim.** 86: 623-629.

Ganster, J., Fink, H.-P., and Pinnow, M. (2006). High-tenacity man-made cellulose fibre reinforced thermoplastics – Injection moulding compounds with polypropylene and alternative matrices. **Compos. Part A.** 37: 1796-1804.

He, Y., Fan, Z., Yanfei Hu, Y., Wu, T., Jia Wei J., and Li, S. (2007). DSC analysis of isothermal melt-crystallization, glasstransition and melting behavior of poly(L-lactide)with different molecular weights. **Europ. Polym. J**. 43: 4431–4439.

Hu, R.-H., Lim, J.-K., Kim, C.-I., and Yoon, H.-C. (2007). Biodegradable Composites Based on Polylactic Acid(PLA) and China Jute Fiber. **Eng. Mater.** 353-358: 1302-1305.

Huda, M. S., Drzal, L. T., Mohanty, A. K., and Misra, M. (2008). Effect of fiber surface-treatments on the properties of laminated biocomposites from poly(lactic acid) (PLA) and kenaf fibers. **Compos. Sci. Technol.** 68: 424-432.

Huda, M. S., Drzal, L. T., Mohanty, A. K., and Misra, M. (2006). Chopped glass and recycled newspaper as reinforcement fibers in injection molded poly(lactic

acid) (PLA) composites: A comparative study. **Compos. Sci. Technol.** 66: 1813-1824.

Iovino, R., Zullo, R., Rao, M. A., Cassar, L., and Gianfreda, L. (2008). Biodegradation of poly(lactic acid)/starch/coir biocomposites under controlled composting conditions. **Polym. Degrad. Stab.** 93: 147-157.

Junga, Y., Kim, S.-S., Kim, Y., Kim, S. H., Byung, S. K., Kim, Y. S., YongChoi, C., and Kim, S. H. (2005). A poly(lactic acid)/calcium metaphosphate composite for bone tissue engineering. **Biomaterials.** 26: 6314-6322.

Kawai, T., Rahman, N., Matsuba, G., Nishida, K., Kanaya, T., Nakana, M., Okamoto, H., Kawada, J., Usuki, A., Honma, N., Nakajima, K., and Mutsuda M. (2007). Crystallization and melting behavior of poly (L-lactic acide). **Macromolecules.** 40: 9463-9469.

Khondker, O. A., Ishiaku, U. S., Nakai, A., and Hamada, H. (2006). A novel processing technique for thermoplastic manufacturing of unidirectional composites reinforced with jute yarns. **Compos. Part A.** 37: 2274-2284.

Krikorian, V., and Pochan, D. J. (2004). Unusual Crystallization Behavior of Organoclay Reinforced Poly(L-lactic acid) Nanocomposites. **Macromolecules.** 37: 6480-6491.

Kuana, C.-F., Kuana, H.-C., M.Mab, C.-C., and Chen, C.-H. (2008). Thermal and electrical conductivity of poly(L-lactide)/multiwalled carbon nanotube nanocomposites. **J. Phys. Chem. Solids.** 69: 1395-1398.

Lee, S.-H., and Wang, S. (2006). Biodegradable polymers/bamboo fiber biocomposite with bio-based coupling agent. **Compos. Part A.** 37: 80-91.

Li, H., and Huneault, M. A. (2007). Effect of nucleation and plasticization on the crystallization of poly(lactic acid). **Polymer.** 48: 6855-6866.

Mathot, V. B.F. (1994). Calorimetry and thermal analysis of polymers. New York : Hanser publishers.

Medeiros, E. S. de., Tocchetto, R. S., Carvalho, L. H. de., Santos, I. M. G., and Souza, A. G. (2001). Nucleating effect and dynamic crystallization of apoly (propylene) /talc system. **J. Therm. Anal. Cal.** 66 : 523-531.

Miyata, T., and Masuko, T. (1998). Crystallization behaviour of poly(-lactide). **Polymer.** 39: 5515-5521.

Nishino, T., Hirao, K., and Kotera, M. (2006). X-ray diffraction studies on stress transfer of kenaf reinforced poly(L-lactic acid) composite. **Compos. Part A.** 37: 2269-2273.

Oksmana, K., Skrifvarsb, M., and Selinc, J.-F. (2003). Natural fibres as reinforcement in polylactic acid (PLA) composites. **Compos. Sci. Technol.** 63: 1317-1324.

Parka, J.-M., Kima, D.-S., and Kimb, S.-R. (2003). Interfacial properties and microfailure degradation mechanisms of bioabsorbable fibers/poly-l-lactide composites using micromechanical test and nondestructive acoustic emission. **Comp. Sci. Technol.** 63: 403-419.

Sanchez-Garcia, M. D., Gimenez, E., and Lagaron, J. M. (2008 ). Morphology and barrier properties of solvent cast composites of thermoplastic biopolymers and purified cellulose fibers. **Carbo. Polym.** 71: 235-244.

S´ anchez, M. S., Ribelles, J.L. G., S´ anchez, F. H., Mano, J.F. (2005). On the kinetics of melting and crystallization of poly(l-lactic acid) by TMDSC. **Thermochimica acta.** 430: 201-210.

Smith, D., Drews. M.J., and Vasanthan, N. (2005). Poly(lactic acid) Derived Fibers with Enhanced Performance. **National Textiles Center Annual Report.** 1-10.

Thanomkiat, P., Phillips, R.A., and Supaphol, P. (2004). Influence of molecular characteristics on overallisothermal melt-crystallization behavior and equilibrium melting temperature of syndiotactic polypropylene. **Euro. Polym. J.** 40: 1671–1682

Tsuji, H., Kawashima, Y., Takikawa, H., and Tanaka, S. (2007). Poly(L-lactide)/nano-structured carbon composites: Conductivity, thermal properties, crystallization, and biodegradation. **Polymer.** 48: 4213-4225.

Vasanthakumari, R., and Penning, A. J. (1983). Crystallization kinetics of poly(L-lactic acid). **Polymer.** 24:175-178.

Wang, Y., and Mano, J. O. F. (2005). Influence of melting conditions on the thermal behaviour of poly(L-lactic acid). **Euro. Polym. J.** 41: 2335-2342.

Wong, S., Shanks, R. A., and Hodzic, A. (2007). Effect of additives on the interfacial strength of poly(L-lactic acid) and poly(3-hydroxy butyric acid)-flax fibre composites. **Compos. Sci. Technol.** 67: 2478-2484.

Yeh, J.T., Huang, C. Y., Chai, W. L., and Chen, K. N. (2009). Plasticized Properties of Poly (lactic acid) and Triacetine Blends. **J. Appl. Polym. Sci.** 112: 2757–2763.

Zhang, Z., Wang, C., Yang, Z., Chen, C., and Mai, K. (2008). Crystallization behavior and melting characteristics of PP nucleated by a novel supported β-nucleating agent. **Polymer.** 49: 5137–5145.

Srimoaon, P., Dangseeyun, N., and Supaphol, P. (2004). Multiple melting behavior in isothermally crystallized poly(trimethylene terephthalate). **Euro. Polym. J.** 40: 599–608.

# CHAPTER IV

# THE STUDY OF GROWTH RATE OF POLY (LACTIC ACID) AND POLY (LACTIC ACID) COMPOSITES

## 4.1 Abstract

In this research, the growth rate of vetiver fiber-PLA composites was investigated. To study the role of vetiver fiber on crystallization of PLA composites, talc as a nucleating agent was used to compare a nucleating effecting between talc and vetiver fiber. Spherulitic growth rate was determined by using a hot stage under a Polarized Light Optical Microscope (POM). Transcrystallization (TC) was observed at the interface between vetiver fiber and PLA. Spherulitic growth rate of PLA in the bulk and on vetiver surface of vetiver fiber-PLA composites was lower than that of neat PLA. In addition, for vetiver fiber-PLA composites, spherulitic growth rate of PLA in TC region was lower than that of PLA in the bulk. Similarly, for talc-PLA composites, spherulitic growth rate of PLA in TC region was lower than that of PLA in the bulk. However, spherulitic growth rate of PLA in the bulk of talc-PLA composites was higher than that of vetiver fiber-PLA composites. Similarly, spherulitic growth rate of PLA in TC region of talc-PLA composites was higher than that of vetiver fiber-PLA composites. Moreover, spherulitic growth rate of PLA in the bulk of talc-PLA composites showed the highest. The Hoffman-Laurizen growth equation was used for determining the growth rate in the bulk and also applied to the

growth rate in TC region. It was found that growth rate of neat PLA and PLA composites was illustrated by a bell-shaped curve as a function of temperature.

KEYWORDS: Growth rate/Poly (lactic acid)/Vetiver fiber/Talc

## 4.2 Introduction

Poly (lactic acid) (PLA) is the first commodity polymer produced from renewable resources. The benefits of PLA manufacturing process include low energy to produce and reduction of green house gas production. Moreover, it inherent has high strength, high modulus that is made from renewable resources. It is one of a few polymers in which the stereochemical structures are easily be modified by polymerizing a controlled mixture of the L - or D-isomers to yield high molecular-weight amorphous or crystalline polymers (Garlotta, 2001). It is a rigid polymer that is either semicrystalline or totally amorphous, depending on the stereopurity of the PLA backbone (Mohanty et al., 2005).

In order for PLA to be processed on large-scale applications such as injection molding, blow molding, thermoforming, and extrusion, the polymer must possess adequate thermal stability to prevent degradation and maintain desired molecular weight and properties. PLA degradation depends on time, temperature, low molecular weight impurities, and catalyst concentration. Catalysts and oligomers decrease the degradation temperature and increase the degradation rate of PLA. In addition, they may cause viscosity changes and poor mechanical properties (Garlotta, 2001).

Generally, which properties of its composites were affected by its crystallization behavior. Therefore, the studies on crystallization behavior of composites are significant. Previously, crystallization of PLA composites in the presence of nucleating agents

was also studied (Li, 2007). Nucleating agent is a chemical substance which initiate nuclei for the growth of crystals in the polymer melt. The nucleating agent has affected the crystalline morphology of the polymer. Usually, the crystallinity increased and the crystallization rate was accelerated with the nucleating agent effect (Xu et al., 2003). Li (2007) found that talc was an effective nucleating agent for PLA. In the same way, natural fibers were reported that they induce crystal nucleation of polymers at the fiber surface. This was so-called transcrystallization in several polymer matrix such as PP (Choudhury, 2008), PE (Vaisman et al., 2003) and PHA (Dufresne et al., 1999).

From previous study, the vetiver grass was shown to be an effective filler in polypropylene (PP) composites. It was found that the presence of vetiver grass led to an increase in tensile strength and Young's modulus of PP composites (Ruksakulpiwat et al., 2007). As mentioned before, PLA is a biodegradable polymer while PP is not, therefore the use of PLA biopolymer instead of PP polymer is interesting. Moreover, the use of vetiver grass as a filler in PLA composites has never been published. In addition, the crystallization of vetiver grass filled PLA composites was comparatively studied to that of talc filled PLA composites.

## 4.3 Experimental

### 4.3.1 Materials and chemical reagents

Poly (lactic acid) (PLA 4042D) was purchased from Nature Works, LLC. Vetiver grass (*Vetiveria Zizanioides*) was obtained from The Land Development Department, Nakhon Ratchasima, Thailand. The ages of vetiver grass are around 6–8 months. Sodium hydroxide (NaOH) (laboratory grade) was purchased from Italmar (Thailand) Co., Ltd. Talc (86255) with average particle size of 45 μm was purchased from Fluka.

### 4.3.2 Vetiver fibers preparation

Vetiver leaves was washed by water to get rid of dirt and dried by sunlight for one day. The washed vetiver leaves were ground by a Retsch grinder machine and sieved into the length of 2 mm to obtain the vetiver fiber. Vetiver fiber with 2 mm length was firstly washed by water to eliminate dirt and dried in an oven at 100°C overnight. After that, the vetiver fiber was immersed in a solution of 4% (wt/v) NaOH for 2 h at 40°C and the vetiver-to-solution ratio was 1:25 (wt/v) to obtain the alkali-vetiver fiber. The alkali-vetiver fiber was then washed thoroughly with water and dried in an oven at 100°C for 24 h. These vetiver fibers were used to prepare the composites throughout this study.

### 4.3.3 Preparation of vetiver fiber-PLA and talc-PLA composites

In this study, 1% (wt/wt) vetiver fiber-PLA composites were used to study the growth rate of vetiver fiber-PLA composites. No effect of vetiver fiber content on growth rate of vetiver fiber-PLA composites was assumed. 1% (wt/wt) vetiver fiber was mixed with neat PLA at 180°C in an internal mixer (Haake Rheomix 3000P). Mixing speed and mixing time were 50 rpm and 13 minutes, respectively. After that, PLA composites were ground and dried before use. In order to compare the role of vetiver fiber and talc on crystallization of PLA composites, the same mixing procedure was applied to mix 1% talc with neat PLA.

### 4.3.4 Sample preparation

Thin films of neat PLA, vetiver fiber-PLA and talc-PLA composites were prepared by a compression molding machine at 180ºC. These thin films were used to investigate the spherulitic growth rate (G) of neat PLA and PLA composites.

### 4.3.5 Spherulitic growth rate

The spherulitic growth rate (G) was measured using a hot stage (Linkam TH600) under a Polarized Light Optical Microscope attached with CCD video camcorder system (Sony). The sample was heated from room temperature to 220ºC with a heating rate 20ºC/min and held at that temperature for 5 min to remove thermal history. Then, the sample was cooled down with a rate of 50ºC/min to various $T_c$. The radius of spherulite was measured as a function of time. The growth rate (G) at each $T_c$ was obtained from the slope of the plot of spherulite radius versus crystallization time. The experimental growth rate was used to fit with the Hoffman and Lauritzen growth rate equation as (Hoffman et al., 1976):

$$G(T) = G_o \exp\left[\frac{-U^*}{R(T_c - T_\infty)}\right]\exp\left[\frac{-K_g}{T_c(\Delta T)f}\right] \tag{4.1}$$

Where G(T) is the radial growth rate.

$G_0$ is the pre-exponential factor containing quantities no strongly dependent on temperature.

$U^*$ is a universal constant characteristic of the activation energy of chain motion (reptation) in the melt.

R is a gas constant.

$K_g$ is the nucleation constant.

$T_\infty$ is the theoretical temperature at which all motion associated with viscous flow or reptation ceases, and is defined as $T_\infty = T_g - 30$ (K).

$f$ is the correction factor $f = 2T_c/(T^\circ_m + T_c)$, which account for the temperature dependence of $\Delta h_f$, $f$ has little effect at small supercoolings, but decrease $\Delta h_f$ considerarable near the glass transition temperature.

$T^\circ_m$ is the equilibrium melting temperature.

$\Delta T$ is the supercooling and is equal to $T^\circ_m - T_c$.

## 4.4 Result and discussion

Figure 4.1 (a)-(d) show optical micrographs of crystallizing PLA of taken during isothermal crystallization at 130°C. It was observed that spherulites of PLA in the bulk of neat PLA were found during isothermal crystallization. The spherulite diameter of PLA in neat PLA increased with increasing time. Figure 4.2 (a)-(d) represented optical micrographs of crystallizing PLA in the bulk and on vetiver fiber surface of vetiver fiber-PLA composites taken during isothermal crystallization at 130°C. Similarly, spherulites of PLA in the bulk of vetiver fiber-PLA composites were observed during crystallization. Transcrystallization (TC) was taken place at the surface of vetiver fiber. TC morphology is formed by a dense heterogeneous nucleation of PLA crystals at the vetiver fiber surface which growing perpendicularly to the fiber axis. The growth of TC proceeds perpendicularly to the fiber until the growing front impinges to spherulites in the bulk. The TC forming at the surface of vetiver fiber was also observed in vetiver fiber-PP composites by Somnuk, U., et al., (2007). Moreover, TC forming at various fiber surface was also found in various polymer matrix such as bamboo-PLA (Tokoro, Okubo, Tanaka, Fujii, and Fujiura, 2008) hemp fibres-poly

(hydroxybutyrate-co-hydroxyvalerate) (PHBV) (Hermida and Mega, 2007), carbon fiber-PP, Kevlar-PP, PET-PP, PTFE-PP (Wang and Liu, 1997), and short flax fiber-PP composites (Arbelaiz, Fernández, Ramos, and Mondragon, 2006). From Figure 4.2 (a)-(d), it was observed that the spherulite diameter of PLA in the bulk of vetiver fiber-PLA composites increased with increasing time. Meanwhile, a width of spherulite of PLA in TC region of vetiver fiber-PLA composites also increased with increasing time. Optical micrographs of crystallized PLA in the bulk and in TC region of talc-PLA composite were shown in Figure 4.3 (a)-(d). Similar to the results of crystallized PLA in the bulk and in TC region of vetiver fiber-PLA composites, the spherulite diameter of PLA in the bulk of talc-PLA composites increased with increasing time. A width of spherulite of PLA in TC region of talc-PLA composites increased with increasing time. Spherulitic growth rate at various crystallization temperatures of PLA in the bulk was determined by measuring radius of spherulite as a function of time. Growth rate of TC in vetiver fiber-PLA composites was evaluated by measuring a width of the TC region perpendicularly preceded to the fiber surface as a function of time. Similarly, spherulitic growth rate of PLA in the bulk and in TC region in talc-PLA composites were measured with the same procedure.

Radius of spherulite plotted against time during isothermal crystallization for neat PLA was shown in Figure 4.4. It was shown that the radius of spherulite increased linearly with the crystallization time at all crystallization temperatures. Similarly, linearly increased of spherulitic radius with the crystallization time was observed in the bulk of vetiver fiber-PLA and talc-PLA composites, as shown in Figure 4.5 and 4.6 respectively. The spherulite width plotted against time during isothermal

crystallization in TC region of vetiver fiber-PLA and talc-PLA composites were also shown in Figure 4.7 and 4.8, respectively.

It was observed that the spherulites of neat PLA (Figure 4.4) were finally larger than that of vetiver fiber-PLA (Figure 4.5) and talc-PLA composites occurring in the bulk (Figure 4.6). Similarly, the spherulites in TC region of vetiver fiber-PLA and talc-PLA composites (Figure 4.7 and Figure 4.8, respectively) were smaller than those occurring in the bulk and those of neat PLA as well. For talc-PLA composites, the final spherulites in the bulk were smallest among neat PLA and vetiver fiber-PLA composites. The smallest spherulites of talc-PLA composites in both bulk compared to those of neat PLA and vetiver fiber-PLA were shown in Figure 4.9. Figure 4.9 (a)-(c) shows optical micrographs of PLA spherulites during crystallization at 115°C in neat PLA, vetiver fiber-PLA and talc-PLA composites, respectively. From Figure 4.9 (a), neat PLA has lower number of nuclei than that of vetiver fiber-PLA and talc-PLA composites. Meanwhile, the size of PLA spherulites in neat PLA was larger than that of vetiver fiber-PLA and talc-PLA composites. When vetiver fiber was added in neat PLA (Figure 4.9 (b)), the number of nuclei of vetiver fiber-PLA composites was higher than that of neat PLA indicating by the higher number of spherulites. By adding talc into neat PLA (Figure 4.9 (c)), it was clearly seen that the amount of spherulites of talc-PLA composites was the highest compared to that of neat PLA and vetiver fiber-PLA composites. This implied that the nucleation density of talc-PLA composites was higher than those of neat PLA and vetiver fiber-PLA composites, led to the smaller size of spherulites of talc-PLA composites. It could be suggested that the vetiver fiber and talc act as a nucleating agent in the PLA composites. Ferrage et al. (2002) also found that the presence of talc particles caused an increase of nuclei

density and led to a large number of PP spherulites. Albano et al. (2003) reported that nucleating agents affected in decreasing the spherulites size and increasing their number as compared with neat polymer.

Then spherulitic growth rates of neat PLA and PLA composites were investigated. Spherulitic growth rates were obtained from the slope of each plot of radius of spherulites and width of spherulites as function of crystallization time as shown in Figure 4.4-4.8 and shown in Figure 4.10. From Figure 4.10, spherulitic growth rate at various crystallization temperatures was showed

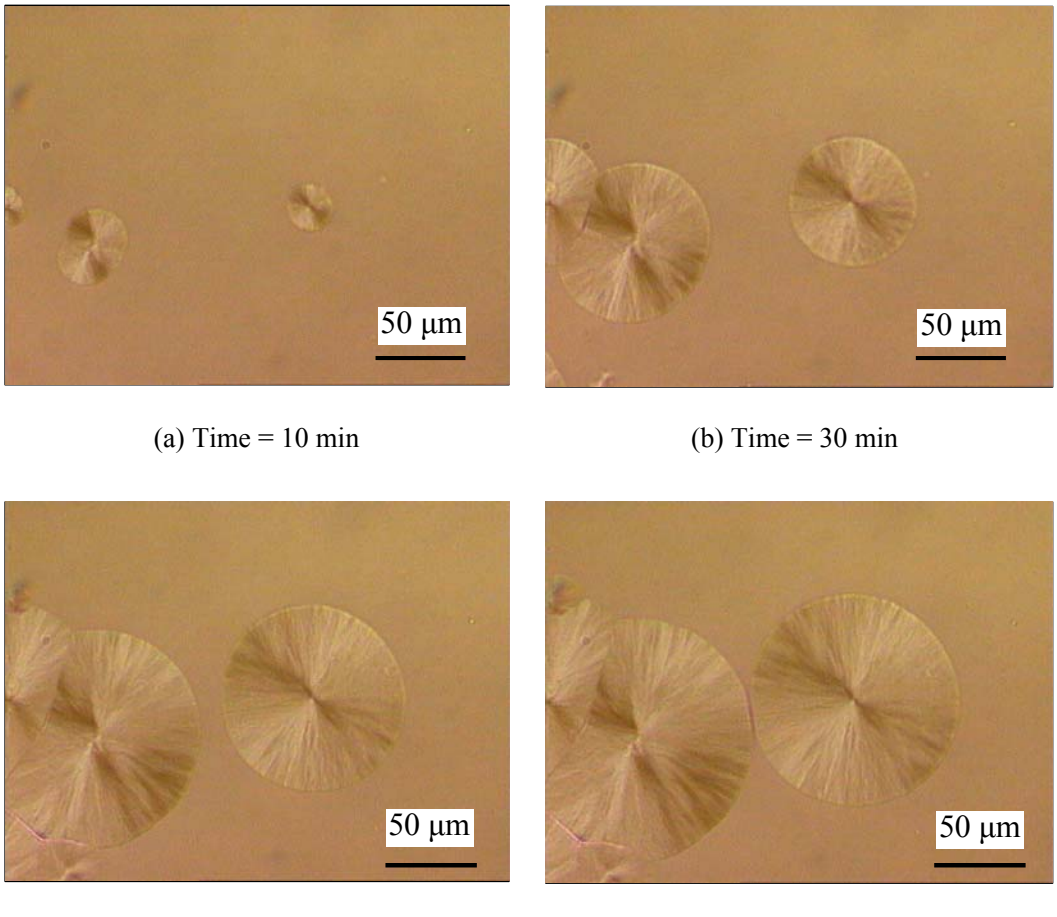


**Figure 4.1** Optical micrographs of spherulites of neat PLA grown from the melt during isothermal crystallization at 130ºC at various crystallization times.

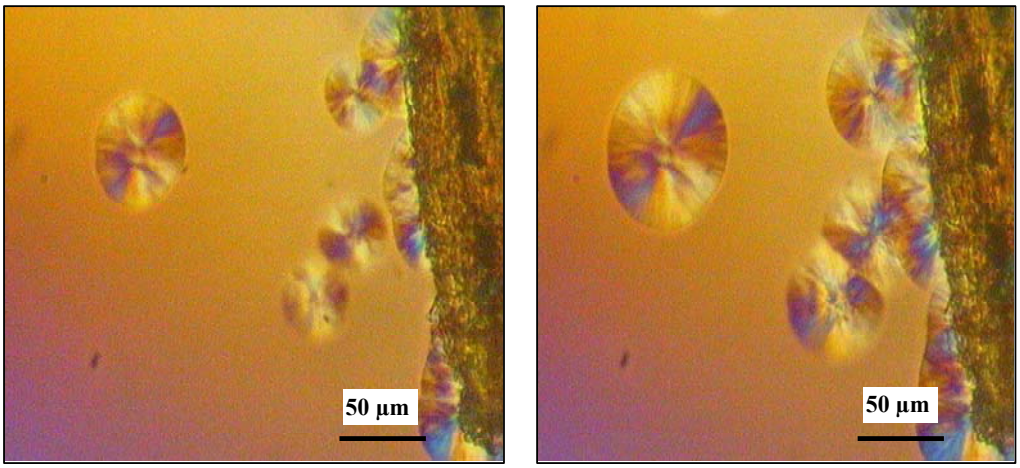


(a) Time = 10 min (b) Time = 30 min

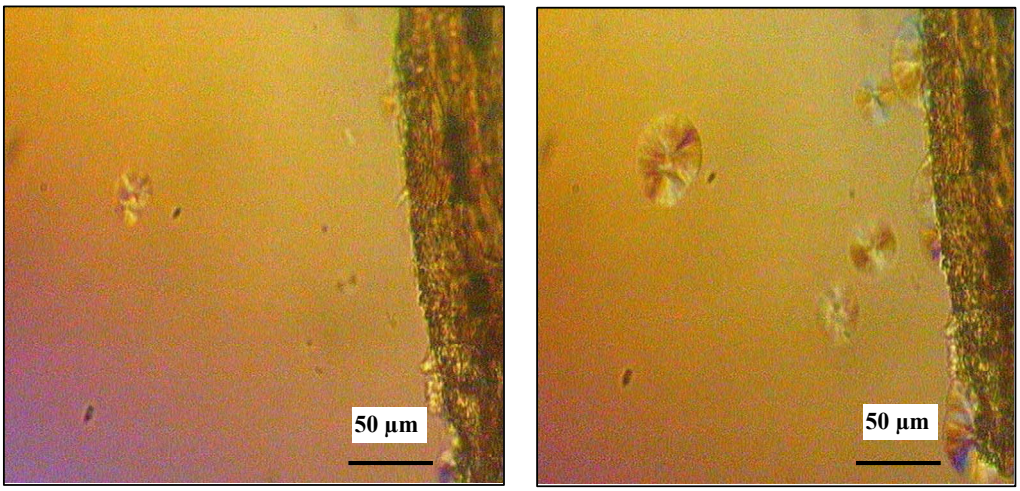


(c) Time = 40 min (d) Time = 50 min

**Figure 4.2** Optical micrographs of spherulites in vetiver fiber-PLA composites grown from the melt during isothermal crystallization at 130ºC at various crystallization times.

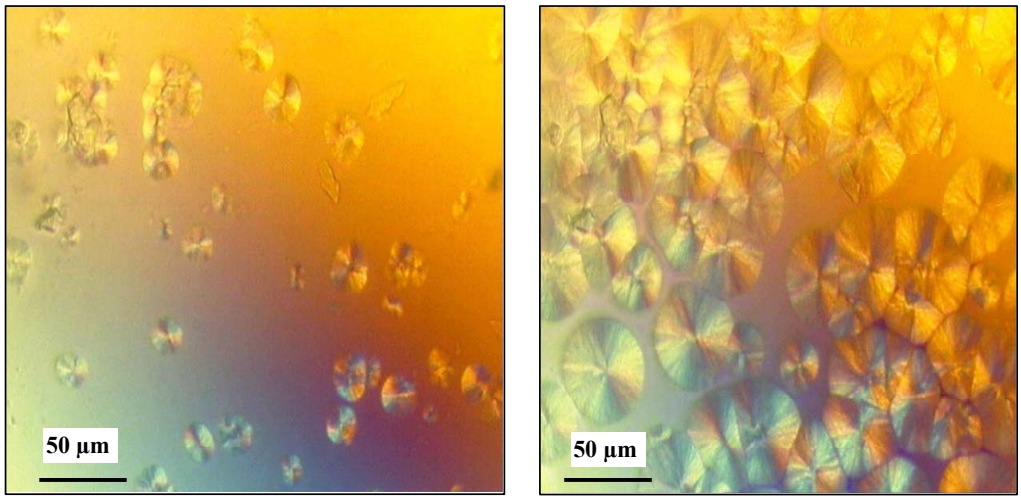


(a) Time = 10 min




(b) Time = 30 min

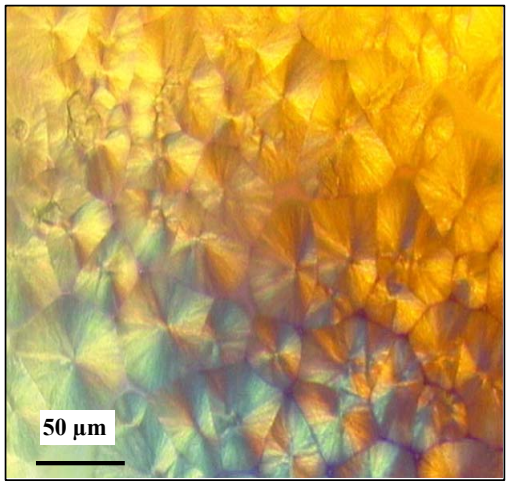


(c) Time = 40 min

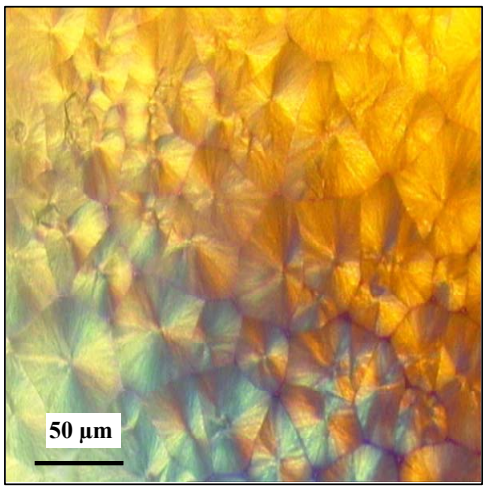


(d) Time = 50 min

**Figure 4.3** Optical micrographs of spherulites in talc-PLA composites grown from the melt during isothermal crystallization at 130ºC at various crystallization time.

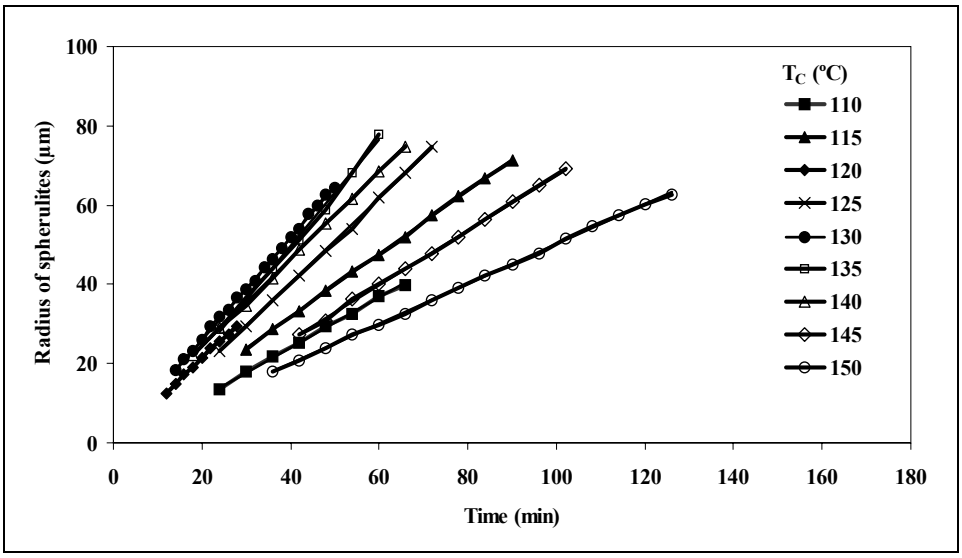


**Figure 4.4** Spherulite radius plotted against crystallization time during isothermal crystallization at various crystallization temperatures ($T_c$) of neat PLA.

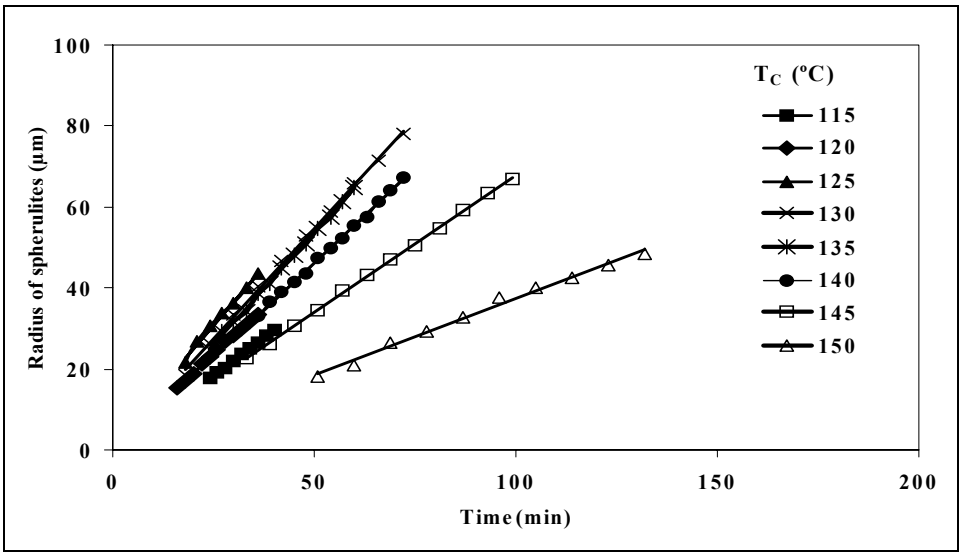


**Figure 4.5** Spherulite radius plotted against crystallization time during isothermal crystallization of bulk PLA in vetiver fiber-PLA composites at various crystallization temperatures ($T_c$).

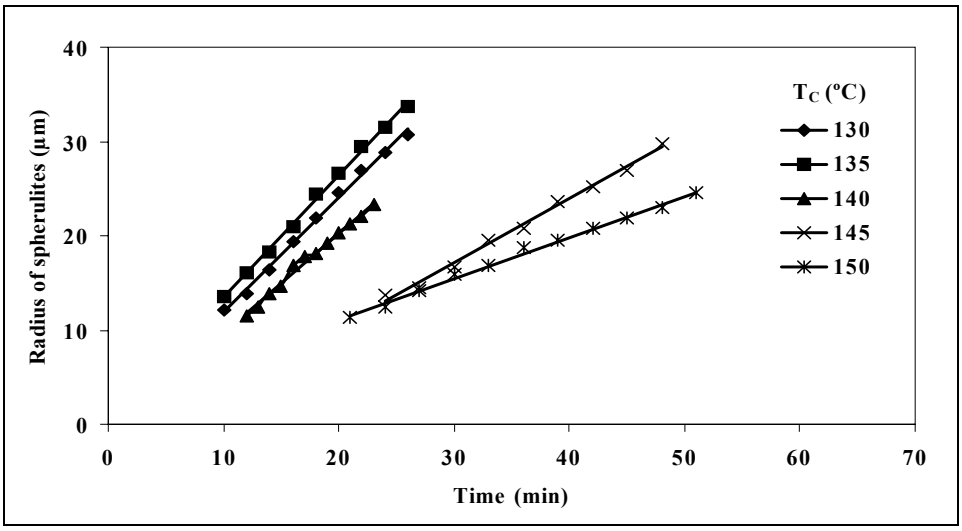


**Figure 4.6** Spherulites radius of bulk PLA in the talc-PLA composites plotted against crystallization time during isothermal crystallization at various crystallization temperatures ($T_c$).

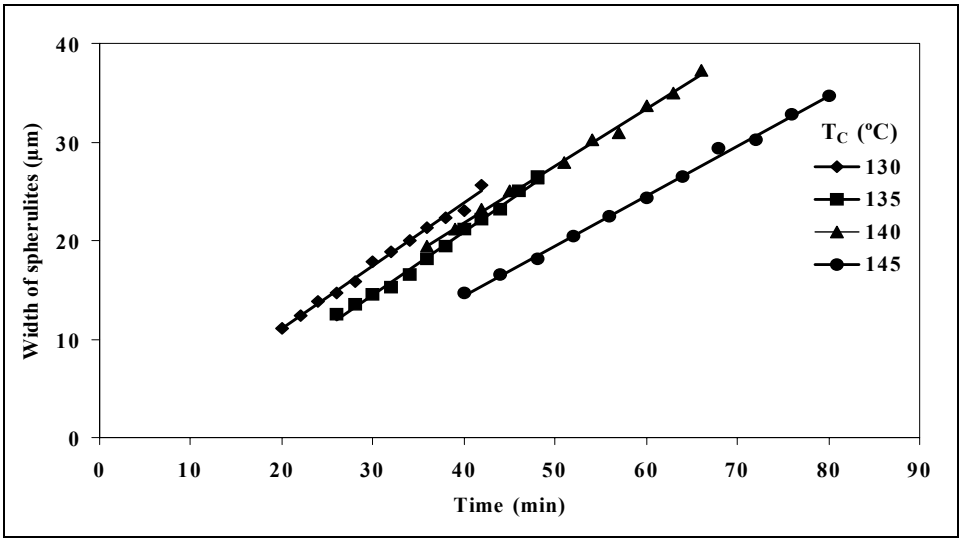


**Figure 4.7** Spherulites radius of PLA at the TC region in talc-PLA composites plotted against crystallization time during isothermal crystallization at various crystallization temperatures ($T_c$).

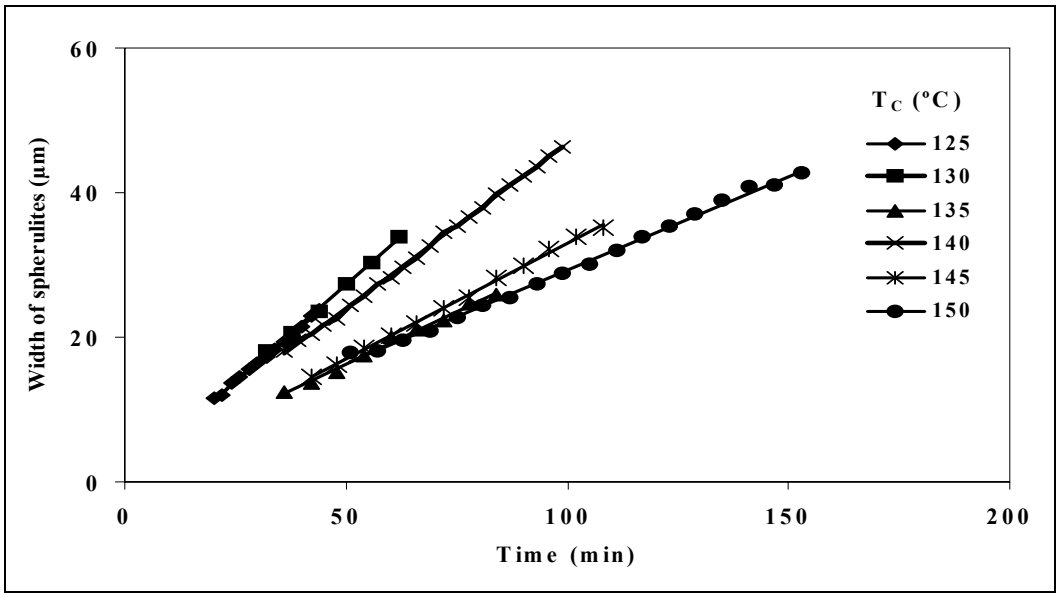


**Figure 4.8** Spherulite radius of PLA at the TC region in vetiver fiber-PLA composites plotted against crystallization time during isothermal crystallization at various crystallization temperatures ($T_c$).

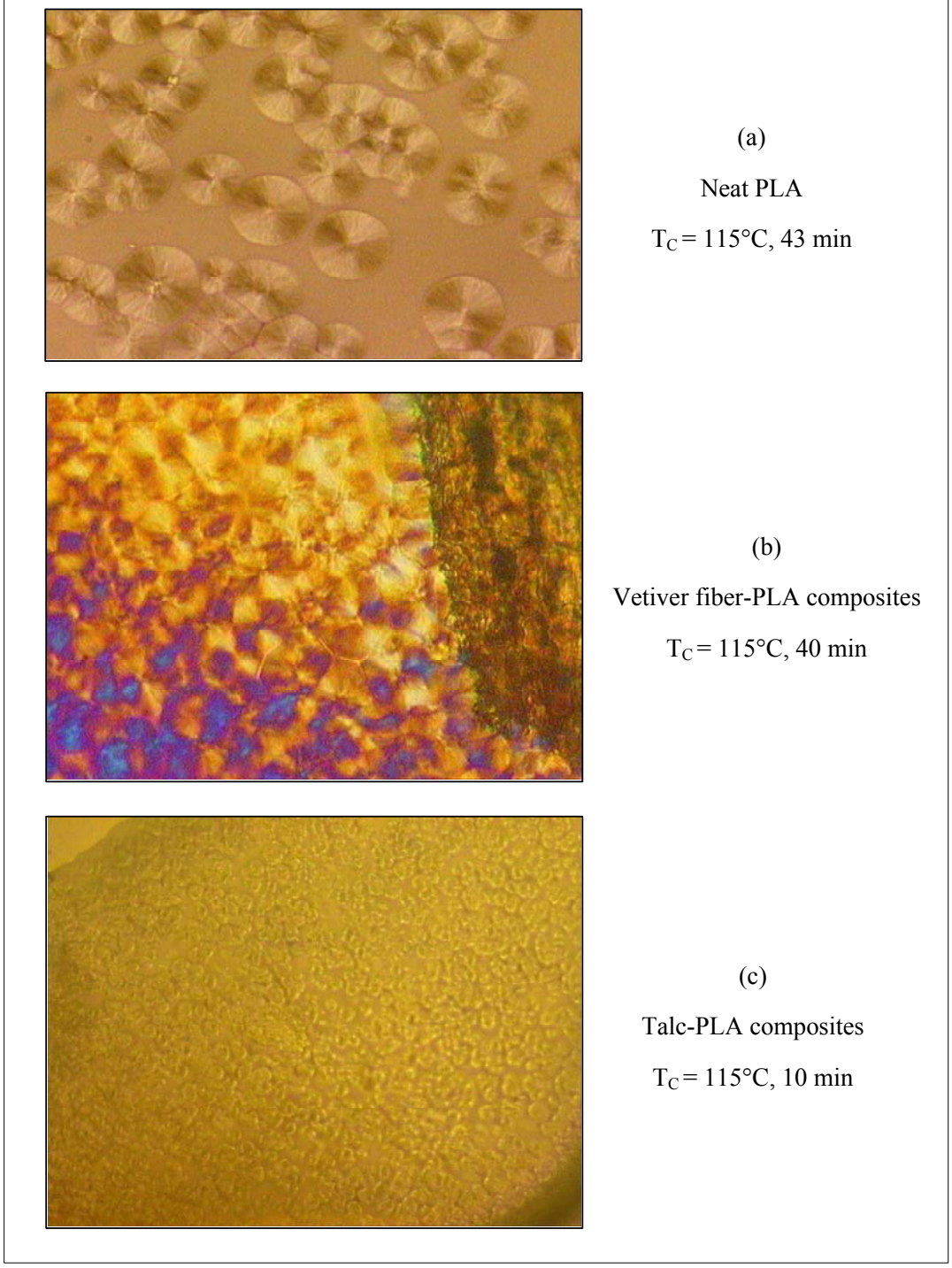


**Figure 4.9** Optical micrographs of PLA spherulites in neat PLA (a) vetiver fiber-PLA (b) and talc-PLA (c) composites during crystallization at temperature of 115°C.

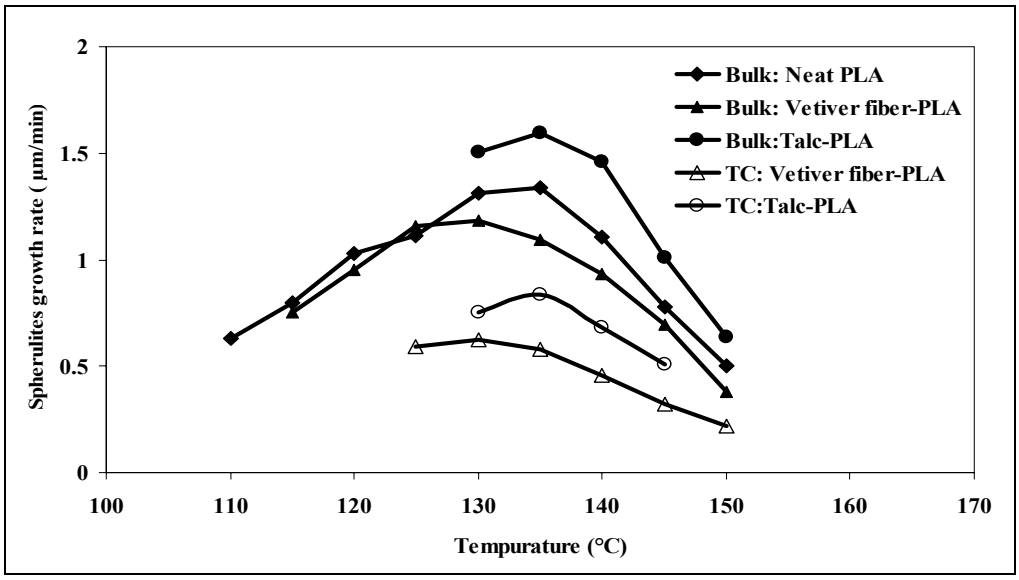


**Figure 4.10** Spherulitic growth rate of neat PLA, vetiver fiber-PLA and talc-PLA composites at various crystallization temperatures.

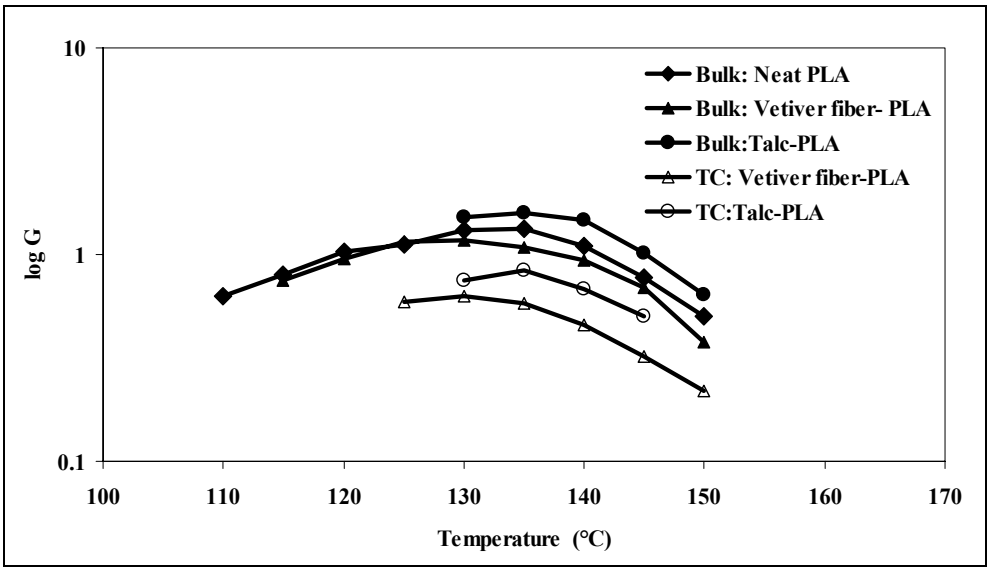


**Figure 4.11** Spherulitic growth rates in logarithmic scale (Log G) as a functionof crystallization temperatures.

Figure 4.11 shows spherulitic growth rate in logarithmic scale (Log G as a function of crystallization temperatures ($T_c$). The spherulitic growth rate as a function of $T_c$ shows a bell shape curve. It has been reported for PLLA that spherulitic growth rate curve showed discontinuity. The discontinuity of spherulitic growth rate curve of PLA was found around 113°C by Yasuniwa et al. (2006) and 120°C by Di Lorenzo (2005). It was known that the discontinuity depends on the molecular weight (Abe, Kikkawa, Inoue, and Doi, 2001), incorporation of co-monomer unit, and tacticity (Tsuji et al., 2005). Most possible explanation for the discontinuity might be the difference in the crystal modification, which was proposed by Zhang et al. (2006). However, the discontinuity was not observed in this study. From Figure 4.11, spherulitic growth rate of neat PLA, PLA in the bulk and in TC region of vetiver fiber and talc can be elucidated.

It was found that the growth rate in the bulk of neat PLA was higher than that of PLA in the bulk of the vetiver fiber-PLA composites. Similar to Somnuk, U., et al., (2007) they also found that the growth rate of neat PP was higher than that of PP in the bulk of the vetiver fiber–PP composites. This may be due to the restriction of chain mobility caused by the fiber.

The growth rate of PLA in the bulk of talc-PLA composites was noticeably higher than that of neat PLA and vetiver fiber-PLA composites. Moreover, it was observed that the growth rate in TC region of talc-PLA composites was greater than that of vetiver fiber-PLA composites. This implied that talc was more favorable for the nucleation of crystallization than vetiver fiber. In addition, it was observed that the growth rate of crystallizing PLA in the bulk of vetiver fiber-PLA and talc-PLA composites were greater than that of crystallizing PLA in TC region.

Generally, the rate of crystallization depends on both nucleation rate and growth rate. In this study, it was found that the growth rate of PLA in the bulk, in TC region of vetiver fiber and talc-PLA composites were lower than that of neat PLA. However, the higher rate of crystallization of PLA in PLA composites than that of neat PLA was observed. This implied that the nucleation rate dominated the growth rate. This was also found in natural fiber-PP composites by Somnuk et al. (2007).

The experimental growth rate of neat PLA and PLA composites at various $T_c$ were then fitted to Equation (4.1). The fitting parameter for the spherulitic growth rate, $K_g$ and $G_0$ in the bulk and at the TC region were elucidated from Figures 4.12 and 4.13 and then listed in Tables 4.1 and 4.2, respectively. From Figures 4.12 and 4.13, it was found that bout Kg of vetiver fiber PLA and talc-PLA composites in bulk and in TC region was lower than that of neat PP in bulk. It is well-known that a foreign surface frequently reduces the nucleus size need for crystal growth. This because the creation of the interface between polymer crystal and substrate might be lee hindered than the creation of the corresponding free polymer crystal surface. Heterogeneous nucleation paths make use of a foreign pre-existing surface to reduce the free energy opposing primary nucleation (Somnuk, U., et al., 2007). Additionally, it showed that the G0 of vetiver-PLA and talc-PLA composites were lower than that of neat PLA. This could be suggested that the incorporation of vetiver fiber and talc into PLA caused a decrease of free volume available for PLA chain to move.

Figure 4.14 shows a plot of growth rate of crystallizing PLA in the bulk and TC region of vetiver fiber-PLA and talc-PLA composites as a function of temperature. It could be found that the Hoffman-Lauritzen equation, Equation (4.1), used for determining the growth rate in the bulk could also be applied to the growth rate in TC

region. From Figure 4.14, it was showed that growth rate of both neat PLA and PLA composites were bell-shaped curve as function of temperature. In this study, the maximum growth rate of neat PLA and PLA composites was found approximately at 135°C. However, two maximum growth rates were reported by other researchers. Kawai et al. (2007) reported that two maximum growth rates were found at 105°C and 130°C. Meanwhile, Di Lorenzo et al. (2008) found the maximum spherulite growth rate around 115°C and 130°C.

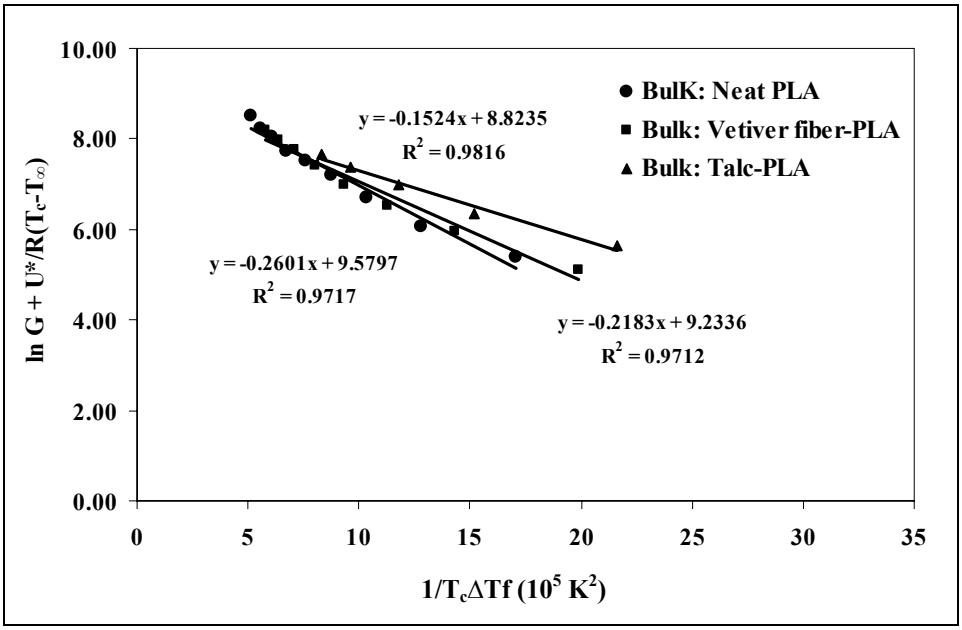


**Figure 4.12** Hoffman-Lauritzen plots for determining $K_g$ and $G_0$ of PLA in the bulk of neat PLA, vetiver fiber-PLA and talc-PLA composites.

**Table 4.1** Nucleation constant ($K_g$) and pre-exponent factor ($G_0$) of PLA in the bulk of neat PLA, vetiver fiber-PLA and talc-PLA composites.

| Samples | $K_g$ ($K^2$) | $G_0$ (μm/min) |
|---|---|---|
| Neat PLA | $2.60x10^4$ | $1.45x10^4$ |
| Vetiver fiber-PLA | $2.18x10^4$ | $1.02x10^4$ |
| Talc-PLA | $1.52x10^4$ | $0.68x10^4$ |

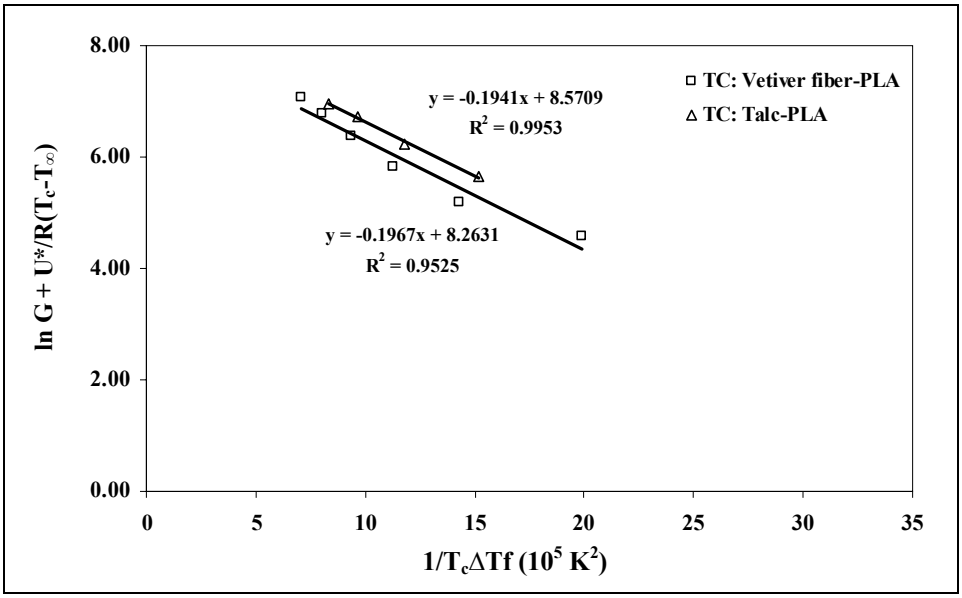


**Figure 4.13** Hoffman-Lauritzen plots for determining $G_0$ and $K_g$ of PLA at TC region of vetiver fiber-PLA and talc-PLA composites.

**Table 4.2** Nucleation constant ($K_g$) and pre-exponent factor ($G_0$) of PLA in TC region of vetiver fiber-PLA and talc-PLA composites.

| Samples | $K_g$ ($K^2$) | $G_0$ (μm/min) |
|---|---|---|
| Vetiver fiber-PLA | $1.97x10^4$ | $0.39x10^4$ |
| Talc-PLA | $1.94x10^4$ | $0.53x10^4$ |

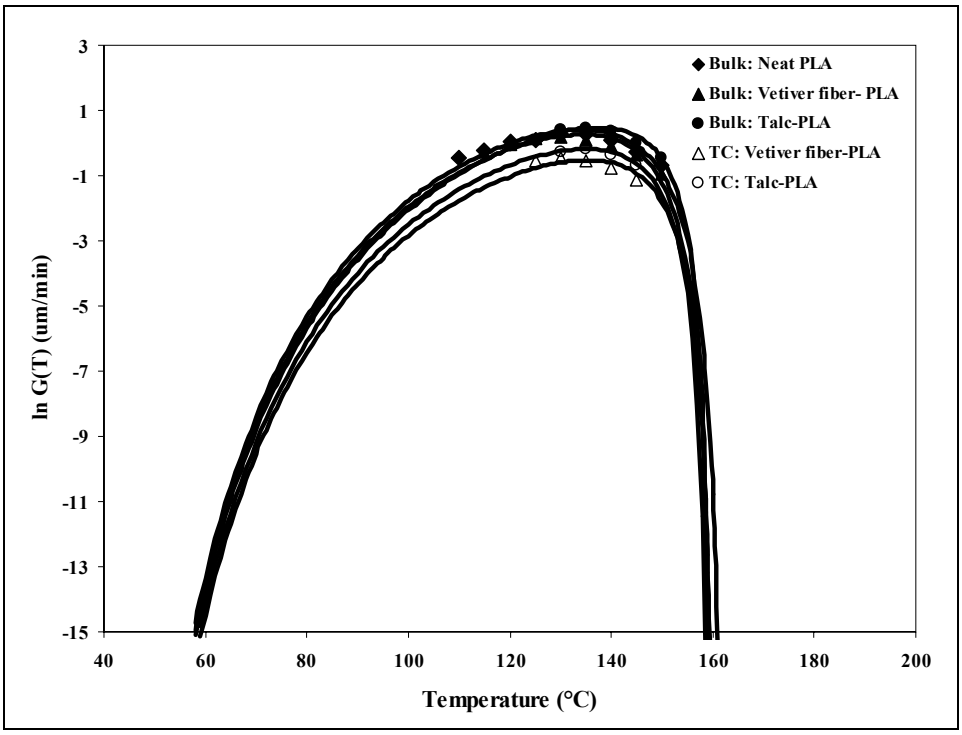


**Figure 4.14** Plot of growth rate of PLA crystallized in the bulk and transcrystallization of PLA on vetiver fiber and talc as a function of temperature. Filled symbols represent experimental data obtained in the bulk, and unfilled symbols indicate experimental data obtained in TC. Lines refer to fitting data to the Hoffman-Lauritzen growth equation (equation 4.1).

## 4.5 Conclusions

From this study, transcrystallization was observed on the surface of vetiver fiber and talc in the PLA composites. The growth rate of PLA in the bulk of talc-PLA composites was the highest. The growth rate of PLA in vetiver fiber-PLA composites was lower than that of neat PLA, both in the bulk and in TC region. The growth rate in the bulk and in TC region of talc-PLA composites was higher than that of vetiver

fiber-PLA composites. The growth rate of crystallized PLA in the bulk was shown to be greater than that of crystallized PLA in the TC region. The Hoffman-Lauritzen growth equation could be used for determining the growth rate in the bulk and also applied to the growth rate in TC region. The maximum growth rate of neat PLA and PLA composites was found approximately at 135 °C.

## 4.6 References

Albano, C., Papa, J., Ichazo, M., González, J., and Ustariz, C. (2003). Application of different macrokinetic models to the isothermal crystallization of PP/talc blends. **Compos. Struct.** 62: 291–302.

Arbelaiz, A., Fernández, B., Ramos, J. A., and Mondragon, I. (2006). Thermal and crystallization studies of short flax fibre reinforced polypropylene metrix composites: Effect of treatments. **Thermochemica Acta.** 440: 111-121.

Choudhury, A. (2008). Isothermal crystallization and mechanical behavior of ionomer treated sisal/HDPE composites. **Mater. Sci. Eng.** 491: 492-500.

Di Lorenzo, M. L. (2001). Determination of spherulite growth rate of poly(L-lactic acid) using combined isothermal and non-isothermal procedures. **Polymer.** 42: 94411-9446.

Dufresne, A., Kellerhals, M. B., and Witholt, B. (1999). Transcrystallization in Mcl-PHAs/Cellulose Whiskers Composites. **Macromolecules.** 32: 7396-7401.

Ferrage, E., and Martin, F. (2002). Talc as nucleating agent of polypropylene: morphology induced by lamellar particles addition and interface mineral-matrix modelization. **J. Mater. Sci.** 37: 1561 – 1573.

Kawai, T., Rahman, N., Matsuba, G., Nishida, K., Kanaya, T., Nakana, M., Okamoto, H., Kawada, J., Usuki, A., Honma, N., Nakajima, K., and Mutsuda M. (2007). Crystallization and melting behavior of poly (L-lactic acide). **Macromolecules.** 40: 9463-9469.

Tokoro, R., Vu, D. M., Okubo, K., Tanaka, T., Fujii, T., and Fujiura, T. (2008). How to improve mechanical properties of polylactic acid with bamboo fibers. **J. Mater. Sci.** 43: 775-787.

Garlotta, D. ( 2001). A Literature Review of Poly(Lactic Acid). **J. Polym. Environ.** 9: 63-84.

Hermida, Élida. B., and Mega, V. I. (2007). Transcrystallization kinetics at the poly(3-hydroxybutyrate-co-3-hydroxyvalerate)/hemp fibre interface. **Compos. Part A.** 38: 1387–1394.

Hoffman, J. D., Davis, G. T., and Lauritzen, L. I. (1976). **Treatise on solid state chemistry: Crystalline and non-crystalline solids** *Vol. 3*. New York: In: Hannay JB Editor.

Li, H., and Huneault, M. A. (2007). Effect of nucleation and plasticization on the crystallization of poly(lactic acid). **Polymer.** 48: 6855-6866.

Mohanty, A. K., Misra, M., and Drzal, L. T. (2005). **Natural fiber, Biopolymer, and Biocomposites.** Boca Raton: Taylor & Francis Group.

Somnuk, U., Eder, G., Phinyocheep, P., Suppakarn, N., Sutapun, W., and Ruksakulpiwat, Y. (2007). Quiescent crystallization of natural fiber-polypropylene composites. **J. Appl. Polym. Sci.** 106: 2997-3006.

Ruksakulpiwat, Y., Suppakarn, N., Sutapun, W., and Thomthong, W. (2007). Vetiver–polypropylene composites: Physical and mechanical properties **Compos. Part A.** 38: 590-601.

Tsuji, H., Sugiura, Y., Sakamoto, Y., Bouapao, Y., and Itsuno, S. (2008). Crystallization behavior of linear 1-arm and 2-arm poly(L-lactide)s: Effects of coinitiators. **Polymer.** 49: 1385-1397.

Vaisman, L., Fernanda Gonzμlez, M., and Marom, G. (2003). Transcrystallinity in brominated UHMWPE fiber reinforced HDPE composites: morphology and dielectric properties. **Polymer.** 44: 1229-1235.

Wang, C., and Liu C. R., (1997). Trancrystallization of polypropylene on carbon fiberes. **Polymer.** 38: 4715-4718.

Xu, T., Lei, H., and Xie, C. S. (2003). The effect of nucleating agent on the crystalline morphology of polypropylene (PP). **Mater. Des.** 24: 227-230.

Yasuniwa, M., Tsubakihara, S., Iura, K., Ono, Y., Dan, Y., and Takahashi, K. (2006). Crystallization behavior of poly(L-lactic acid). **Polyme.** 47, 7554-7563.

Yuryev, Y., Wood-Adams, P., Heuzey, M.-C., Dubois, C., and Brisson, J. (2008). Crystallization of polylactide films: An atomic force microscopy study of the effects of temperature and blending. **Polymer.** 49, 2306-2320.

# CHAPTER V

# CONCLUSIONS

In this study, the role of vetiver fiber on crystallization behavior of vetiver fiber-PLA composite was evaluated. Talc as a nucleating agent was used to compare the nucleating effecting between talc and vetiver fiber. From isothermal crystallization, rate of crystallization of talc-PLA composites was the highest among that of neat PLA and vetiver fiber-PLA composites. Additionally, the equilibrium melting temperature of vetiver fiber-PLA and talc–PLA composites was lower than that of neat PLA. An increase in vetiver fiber content in vetiver fiber-PLA composites led to a decrease of equilibrium melting temperature of the PLA composites.

In addition, at a cooling rate of 10°C/min, crystallization peak of talc-PLA composites was not observed. However, when a cooling rate was lower to 5°C/min, the crystallization peak of talc-PLA composites was observed. Moreover, upon the second heating scan, re-crystallization peak of talc-PLA composites was found with a heating rate of 10°C/min. While re-crystallization peak of talc-PLA composites was not found with a heating rate of 5°C/min.

In contrast, the crystallization peak of PLA in vetiver fiber-PLA composites was not observed upon a cooling even though with lowering of cooling rate to 1°C/min. Upon the second heating scan, re-crystallization peak of vetiver fiber-PLA composites were observed. When the heating rate higher than of 10°C/min, re-crystallization peak of vetiver fiber-PLA composites was not observed. The crystallinity of PLA increased

with the presence of talc and vetiver fiber. These indicated that talc and vetiver fiber act as a nucleating agent for the PLA composites.

Additionally, the spherulitic growth rate of neat PLA and PLA composites were investigated. The transcrystallization (TC) was observed at the vetiver fiber and talc surface. The radius of spherulite increased linearly with the crystallization time at all crystallization temperatures. The growth rate of neat PLA was higher than that of PLA in the bulk of the vetiver fiber-PLA composites. While the growth rate of PLA in the bulk of talc-PLA composites was noticeably higher than that of neat PLA and vetiver fiber-PLA composites. Moreover, it was observed that the growth rate in TC region of talc-PLA composites was greater than that of vetiver fiber-PLA composites. In addition, it was observed that the growth rate of crystallized PLA in the bulk of PLA composites were greater than that of crystallized PLA in TC region. In addition, the Hoffman-Lauritzen growth equation was used for determining the growth rate in the bulk and also applied to the growth rate in TC region. It was found that growth rate of both neat PLA and PLA composites were illustrated by a bell-shaped curve as function of temperature. The maximum growth rate of neat PLA and PLA composites was found approximately at 135°C.

# REFERENCES


Albano, C., Papa, J., Ichazo, M., González, J., and Ustariz, C. (2003). Application of different macrokinetic models to the isothermal crystallization of PP/talc blends. **Compos. Struct.** 62: 291–302.

Anderson, K. S., and Hillmyer, M. A. (2006). Melt preparation and nucleation efficiency of polylactide stereocomplex crystallites. **Polymer.** 47: 2030-2035.

Arbelaiz, A., Fernández, B., Ramos, J. A., and Mondragon, I. (2006). Thermal and crystallization studies of short flax fibre reinforced polypropylene metrix composites: Effect of treatments. **Thermochemica Acta.** 440: 111-121.

Arroyoa, M., Zitzumbob, R., andAvalos, F. (2000). Composites based on PP/EPDM blends and aramid short fibres. Morphology/behaviour relationship. **Polymer.** 41: 6351–6359.

Bledzki, A. K., and Gassan, J. (1999). Composites reinforced with cellulose based fibres. **Prog. Polym. Sci.** 24: 221-274.

Chen, X., Hou, G., Chen, Y., Yang, K., Dong, Y., and Zhou, H. (2007). Effect of molecular weight on crystallization, melting behavior and morphology of poly(trimethylene terephalate). **Polym. Test.** 26: 144–153.

Cheung, H.-Y., Lau, K.-T., Tao, X.-M., and Hui, D. (2008). A potential material for tissue engineering: Silkworm silk/PLA biocomposite. **Compos. Part B: Eng.** 39: 1026-1033.

Choudhury, A. (2008). Isothermal crystallization and mechanical behavior of ionomer treated sisal/HDPE composites. **Mater. Sci. Eng.** 491: 492-500.

Day, M., Victoria, A., Nawaby, and Liao, X. (2006). A DSC study of the crystallization behavior of polylactic acid its nanocomposites. **J. Therm. Anal. Calorim.** 86: 623-629.

Di Lorenzo, M. L., (2001). Determination of spherulite growth rate of poly(L-lactic acid) using combined isothermal and non-isothermal procedures. **Polymer.** 42: 94411-9446.

Dufresne, A., Kellerhals, M. B., and Witholt, B. (1999). Transcrystallization in Mcl-PHAs/Cellulose Whiskers Composites. **Macromolecules**. 32: 7396-7401.

Dutkiewicz, S., Grochowska-Łapienis, D., and Tomaszewski, W. (2003). Synthesis of Poly(L(+) Lactic Acid) by Polycondensation Method in Solution. **Fibres&Textiles in Eastern Europe.** 11: 66-70.

Ferrage, E., and Martin, F. (2002). Talc as nucleating agent of polypropylene: morphology induced by lamellar particles addition and interface mineral-matrix modelization. **J. Mater. Sci.** 37: 1561 – 1573.

Ganster, J., Fink, H.-P., and Pinnow, M. (2006). High-tenacity man-made cellulose fibre reinforced thermoplastics – Injection moulding compounds with polypropylene and alternative matrices. **Compos. Part A.** 37: 1796-1804.

Garlotta, D. ( 2001). A Literature Review of Poly(Lactic Acid). **J. Polym. Environ.** 9: 63-84.

Hartmann, M. H. (1998). **Biopolymers from Renewable Resources.** Berlin: Springer-Verlag.

He, Y., Fan, Z., Yanfei Hu, Y., Wu, T., Jia Wei J., and Li, S. (2007). DSC analysis of isothermal melt-crystallization, glasstransition and melting behavior of poly(L-lactide)with different molecular weights. **Euro. Polym. J.** 43: 4431–4439.

Hermida, Élida. B., and Mega, V. I. (2007). Transcrystallization kinetics at the poly (3-hydroxybutyrate-co-3-hydroxyvalerate)/hemp fibre interface. **Compos. Part A.** 38: 1387–1394.

Hoffman, J. D., Davis, G. T., and Lauritzen, L. I. (1976). **Treatise on solid state chemistry: Crystalline and non-crystalline solids Vol. 3.** New York: In: Hannay JB Editor.

Hongbo Li, M. A. H. (2007). Effect of nucleation and plasticization on the crystallization of poly(lactic acid). **Polymer.** 48: 6855-6866.

Hu, R.-H., Lim, J.-K., Kim, C.-I., and Yoon, H.-C. (2007). Biodegradable Composites Based on Polylactic Acid(PLA) and China Jute Fiber. **Eng. Mater.** 353-358: 1302-1305.

Huda, M. S., Drzal, L. T., Mohanty, A. K., and Misra, M. (2008). Effect of fiber surface-treatments on the properties of laminated biocomposites from poly(lactic acid) (PLA) and kenaf fibers. **Compos. Sci. Technol.** 68: 424-432.

Huda, M. S., Drzal, L. T., Mohanty, A. K., and Misra, M. (2006). Chopped glass and recycled newspaper as reinforcement fibers in injection molded poly(lactic acid) (PLA) composites: A comparative study. **Compos. Sci. Technol.** 66: 1813-1824.

Iovino, R., Zullo, R., Rao, M. A., Cassar, L., and Gianfreda, L. (2008). Biodegradation of poly(lactic acid)/starch/coir biocomposites under controlled composting conditions. **Polym. Degrad. Stab.** 93: 147-157.

Junga, Y., Kim, S.-S., Kim, Y., Kim, S.-H., Byung-Soo Kimb, SukyoungKim, Yong Choi, C., and Kim, S. H. (2005). A poly(lactic acid)/calcium metaphosphate composite for bone tissue engineering. **Biomaterials.** 26: 6314-6322.

Kalb, B., and Pennings, A. J. (1980). General crystallization behavior of poly(L-lactic acid) **Polymer.** 21: 607-612.

Kawai, T., Rahman, N., Matsuba, G., Nishida, K., Kanaya, T., Nakano, M., Okamoto, H., Kawada, J., Usuki, A., Honma, N., Nakajima, K., and Matsuda, M. (2007). Crystallization and Melting Behavior of Poly (L-lactic Acid). **Macromolecules.** 40: 9463-9469.

Khondker, O. A., Ishiaku, U. S., Nakai, A., and Hamada, H. (2006). A novel processing technique for thermoplastic manufacturing of unidirectional composites reinforced with jute yarns. **Compos. Part A.** 37: 2274-2284.

Krikorian, V., and Pochan, D. J. (2004). Unusual Crystallization Behavior of Organoclay Reinforced Poly(L-lactic acid) Nanocomposites. **Macromole-cules.** 37: 6480-6491.

Kuana, C.-F., Chena, C.-H., Kuana, H.-C., Kun-Chang Lina, Chiangb, C.-L., and Peng, H.-C. (2008). Multi-walled carbon nanotube reinforced poly (L-lactic acid) nanocomposites enhanced by water-crosslinking reaction. **J. Phys. Chem. Solids.** 69: 1399-1402.

Kuana, C.-F., Kuana, H.-C., M.Mab, C.-C., and Chen, C.-H. (2008). Thermal and electrical conductivity of poly(L-lactide)/multiwalled carbon nanotube nanocomposites. **J. Phys. Chem. Solids.** 69: 1395-1398.

Lee, C. (2007). Production of D-lactic acid by bacterial fermentation of rice. **Fiber Polym.** 8: 571-578.

Lee, S.-H., and Wang, S. (2006). Biodegradable polymers/bamboo fiber biocomposite with bio-based coupling agent. **Compos. Part A.** 37: 80-91.

Lee, S.-Y., Kang, I.-A., Doh, G.-H., Yoon, H.-G., Park, B.-D., and Wu, Q. (2008). Thermal and Mechanical Properties of Wood Flour/Talc-filled Polylactic Acid Composites: Effect of Filler Content and Coupling Treatment. **J. Thermo. Compos. Mater.** 21: 209-223.

Li, H., and Huneault, M. A. (2007). Effect of nucleation and plasticization on the crystallization of poly(lactic acid). **Polymer.** 48: 6855-6866.

Mathot, V. B.F. (1994). Calorimetry and thermal analysis of polymers. Newyork : Hanser publishers.

Medeiros, E. S. D., Tocchetto, R. S., Carvalho, L. H. de., Santos, I. M. G., and Souza, A. G. (2001). Nucleating effect and dynamic crystallization of a poly (propylene)/talc system. **J. Therm. Anal. Cal.** 66: 523-531.

Miyata, T., and Masuko, T. (1998). Crystallization behaviour of poly(-lactide). **Polymer.** 39: 5515-5521.

Mohanty, A. K., Misra, M., and Drzal, L. T. (2005). **Natural fiber, Biopolymer, and Biocomposites.** Boca Raton: Taylor & Francis Group.

Nam, J. Y., Okamoto, M., Okamoto, H., Nakano, M., Usuki, A., and Matsuda, M. (2006). Morphology and crystallization kinetics in a mixture of low-molecular weight aliphatic amide and polylactide. **Polymer.** 47: 1340-1347.

Nishino, T., Hirao, K., and Kotera, M. (2006). X-ray diffraction studies on stress transfer of kenaf reinforced poly(L-lactic acid) composite. **Compos. Part A**. 37: 2269-2273.

Nishino, T., Hiraoa, K., Koteraa, M., Nakamaea, K., and Inagakib, H. (2003). Kenaf reinforced biodegradable composite. **Compos. Sci. Technol.** 63: 1281-1286.

Oksmana, K., Skrifvarsb, M., and Selinc, J.-F. (2003). Natural fibres as reinforcement in polylactic acid (PLA) composites. **Compos. Sci. Technol.** 63: 1317-1324.

Parka, J.-M., Kima, D.-S., and Kimb, S.-R. (2003). Interfacial properties and microfailure degradation mechanisms of bioabsorbable fibers/poly-l-lactide composites using micromechanical test and nondestructive acoustic emission. **Compos. Sci. Technol.** 63: 403-419.

Paul, M.-A. l., Alexandre, M. l., Dege´e, P., Henrist, C., Rulmont, A., and Dubois, P. (2003). New nanocomposite materials based on plasticized poly(L-lactide) and organo-modified montmorillonites: thermal and morphological study. **Polymer.** 44: 443-450.

Quan, H., Li, Z.-M., Yang, M.-B., and Huang, R. (2005). On transcrystallinity in semi-crystalline polymer composites. **Compos. Sci. Technol.** 65: 999-1021.

Ruksakulpiwat, Y., Suppakarn, N., Sutapun, W., and Thomthong, W. (2007). Vetiver–polypropylene composites: Physical and mechanical properties

**Compos. Part A.** 38: 590-601.

Sanchez-Garcia, M. D., Gimenez, E., and Lagaron, J. M. (2008 ). Morphology and barrier properties of solvent cast composites of thermoplastic biopolymers and purified cellulose fibers. **Carbo. Polym.** 71: 235-244.

S´ anchez, M. S., Ribelles, J.L. G., S´ anchez, F. H., Mano, J.F. (2005). On the kinetics of melting and crystallization of poly(l-lactic acid) by TMDSC. **Thermochimica acta.** 430: 201-210.

Somnuk, U., Eder, G., Phinyocheep, P., Suppakarn, N., Sutapun, W., and Ruksakulpiwat, Y. (2007). Quiescent crystallization of natural fiber-polypropylene composites. **J. Appl. Polym. Sci.** 106: 2997-3006.

Srimoaon, P., Dangseeyun, N., and Supaphol, P. (2004). Multiple melting behavior in isothermally crystallized poly(trimethylene terephthalate)**. Euro. Polym. J.** 40: 599–608.

Thanomkiat, P., Phillips, R.A., and Supaphol, P. (2004). Influence of molecular characteristics on overallisothermal melt-crystallization behavior and equilibrium melting temperature of syndiotactic polypropylene**. Euro. Polym. J.** 40: 1671–1682

Tokoro, R., Vu, D. M., Okubo, K., Tanaka, T., Fujii, T., and Fujiura, T. (2008). How to improve mechanical properties of polylactic acid with bamboo fibers. **J. Mater. Sci.** 43: 775-787.

Tsuji, H., Sugiura, Y., Sakamoto, Y., Bouapao, Y., and Itsuno, S. (2008). Crystallization behavior of linear 1-arm and 2-arm poly(L-lactide)s:

Effects of coinitiators. **Polymer.** 49: 1385-1397.

Tsuji, H., Kawashima, Y., Takikawa, H., and Tanaka, S. (2007). Poly(L-lactide)/ nano-structured carbon composites: Conductivity, thermal properties, crystallization, and biodegradation. **Polymer.** 48: 4213-4225.

Tsuji, H., Takai, H., and Saha, S. K. (2006). Isothermal and non-isothermal crystallization behavior of poly(L-lactic acid):Effects of stereocomplex as nucleating agent. **Polymer.** 47: 3826-3837

Varga, J., and Karger-Kocsis, J. (1995). Interfacial morphologies in carbonfiber-reinforced polypropylene microcomposites. **Polymer.** 36: 4877-4881.

Vaisman, L., Fernanda Gonzαlez, M., and Marom, G. (2003). Transcrystallinity in brominated UHMWPE fiber reinforced HDPE composites: morphology and dielectric properties. **Polymer.** 44: 1229-1235.

Vasanthakumari, R., and Penning, A. J. (1983). Crystallization kinetics of poly(L-lactic acid). **Polymer.** 24: 175-178.

Wang, C., and Liu C. R., (1997). Trancrystallization of polypropylene on carbon fiberes. **Polymer.** 38: 4715-4718.

Wang, Y., and Mano, J. o. F. (2005). Influence of melting conditions on the thermal behaviour of poly(L-lactic acid). **Euro. Polym. J.** 41: 2335-2342.

Wong, S., Shanks, R. A., and Hodzic, A. (2007). Effect of additives on the interfacial strength of poly(L-lactic acid) and poly(3-hydroxy butyric acid)-flax fibre composites. **Compos. Sci. Technol.** 67: 2478-2484.

Xu, T., Lei, H., and Xie, C. S. (2003). The effect of nucleating agent on the crystalline morphology of polypropylene (PP). **Mater. Des.** 24: 227-230.

Yasuniwa, M., Iura, K., and Dan, Y. (2007). Melting behavior of poly(L-lactic acid): Effects of crystallization temperature and time. **Polymer.** 48: 5398-5407.

Yasuniwa, M., Tsubakihara, S., Iura, K., Ono, Y., Dan, Y., and Takahashi, K. (2006). Crystallization behavior of poly(L-lactic acid). **Polymer.** 47: 7554-7563.

Yeh, J.T., Huang, C. Y., Chai, W. L., and Chen, K. N. (2009). Plasticized Properties of Poly (lactic acid) and Triacetine Blends. **J. Appl. Polym. Sci.** 112: 2757–2763.

Yuryev, Y., Wood-Adams, P., Heuzey, M.-C., Dubois, C., and Brisson, J. (2008). Crystallization of polylactide films: An atomic force microscopy study of the effects of temperature and blending. **Polymer.** 49: 2306-2320.

Zhang, Z., Wang, C., Yang, Z., Chen, C., and Mai, K. (2008). Crystallization behavior and melting characteristics of PP nucleated by a novel supported β-nucleating agent. **Polymer.** 49: 5137–5145.

# APPENDIX A

# LIST OF PUBLICATIONS

# THE STUDY OF GROWTH RATE OF VETIVER GRASS-POLYLACTIC ACID COMPOSITES

**Somruetai Boonying**[1,2], Wimonlak Sutapun[1,2], Nitinat Supakarn[1,2], and Yupaporn Ruksakulpiwat[1,2]*

[1]School of Polymer Engineering, Institute of Engineering, Suranaree University of Technology, Nakhon Ratchasima 30000, Thailand
[2]Center of Excellence for Petroleum, Petrochemicals and Advanced Materails, Chulalongkorn University, Bangkok 10330, Thailand

* Corresponding Author E-mail address: yupa@sut.ac.th

**Abstract: In this research, the crystallization behavior of vetiver grass-PLA composites was investigated. Sperulitic growth rate was determined by using a Hot Stage under a Polarized Light Optical Microscope (POM). Transcrystallization was observed at the interface between vetiver grass and PLA. It was found that sperulitic growth rate of PLA at transcrystalline region was lower than that of PLA in the bulk.**

## 1. Introduction

Poly (lactic acid) (PLA) becomes an interesting bioplastic nowadays because it has high strength and modulus and can be made from renewable resources. The crystallinity of PLA depends on the stereopurity (L- or D-isomers) of the polymer backbone. This made PLA either semicrystalline or totally amorphous. PLA is a brittle polymer. It needed modification for more practical applications. A way to improve the properties of PLA is addition of filler or reinforcing material. One of reinforcing materials for PLA composite is natural fiber such as kenaf [1], flax [2], bamboo [3], coir [4] and jute [5].

From our previous study, the vetiver grass was shown to be an effective filler in polypropylene (PP) composites. It was found that the presence of vetiver grass led to an increase in tensile strength and Young's modulus of PP composites [6]. As mentioned above, PLA is biodegradable polymer while PP is not. Therefore, the use of PLA biopolymer in the composites instead of PP polymer is interesting. The properties of composites were affected by its crystallization behavior. Therefore, the studies on crystallization behavior of composites are significant.

## 2. Experimental

### 2.1 Materials

Poly (lactic acid) (PLA 4042D) with density of 1.24 g/ml was purchased from Nature Works. Vetiver grass (*Vetiveria Zizanioides*) was obtained from The Land Development Department, Nakhon Ratchasima, Thailand. The ages of vetiver grass are around 6–8 months. Sodium hydroxide (NaOH) (laboratory grade) was purchased from Italmar (Thailand) CO., LTD.

### 2.2 Sample preparation

#### 2.2.1 Vetiver fibers preparation

Vetiver grass was washed by water to get rid of dirt and dried by sunlight for one day. The washed vetiver leaves were ground by a Retsch grinder machine and sieved into the length of 2 mm. Vetiver fiber with 2 mm. length was firstly washed by water to eliminate dirt and dried in an oven at 100°C overnight. After that, the vetiver fiber was immersed in a solution of 4% (wt) NaOH for 2 h at 40°C and the vetiver-to-solution ratio is 1:25 (w/v). The alkali-vetiver fiber was then washed thoroughly with water and dried in an oven at 100°C for 24 h.

#### 2.2.2 Preparation of vetiver fiber-PLA composites

Vetiver fiber was mixed with PLA at 170 °C in an internal mixer (Haake Rheomix 3000P model 557-1306).The ratio of vetiver fiber to PLA is 1% by weight. Mixing speed and mixing time were 50 rpm and 13 minutes, respectively. After that, PLA composites were ground and dried before using.

### 2.3 Growth rate measurement

Thin films of neat PLA and vetiver fiber-PLA composite were prepared by compression molding at 180 ºC. A small piece of neat PLA and PLA composites were squeezed between two glass slides, and then inserted in the hot stage. These film samples were used to obtain spherulite growth rate of neat PLA and PLA composites by using a Hot stage (Linkam TH600) under a Polarized Light Optical Microscope attached with CCD video camcorder system (Sony). The sample was heated from room temperature to 220 ºC with a heating rate 20 ºC/min and held at that temperature for 5 min. Then, the sample was cooled down with a rate of 50 ºC/min to various crystallization temperatures ($T_c$). The radius of spherulite was measured as a function of time. The growth rate (G) at various $T_c$ was obtained from the slope of the plots of spherulite radius versus time.

Comparisons among the growth rate of neat PLA, PLA in bulk of composite and PLA at fiber surface were made.

**3. Result and discussion**

From the optical microscope, spherulites of PLA in bulk were observed during crystallization. Moreover, transcrystallization (TC) were taken place at the fiber surface. TC morphology can be formed by a dense heterogeneous nucleation of PLA crystals at the vetiver fiber surface which grow perpendicular to the fiber axis. The growth of TC proceeds perpendicularly to the fiber until the growing front impinges with spherulites nucleated in the bulk. TC morphology was also observed at the surface of fiber in other fiber composites [7]. Examples of optical micrographs of crystallized PLA in the bulk of composite and on vetiver fiber taken during isothermal crystallization process were shown in Figure 1. It was observed that the spherulite diameter of PLA in bulk increased with increasing time as shown in Figure 2. Spherulitic growth rate of PLA in the bulk was determined by measuring radius of spherulite as a function of time. Growth rate of TC was evaluated by measuring a width of the TC region perpendicularly preceded to the fiber surface as a function of time. Radius of spherulite plotted against time during isothermal crystallization for neat PLA, bulk PLA in the composites and PLA at the TC region at various $T_c$ are shown in Figure 3 (a)-(c), respectively. It was shown that the radius of spherulite increased linearly with the crystallization time at all crystallization temperatures. Spherulitic growth rates were obtained from the slope of each plot in Figure 3 and shown in Figure 4.

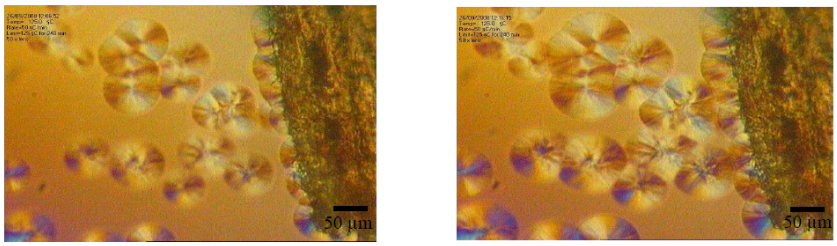


time=25min time=35 min

Figure 1. Optical micrographs of PLA in bulk and on vetiver fiber during crystallization at temperature of 125 °C.

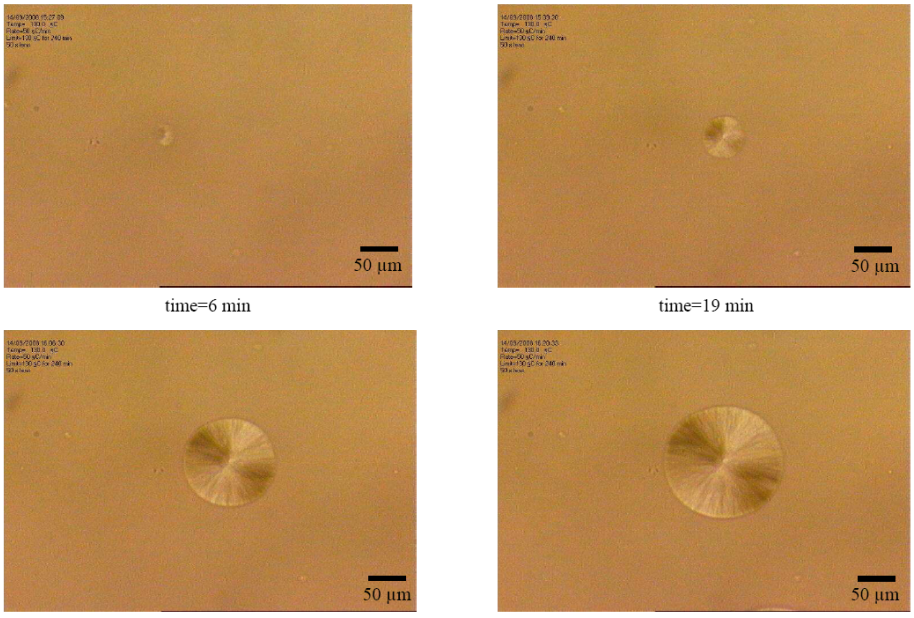


time=6 min time=19 min

time=48 min time=63 min

Figure 2. Optical micrographs of PLA spherulites grown from the melt during isothermal crystallization at 130 ºC at various crystallization time.

Figure 5 shows spherulitic growth rate in logarithmic scale (Log G) at various crystallization temperatures ($T_c$). The spherulitic growth rate as a function of $T_c$ shows a bell shape curve. It has been reported for PLLA that spherulitic growth rate curve shows discontinuity [8]. It is known that the discontinuity is dependent on the molecular weight, incorporated co-monomer unit, and tacticity. This phenomenon has been assumed to be of a regime transition. In this study, the discontinuity was not observed. From Figure 5, comparison among spherulitic growth rate at various $T_c$ of neat PLA, PLA in bulk of the composite and PLA at fiber surface of the composites can be elucidated. It was found that the growth rate of neat PLA was higher than those of PLA in bulk of the vetiver-PLA composites. Similar to Somnuk and co-worker, they also found that the growth rate of neat PP was higher than those of PP in the bulk of the vetiver fiber–PP composites [9]. This may be due to the restriction of chain mobility caused by the fiber. In addition, it was observed that the growth rate of crystallized PLA in the bulk were greater than that of crystallized PLA in the TC region.

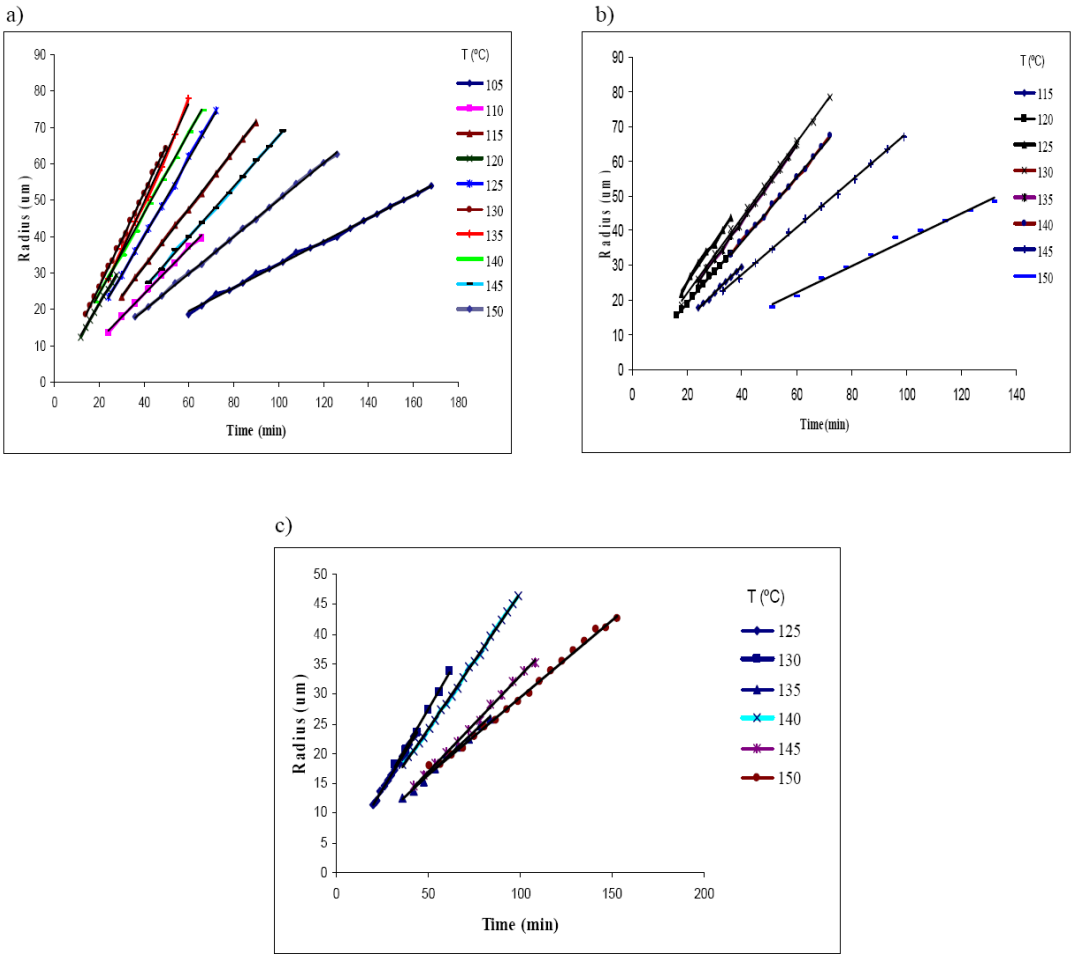


Figure 3. Spherulite radius plotted against crystallization time during isothermal crystallization at various crystallization temperatures of (a) neat PLA, (b) bulk PLA in the composites and (c) PLA in the TC region.

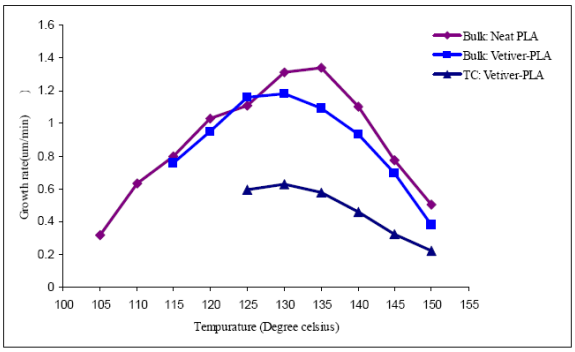


Figure 4. Spherulitic growth rate (G) at various crystallization temperatures ($T_c$).

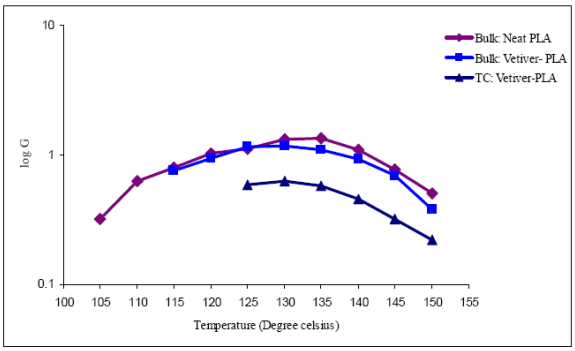


Figure 5 Spherulitic growth rates in logarithmic scale (Log G) at various crystallization temperatures ($T_c$).

## 4. Conclusion

From this study, transcrystallization was observed on the surface of vetiver fiber in the PLA composites. Comparison among spherulitic growth rate at various $T_c$ of neat PLA, PLA in bulk of the composite and PLA at fiber surface of the composites was made. The growth rate of neat PLA was shown to be the highest. When vetiver fibers were added in PLA, the growth rate of PLA was lower, both in the bulk and on the surface of vetiver fiber in the composites. The growth rate of crystallized PLA in the bulk was shown to be greater than that of crystallized PLA in the TC region.

## 5. References

[1] Huda, M. S., Drzal, L. T., Mohanty, A. K., and Misra, M., *Compos Sci Technol.* **68** (2008), pp.424-432.

[2] Wong, S., Shanks, R. A., and Hodzic, A., *Compos Sci Technol.* **67** (2007), pp. 2478-2484.

[3] Lee, S.-H., and Wang, S., *Compos Sci Technol.* **37** (2006), pp. 80-91.

[4] Iovino, R., Zullo, R., Rao, M. A., Cassar, L., and Gianfreda, L., *Polym Degrad Stab*. 93 (2008), pp. 147-157.

[5] Khondker, O. A., Ishiaku, U. S., Nakai, A., and Hamada, H., *Composites Part A*. **37** (2006), pp. 2274-2284.

[6] Ruksakulpiwat, Y., Suppakarn, N., Sutapun, W., and Thomthong, W., *Composites Part A*. **38** (2007), pp. 590-601.

[7] Zafeiropoulos, N. E., Baillie, C. A., and Matthews, F. L., *Composites Part A*. **32** (2001), pp. 525-543.

[8] Kawai, T., Rahman, N., Matsuba, G., Nishida, K., Kanaya, T., Nakano, M., Okamoto, H., Kawada, J., Usuki, A., Honma, N., Nakajima, K., and Matsuda, M., *Macromolecules*. **40** (2007), pp. 9463-9469.

[9] Somnuk, U., Eder, G., Phinyocheep, P., Suppakarn, N., Sutapun, W., and Ruksakulpiwat, Y., *J Appl Polym Sci*. **106** (2007), pp. 2997-3006.

# BIOGRAPHY

Ms. Somruetai Boonying was born on September 26, 1979 in Yasothon, Thailand. She finished primary school from Ban Ponlawai School and secondary school from Mahachanachaiwittayakom School. After that, she continued her study in faculty of science at Mahasarakham University (MSU), Mahasarakham and earned her Bachelor's degree in Chemistry in 2002. Then, she continued with her graduate study in Polymer Engineering Program, Institute of Engineering, Suranaree University of Technology. During her graduate study, she got a research assistant scholarship from the Center of Excellence for Petroleum, Petrochemical and Advanced Materials, Chulalongkorn University, Thailand. Her research was about "*Crystallization behavior of poly(lactic acid) composites*". Several parts of her work were presented at Pure and Applied Chemistry International Conference (PACCON 2009), Phitsanulok, Thailand.